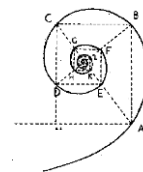




UNIVERSITÀ DEGLI STUDI DI MILANO



SCUOLA DOTTORATO

IN MEDICINA MOLECOLARE E TRASLAZIONALE

CICLO XXX

TESI DI DOTTORATO DI RICERCA

Settore Scientifico Disciplinare **MED/07**

**Gene editing technologies based on Crispr-
Cas9 system for the treatment of HIV: studies in
vitro and *in vivo***

Dottorando: Ramona **BELLA**
Matricola N° **R10845**

Tutor: Prof. Pasquale **Ferrante**

Co-Tutor: Dr. Kamel **Khalili**

Coordinatore del dottorato: Prof. Riccardo **GHIDONI**

Anno Accademico 2016/2017

ABSTRACT

Retroviruses include two subfamilies, orthoretrovirinae and spumaretrovirinae. The human immunodeficiency virus 1 (HIV-1) belongs to the orthoretrovirinae subfamily and is the causative agent of acquired immunodeficiency syndrome (AIDS). HIV-1 infects 36.9 million people and 2.6 million children throughout the world. During primary infection HIV converts its RNA genome into DNA, which integrates into the host genome. The cellular environment present at the site of the integration may influence viral transcriptional activity. The sequestration of host transcription factors, the presence of repressor of transcription and nucleosomes and epigenetic modifications on the HIV promoter, or transcriptional modification of Tat are all conditions that influence the formation of long term viral reservoirs. The use of antiretroviral drugs has been proposed as a functional cure to control the viral load but lacks the ability to obtain viral sterilization since antiretroviral drugs can not remove the virus from latently infected cells and anatomical sanctuaries such as brain and the gut associated lymphoid tissue. In recent years gene editing strategies have been largely employed for the treatment of HIV-1. In this present study, we aimed to discover an innovative CRISPR technology specific against the HIV viral genome that can target latently infected cells and be delivered in all tissues. Initially, we performed in vitro analysis, where TZMB-1 cells containing the luciferase gene under the control of LTR were transfected with pCMV-Tat and three plasmids harboring Cas9 under the control of different regions of LTR promoter to evaluate by western blot analysis the minimal LTR promoter region able to activate Cas9 in presence of Tat. TZMB-1 cells were transduced with the lentiviruses, harboring Cas9 or gRNAs specific for the promoter region, and infected with HIV-1 to test, by PCR and luciferase assay, the presence of gene editing. Then PCR and flow cytometric analyses were performed on

2D10 cells, HIV-1 latently infected cells, to test the ability of Tat-induced Cas9 to excise viral DNA. Subsequently, was evaluated the ability of Cas9, in presence of gRNAs, to protect Jurkat cells from viral reinfection by eliminating the virus during the early stages of infection. The second part of our study was performed to test Cas9 and gRNAs specific for HIV-1 LTR and Gag regions in vivo using adeno-associated virus (AAV) as the delivery system. Tissues of HIV-1 transgenic mice and rats and humanized mice were provided by collaborators for evaluation by analyzing DNA and RNA for the presence of viral editing. Results from in vitro experiments showed the ability of Tat to activate the minimal promoter LTR, inducing gene editing in TZMb-1 and 2D10 cells. The presence of Cas9 in Jurkat cells induces a reduction of viral RNA of 96% at five days from infection. Studies in vivo showed the presence of viral excision in blood, heart, liver, lung, kidney, spleen and brain in transgenic mice and a reduction of viral RNA in the blood of transgenic rats. Excision of HIV-1 was reported in the spleen, gut associated lymphoid tissue, liver, kidney, lung and brain of humanized mice with complete viral sterilization in 29% of the infected animals that were subjected to antiretroviral treatment. The absence of off-target effects was confirmed by deep sequencing analysis. Together, these data show the ability to create a Cas9-inducible system generating negative feedback against the virus while avoiding persistent Cas9 expression in the cells. The use of AAV vectors in vivo showed high delivery efficiency in the different tissues, obtaining viral sterilization for the first-time. Further experiments on humanized mice and SIV infected monkey models will show this approach combined with ART therapy may have important application for HIV-1 sterilization in clinical trials.

SOMMARIO

Retroviruses includono due sottofamiglie, gli *Orthoretrovirinae* e *Spumaretrovirinae*. Il virus dell'immunodeficienza umana (HIV) appartiene alla sottofamiglia degli *Orthoretrovirinae* ed è considerato l'agente causativo della sindrome dell'immunodeficienza acquisita (AIDS). Ad oggi 36,9 milioni di individui, di cui 2,6 milioni di bambini nel mondo convivono con l'infezione da HIV-1. Durante l'infezione primaria, dopo la conversione di HIV-1 RNA in DNA, il virus integra il suo genoma nel DNA dell'ospite. L'ambiente cellulare presente a livello del sito di integrazione influenza la replicazione e la trascrizione virale. Il sequestro di fattori di trascrizione cellulari, la presenza di repressori di trascrizione e nucleosomi e modificazioni genetiche a livello del promotore virale o modificazioni trascrizionali di Tat sono tutte condizioni che incidono sulla formazione di reservoir virali a lungo termine. L'uso di farmaci antiretrovirali è stato proposto come cura funzionale in grado di mantenere la carica virale sotto il limite di detezione, ma la mancanza di azione a livello delle cellule reservoir e il mancato raggiungimento di organi come il sistema nervoso centrale (SNC) o il tessuto linfoide associate all'intestino rappresenta un grosso limite di questi farmaci. In questi ultimi anni l'uso di gene editing per il trattamento di HIV-1 è stato impiegato da differenti laboratori. Il presente studio ha come scopo la realizzazione di un nuovo costrutto usando un efficace sistema di delivery per targettare le cellule reservoir e raggiungere i diversi tipi di tessuti. Inizialmente è stato condotto uno studio in vitro, cellule TZMB-1 contenenti il gene per la luciferasi sotto il controllo di LTR sono state transfettate con pCMV-Tat e tre plasmidi contenenti Cas9 sotto il controllo di diverse regioni del promotore per individuare attraverso western blot la minima regione di LTR in grado di attivare la trascrizione di Cas9 in presenza di Tat. TZMB-1 cellule sono state trasdotte con lentivirus contenenti Cas9 e gRNAs specifici per il promotore

LTR e infettate con HIV-1 per valutare la presenza di LTR editing mediante saggi di PCR e luciferasi. Successivamente analisi di PCR e citofluorimetriche sono state condotte per valutare l'abilita' del costrutto Cas9, Tat-indotto, di escidere il virus in cellule 2D10, modello cellulare di infezione latente. Infine e' stata testata la capacita' di Cas9 in presenza dei gRNAs di proteggere le cellule Jurkat da reinfezione virale eliminando il virus nello stadio iniziale dell'infezione. La seconda parte del nostro studio e' stata condotta per testare Cas9 e gRNAs specifici per il promotore LTR e la regione Gag, in vivo usando adeno-associati virus (AAV) come sistema di delivery. Tessuti di topi e ratti HIV-1 transgenici e di topi umanizzati, sono stati forniti da collaboratori per valutare attraverso analisi del DNA e RNA la presenza di editing virale. Risultati ottenuti dagli esperimenti in vitro hanno dimostrato l'abilita' di Tat di attivare la minima regione del promotore LTR, inducendo gene editing in cellule TZMb-I e 2D10. La presenza di Cas9 nelle cellule Jurkat induce una riduzione dei trascritti virali del 96% a cinque giorni dall'infezione. Studi in vivo hanno dimostrato la presenza di eliminazione virale in diversi tessuti come sangue, fegato, polmoni, rene, milza e cervello in topi transgenici ed una riduzione del RNA virale nel sangue dei ratti transgenici. Editing di HIV-1 e' stato osservato nei tessuti di milza, tessuto linfoide associato all'intestino, fegato, rene, polmone e cervello dei topi umanizzati con completa sterilizzazione virale nel 29% degli animali precedentemente trattati con terapia antiretrovirale. Questi risultati, hanno dimostrato la capacita' di creare un nuovo sistema di gene editing attivato dalla presenza del virus nella cellula creando un feedback negativo contro lo stesso virus ed evitando la persistente espressione di Cas9 nelle cellule. L'uso di AAV in vivo, ha dimostrato alta efficienza di delivery nei diversi tessuti, ottenendo completa sterilizzazione virale. Questi dati, se confermati da ulteriori esperimenti sui topi umanizzati e modelli di scimmia infettati con SIV,

combinati con la terapia antiretrovirale possono avere importanti implicazioni per la cura di HIV-1 in trial clinici.

INDEX

	<u>Page</u>
Abstract.....	II
Sommario.....	IV
List of Symbols.....	XIII
List of Figures.....	1
List of Tables	4

Chapters

1. Introduction.....	5
1.1. <i>Human Immunodeficiency Virus</i>	5
1.1.1. Epidemiology	5
1.1.2. HIV Transmission and Pathogenesis.....	8
1.1.3. HIV-1 Diagnosis.....	10
1.1.4. HIV Genome.....	11
1.1.5. HIV Structural Biology	13
1.1.6. Regulatory Tat Protein.....	18
1.1.7. HIV-1 Replication Cycle	20
1.1.8. Latency	23
1.2. <i>HIV-1 Treatment</i>	26
1.2.1. Antiretroviral Treatment	26
1.2.2. Vaccines	28
1.2.3. Transplantation of Hematopoietic Stem Cells	28

1.2.4.	Shock and Kill Approach Therapy	29
1.2.5.	Gene Therapy Strategies	30
1.2.6.	Cre Recombinase.....	30
1.2.7.	Homing Endonucleases.....	31
1.2.8.	The Zinc Finger Nuclease (ZFN).....	31
1.2.9.	Transcription Activator-Like Effector Nucleases (TALENs)	33
1.2.10.	Double Strand Break (DSB).....	34
1.2.11.	CRISPR System.....	36
1.2.12.	CRISPR/Cas9 Delivery	41
1.2.13.	CRISPR/Cas9 System for HIV-1 Genome Editing.....	42
2.	Aim of the Study	46
3.	Materials and Methods	47
3.1.	<i>Plasmid Preparation</i>	47
3.2.	<i>Cell Culture</i>	48
3.3.	<i>Co-Transfection of TZM-bl with px260-LTR-Cas9 and pCMV-Tat</i>	49
3.4.	<i>Lentiviral Packaging</i>	50
3.5.	<i>Viral Titer</i>	50
3.6.	<i>Immunohistochemistry for Cas9</i>	51
3.7.	<i>TZM-bl Transduction with pLENTI-LTR-Cas9</i>	51
3.8.	<i>Stable Cell Lines</i>	52

3.9.	<i>Infection of TZM-bl with HIV-1_{JRFL} or HIV-1_{SF162}</i>	53
3.10.	<i>Electroportation of the 2D10 Cell Line with LTR (-80/+66)- Cas9</i>	54
3.11.	<i>Viral Stock</i>	55
3.12.	<i>Jurkat HIV-1 Infection</i>	55
3.13.	<i>Cellular Viability Assay</i>	56
3.14.	<i>Luciferase Assay</i>	56
3.15.	<i>Western Blot</i>	57
3.16.	<i>DNA and RNA Isolation</i>	57
3.17.	<i>HIV-1 DNA Detection and Quantification</i>	57
3.18.	<i>Selection of gRNAs</i>	58
3.19.	<i>Transduction of Tg26 MEFs</i>	58
3.20.	<i>In vivo rAAV9:saCas9/gRNA Administration</i>	59
3.21.	<i>Analysis of DNA in Animal Models</i>	59
3.22.	<i>RNA Analysis of Rats and Humanized Mice Samples</i>	60
3.23.	<i>Statistical Analysis</i>	61
4.	Results	65
4.1.	<i>Determination of the minimal promoter region activated by Tat</i>	65
4.2.	<i>Increase of Cas9 expression in the presence of Tat</i>	66
4.3.	<i>Viral excision increases in presence of Tat and gRNAs</i> ..	67
4.4.	<i>Decreased LTR promoter activity in presence of Tat</i>	69

4.5.	<i>Cas9 expression is activated during HIV-1 infection.....</i>	70
4.6.	<i>Tat protein expression drives viral excision</i>	71
4.7.	<i>Decreased LTR promoter activity during HIV-1 infection</i>	72
4.8.	<i>Cas9 expression in Jurkat 2D10 cells as model of latently infected cells</i>	73
4.9.	<i>Viral excision in the Jurkat 2D10 cell model of latently infected cells</i>	74
4.10.	<i>GFP reduction in Jurkat 2D10 cells as model of latently infected cells</i>	76
4.11.	<i>Viral excision in Jurkat cells during the early stage of infection.....</i>	77
4.12.	<i>GFP reduction in Jurkat cells on the early stage of infection</i>	79
4.13.	<i>Reduction of GFP protein levels in presence of gRNAs and Cas9 in Jurkat cells.....</i>	80
4.14.	<i>Gag DNA and RNA reduction in Cas9 treated Jurkat cells at the early stage of infection</i>	82
4.15.	<i>Viral Excision in MEF cells treated with rAAV9 SaCas9/gRNAs.....</i>	83
4.16.	<i>Viral excision in vivo in Tg26 mice treated with rAAV9 SaCas9/gRNAs.....</i>	84

4.17. <i>Viral excision in vivo in Tg26 rats treated with rAAV9 SaCas9/gRNAs</i>	86
4.18. <i>Viral excision in vivo in humanized mice treated with rAAV9 SaCas9/gRNAs</i>	88
4.19. <i>Cas9 and gRNAs expression in the tissues Humanized mice</i>	93
4.20. <i>No viral DNA was observed in two LASER ART/AAV9 CRISPR/Cas9 treated mice</i>	94
5. Discussion	96
6. Conclusions	102
7. References	105
APPENDIX A: Molecular Cloning	133
A1. <i>PCR Products</i>	133
A2. <i>Gel Purification of PCR Products</i>	134
A3. <i>Ligation of PCR Products and Transformation</i>	134
A4. <i>DNA Isolation from Bacteria</i>	136
A5. <i>Digestion of pCR™4-TOPO® TA Vector and pX260-U6-DR-BB-DR-Cbh-NLS-hSpCas9-NLS-H1-shorttracr-PGK-puro vector</i>	136
A6. <i>Creation of Lenti-LTR (-80/+66) Cas9-BLAST Construct</i> .	138
A7. <i>Creation of px601-CMV/saCas9-LTR-GagD</i>	139

APPENDIX B: Lentiviral Packaging	143
APPENDIX C: Western Blot.....	144
APPENDIX D: DNA and RNA Analysis	145
D1. <i>Genomic DNA Extraction from Cells and Tissues</i>	145
D2. <i>RNA Isolation from Cells and Blood</i>	145
D3. <i>Retrotranscription</i>.....	146
D4. <i>RNA Extraction from Rat Tissues</i>	146
D5. <i>PCR on TZM-bl Cells</i>.....	147
D6. <i>qPCR on Jurkat 2D10 Cells</i>	147
D7. <i>PCR on Jurkat 2D10 Cells</i>.....	148
APPENDIX E: Tg26 Mice and Rat Model	149
APPENDIX F: Humanized Mice AAV9/CRISPR/Cas9 Treatment.....	150
Scientific Products	151
Scientific Products Related to this Work	152
Acknowledgements	154

LIST OF SYMBOLS

AIDS	Acquired Immunodeficiency Syndrome
AP-1	Clathrin Adapter Protein Complex 1
AP-2	Clathrin Adapter Protein Complex 2
APOBEC3F
.....	Apopolipoprotein B mRNA Editing Enzyme Catalytic Subunit 3F
APOBEC3G
.....	Apopolipoprotein B mRNA Editing Enzyme Catalytic Subunit 3G
ART	Antiretroviral Therapy
BBB	Blood-Brain Barrier
CA	Capsid
Cas	CRISPR-Associated Protein
Cas9 RNPS	Cas9/sgRNA Ribonucleoproteins
CIP	Alkaline Phosphatase, Calf Intestinal
Cpf1	CRISPR from Prevotella and Francisella 1
CREBBP	cAMP-Response Element Binding Protein
CRISPR
.....	Clustered Regulatory Interspaced Short Palindromic Repeat System
CTIP2
.....	Chicken Upstream Promoter Transcription Factor Interacting Protein 2
COUP-TFII	COUP Transcription Factor 2
CTLs	Cytotoxic T Lymphocytes
DDB1	DNA Damage-Binding Protein 1
DMEM	Dulbecco's Modified Eagle Medium
DSB	Double Strand Breaks
DSIF	DRB Sensitivity Inducing Factor
EP300	E1A Binding Protein p300
ESCRT	Endosomal Sorting Complex Required for Transport
FasL	Fas Ligand
FBS	Inactivated Fetal Bovine Serum
GFP	Green Fluorescent Protein
HAART	Highly Active Anti-Retroviral Therapy
HAND	HIV-Associated Neurocognitive Disorders
HATs	Histone Acetyltransferases
HBSS	Hank's Balanced Salt Solution
HDR	Homology Directed Repair
HIV-1 and HIV-2	Human Immunodeficiency Virus 1 and 2
HKMT	Histone Methyltransferase
IN	HIV-1 Integrase
ITGB2	Integrin Subunit Beta-2
KS	Kaposi's Sarcoma
LASER ART	Long-Acting Slow Effective Release Antiretroviral Therapy
LBH-589	Panobinostat

LRA	Latency Reversing Agents
LTRs	Long Terminal Repeats
MA	Matrix
MEFs	Mouse Embryonic Fibroblasts
MHC-1	Major Histocompatibility Complex Class 1
NC	Nucleocapsid
Nef	Negative Regulatory Factor
NELF	Negative Elongation Factor
NES	Nuclear Export Signal
NFAT	Nuclear Factor of Activated T-Cells
NF-KB	Nuclear Factor Kappa-Light-Chain-Enhancer of Activated B Cells
NHEJ	Non-Homologous End Joining
NIH	National Institute of Health
NLS	Nuclear Localization Signal
NNRTIs	Non-Nucleoside Reverse Transcriptase Inhibitors
NUC	Nucleosome
O/N	Overnight
ORF	Open Reading Frame
PACS1	Phophofurin Acidic Cluster Sorting Protein 1
PAMs	Protospacer Adjacent Motifs Region
PBLs	Human Peripheral Blood Lymphocytes
PBMCs	Peripheral Blood Mononuclear Cells
PBS	Primer Binding Site
PCAF	Acetyl-CoA Acetyltransferase
PCP	Pneumocystis Carinii Pneumonia
PD-1	Programmed Cell Death Protein 1
PEI	Polymer Polyethyleneimine
PHA	Phytohemagglutinin
PI	PAM-Interacting
PIC	Pre-Integration Complex
PolyA	Polyadenylation Signal
PTD	Portein Transduction Domain
P-TEFb	Positive Transcription Elongation Factor
PTPC	Permeability Transition Pore Complex
rAAV	Recombinant Adeno-Associated Virus
RPMI	Roswell Park Memorial Institute
RRE	Rev Response Element
RT	Reverse Transcriptase
saCas9	Staphylococcus aureus Cas9 protein
SAHA	Suberohylanilide Hydroxamic Acid
SERINC3/5	Serine Incorporator 3 and 5, antiviral proteins
SIV	Simian Immunodeficiency Virus
SLiPE	Substrate-Linked Protein Evolution
SP1	Stimulatory Protein 1

spCas9	Streptococcus Pyogenes Cas9
SRC	Sarcoma
TAF	TBP-Associated Factor
TAK	Tat-Associated Kinase
TALEN	Transcription Like Effector Nuclease
TAR	Transcription Response Region
TCF-4	T Cell Factor 4
tracrRNA	Trans-activating crRNA
TRIM	Tripartite motif-containing
TSA	Trichostatin A
UNAIDS	Joint United Nations Program on HIV/AIDS
VPA	Valporic Acid
Vpu	Viral Protein U
ZFN	Zinc Finger Nuclease

LIST OF FIGURES

- Figure 1.** Illustration of the *Retroviridae* Family
- Figure 2.** 2016 Global HIV patients testing and treatment
- Figure 3.** HIV-1 Infection Phases
- Figure 4.** HIV-1 Genome Map and Structural Biology
- Figure 5.** Reverse transcription of HIV-1 RNA
- Figure 6.** Interaction of Tat with NF- κ B and p-TEFb
- Figure 7.** HIV-1 Life Cycle
- Figure 8.** HIV-1 RNA copies/ml in the plasma in patients treated with antiretroviral therapy
- Figure 9.** Global Incidence of HIV-1 Infected Patients under ART Therapy between 2010-2015
- Figure 10.** Zinc Finger Nuclease Model
- Figure 11.** TALEN Model System
- Figure 12.** Induction of Double Strand Breaks after Gene Editing
- Figure 13.** Cas9-gRNAs Interactions
- Figure 14.** Determination of the minimal promoter region activated by Tat
- Figure 15.** Cas9 expression is activated by Tat
- Figure 16.** Increased viral excision in presence of Tat and gRNAs
- Figure 17.** DNA analysis of truncated LTR confirms viral excision
- Figure 18.** Decrease of LTR promoter activity in presence of Tat
- Figure 19.** Cas9 expression during HIV-1 infection
- Figure 20.** Tat protein production drives viral excision
- Figure 21.** Decreased LTR promoter activity in presence of Tat
- Figure 22.** Cas9 expression in Jurkat 2D10 cells
- Figure 23.** Viral excision in a model of HIV-latent infection
- Figure 24.** Sequence analysis of the truncated LTR Fragment

- Figure 25.** Excision Percentage of the LTR Promoter region
- Figure 26.** Decrease of viral reactivation
- Figure 27.** Viral excision in Jurkat Cells at the early stage of infection
- Figure 28.** Sequence Analysis of Truncated LTR Fragments
- Figure 29.** Excision of the viral DNA between LTR regions
- Figure 30.** GFP reduction in Jurkat cells on the early stage of infection
- Figure 31.** Reduction of GFP protein levels in presence of gRNAs and Cas9
- Figure 32.** Quantification of Viable Jurkat Cells
- Figure 33.** Cas9 DNA and RNA reduction in Jurkat cells
- Figure 34.** Viral excision on DNA of MEF cells
- Figure 35.** Viral excision in vivo in tissues of Tg26 mice
- Figure 36.** Sequence analysis of truncated fragments from liver DNA.
- Figure 37.** Viral excision in blood DNA of rats treated with rAAV9SaCa9 gRNAs
- Figure 38.** Sequence analysis of the 221 bp truncation fragment
- Figure 39.** Percent of viral RNA decrease in the blood of treated Tg26 rats
- Figure 40.** HIV-1 genome map
- Figure 41.** Viral excision in spleen, GALT, and kidney of humanized mice HIV-1 infected
- Figure 42.** Viral excision in lung, liver and brain of humanized mice HIV-1 infected
- Figure 43.** Analysis of truncated/end joined viral DNA sequence
- Figure 44.** Quality control on spleen, GALT, kidney DNA of humanized mice HIV-1 infected
- Figure 45.** Detection of human beta globin in spleen tissue of humanized mice HIV-1 infected

- Figure 46.** Cas9 and gRNAs expression in spleen tissue of humanized mice HIV-1 infected
- Figure 47.** Decreased pol and env copies on DNA spleen tissue of humanized mice HIV-1 infected
- Figure 48.** Illustration of the LTR HIV-1 Promoter
- Figure 49.** pCR2.1 Vector Map and Sequence
- Figure 50.** Vector Map of pX260-U6-DR-BB-DR-Cbh-NLS-hSpCas9-NLS-H1-shorttracr-PGK-puro Plasmid
- Figure 51.** LentiCas9-Blast Plasmid Vector Map
- Figure 52.** Position of the T795 and T796 Primers used to amplify the gRNA sequence for the Cloning of multi-gRNAs in one px601 Vector
- Figure 53.** Schematic Representation of the Tg26 Mouse Strain Transgene containing HIV-1 DNA
- Figure 54.** Schematic Representation of Mouse Humanization, Viral Infection, ART Initiation and CRISPR/Cas9 Treatment
- .

LIST OF TABLES

- Table 1.** 2016 Regional HIV and AIDS Statistics
- Table 2.** CRISPR/Cas9 Studies Related to HIV-1 Treatment
- Table 3.** Transduction Conditions for TZM-bl Cells with Adenoviral Vectors
- Table 4.** Transduction Conditions for TZM-bl Cells with Lentiviral Vectors
- Table 5.** Electroporation Conditions for the Jurkat 2D10 Stable Cell Line with Lentiviral Vectors Expressing gRNAs and a Tat Plasmid
- Table 6.** Primers sequence for PCR and qPCR assays
- Table 7.** PCR conditions for the LTR Promoter Amplification
- Table 8.** Ligation Condition for LTR Cloning into the TA Vector
- Table 9.** Digestion Conditions for LTR Cloning into pX260-U6-DR-BB-DR-Cbh-NLS-hSpCas9-NLS-H1-shorttracr-PGK-puro
- Table 10.** De-phosphorylation Conditions of px601-AAV-CMV:NLS-saCas9-NLS-3xHA-bGHpA;U6:Bsa1-SgRNA after Bsa1 digestion
- Table 11.** Phosphorylation of Annealed Oligonucleotides Mixture
- Table 12.** Ligation Condition for Phosphorylated Oligonucleotides with the px601 Vector
- Table 13.** Infusion Treatment Conditions to create the px601 LTR1 GagD Construct
- Table 14.** Lentiviral Vector Packaging Conditions
- Table 15.** qPCR Conditions to Detect Viral DNA in Jurkat 2D10 cells

1. Introduction

1.1 Human Immunodeficiency Virus

Retroviruses are spherical viruses of 80-120 nm in diameter [1] sharing similar structure, genomic organization and replicative strategy. The *retroviridae* family is composed of two virus subfamilies, *Orthoretrovirinae* and *Spumaretrovirinae*. The *Spumaretrovirinae* subfamily only includes Spumaviruses, and the *Orthoretrovirinae* subfamily includes six viral genera, *Alpharetrovirus*, *Betaretrovirus*, *Deltaretrovirus*, *Epsilonretrovirus*, *Gammaretrovirus* and *Lentivirus*. *Lentiviruses* are characterized by persistent infection in humans and animals. *Lentiviruses* include human immunodeficiency viruses 1 and 2, HIV-1 and HIV-2.

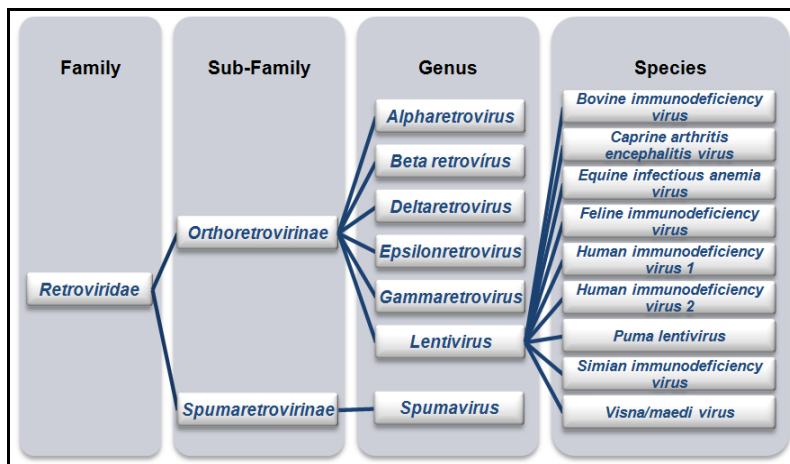


Figure 1: Illustration of the *Retroviridae* family (Reproduced under open access) [2].

1.1.1 Epidemiology

The HIV-1 epidemic initiated with zoonotic transmission from primates of Africa infected with Simian Immunodeficiency Viruses (SIV) throughout the 1900s. There are two recognized types of HIV, HIV type 1 and HIV type 2, which have different original transmission origins. Chimpanzees and

mangabey monkey are hypothesized to have transmitted HIV-1 and HIV-2 to humans, respectively [3]. HIV-2 is restricted to Western Africa and causes a disease like HIV-1, but is less transmissible and has decreased virulence [4]. HIV-1 originated from four different transmission to human, three from chimpanzee and one from gorillas. The groups N and P derive from chimpanzee and gorillas respectively and are diffused throughout Western Africa. The main group (M) derives from chimpanzees and is the source of the worldwide HIV pandemic. The M group includes nine viral subtypes: A-D, F-H, J and K. The most widespread subtypes are C, which is responsible of 48 % of infection in Africa and India [5], and B, which is diffused throughout Western Europe, America and Australia. Different HIV subtypes have different rates of transmission and disease progression.

In 1980 a new disease, acquired immunodeficiency syndrome (AIDS), was recognized by studying cases of young homosexual men in the United States affected with *Pneumocystis carinii* pneumonia (PCP) and Kaposi's sarcoma (KS) [6]. After two years, HIV-1 was recognized as the causative agent of AIDS. Since then 76.1 (65.2 - 41.5) million people in the world became infected with HIV-1 and today roughly 36.5 (30.8 – 42.9) million people live with HIV infection, including 2.1 million children under the age of 15 [7]. HIV-1 infection in 2010 was the main cause of morbidity in the world for people aged 30-44 years [8] with the highest incidence in sub-Saharan Africa. HIV prevalence is higher in people with risk behaviors such as homosexual men and drug users [9]. One million (830.000 - 1.200.000) AIDS related deaths were reported in 2016, while 35.0 million (28.9 – 41.5) AIDS related deaths have been reported since the start of the HIV-1 epidemic. The number of AIDS related deaths decreased by 48 % after peaking in 2005 when there were 1.9 million AIDS related deaths. Tuberculosis is the main source of death among HIV-1 infected patients (350.000 deaths in 2015) with 1.2 million of people living with HIV also

having tuberculosis. The global prevalence of HIV-1 after the introduction of antiretroviral therapy (ART) decreased by 11% among adult and by 47% among children from 2010 to 2016. [7]. In 2014, the Joint United Nations Program on HIV and AIDS (UNAIDS) set up the program “90-90-90 targets”. The goal of this program is to reach these three important results by 2020 [10]:

- 1) Diagnose HIV-1 infection in 90% of people living with HIV-1
- 2) Start ART treatment in 90% of diagnosed people
- 3) Reach fully suppressed viral load in 90% of ART patients

So far, it is hypothesized that 70% of all HIV-1 positive people are diagnosed, with 53% of patients undergoing ART and around 44% demonstrating viral suppression. Large disparities exist for these statistics between different countries [7].

	People living with HIV (all ages) - by region	AIDS-related deaths (all ages) - by region
REGION		
Asia and the Pacific	5.1 million	170000
Caribbean	311000	9400
East and Southern Africa	19.4	420000
Eastern Europe and Central Asia	1.6	40000
Latin America	1.8	36000
Middle East and North Africa	231000	11000
West and Central Africa	6.1	310000
Western & Central Europe and North America	2.1	18000

Table 1: 2016 Regional HIV and AIDS Statistics. Data from UNAIDS showing the number of patients with HIV and number of AIDS-related deaths in different regions of the world in 2016. (Table created using the official data from UNAIDS, special analysis, 2017) [7].

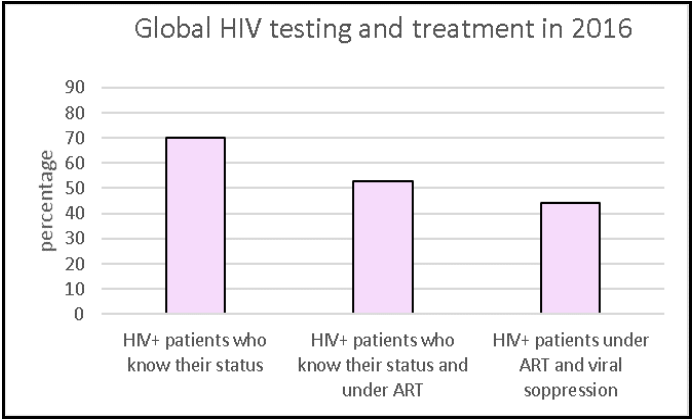


Figure 2: 2016 Global HIV patients testing and treatment. Percentage of HIV-1-positive patients aware of their status, patients undergoing ART therapy, and patients with viral suppression in the world during 2016. (Figure created using the official data from UNAIDS, special analysis, 2017) [7]

1.1.2 HIV Transmission and Pathogenesis

HIV-1 sexual transmission risk increases in the initial months of HIV-1 infection, which is characterized by high viral plasma load, and is also influenced by other factors including seminal and cervical viral load [11]. Genital ulcers, herpes simplex type 2 infection, bacterial vaginosis, pregnancy, anal intercourse and injection drug use are factors increasing HIV-1 transmission risk [12]. The HIV-1 mother to child transmission risk is about 15-25% during pregnancy, increasing to 35-40% during breastfeeding [13]. Initiation of ART therapy reduces the probability of transmission to the infant by reducing maternal viral load. CD4+ T cells in mucosal tissues are the first targets of HIV-1 during the early stages of infection, followed by viral spread throughout the lymphoid system, a stage called the eclipse phase. HIV-1 RNA levels are detectable after several

days of infection and reach 10^6 - 10^7 copies/ml after a month. This stage of primary or acute infection can be asymptomatic or characterized by fever, lymphadenopathy, rash, malaise or myalgias and more rarely by meningitis. Rash is present in 40-80% of cases and is typically maculopapular and involves the trunk [14]. After progressive depletion of infected CD4+ T cells, the immune system establishes partial control of the virus. However, the antibody response is unsuccessful against HIV-1 variants, resulting in viral escape. After 4-6 months, the plasma viral load decreases by about 100-fold, reaching a viral set point ranging from few copies of virus/ml to 10^6 copies/ml due the action of CD8+ cytotoxic T lymphocytes (CTLs). The viral plasma load directly influences disease outcome and progression towards AIDS [15]. This phase is generally asymptomatic and can exist for up to 15 years, resulting in the constant destruction of CD4+ cells and the presence of chronic inflammation (chronic phase) and inactivation of CTLs. In the final stage of infection, AIDS phase, the level of CD4+ T cells per μ l of blood reaches < 100 cells/ μ l [9]. This phase is characterized by weight loss, fever, cough, increased risk of myocardial infarctions, liver disease in presence of coinfection of hepatitis B and C, HIV-1-related tuberculosis mortality and the development of opportunistic illnesses such as Candida in the esophagus, trachea, bronchi and lungs, invasive cervical cancer, cytomegalovirus disease, HIV-related encephalopathy, Kaposi's sarcoma, Burkitt lymphoma, immunoblastic or primary brain lymphoma, toxoplasmosis of the brain, Salmonella septicemia and Herpes Simplex Virus infection involving skin or lungs problems [16], [17], [18], [19].

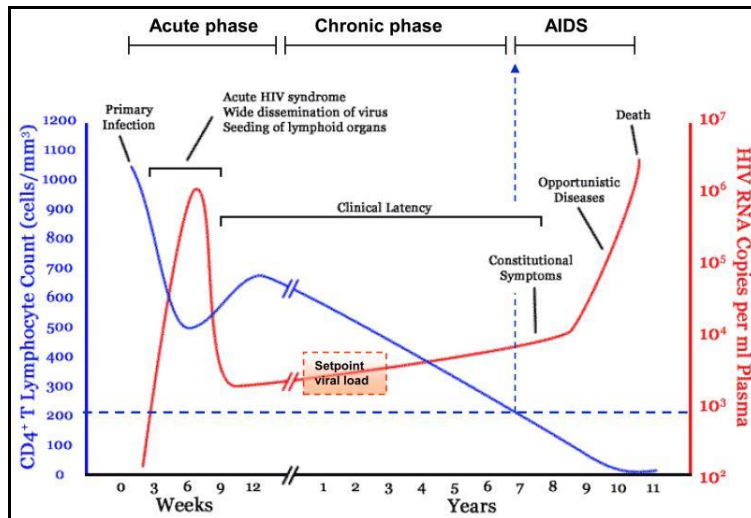


Figure 3: HIV-1 Infection Phases. Acute phase (6-12 weeks) is characterized by flu-like symptoms, a peak in viral load and acute loss of CD4+T cells. Chronic phase can last between 7 to 10 years and is characterized by clinical latency. Symptoms appear during the AIDS phase where a high viral load and the decline of the CD4 T cells results in the development of opportunistic diseases and death. (Figure reproduced with permission from An P. *et al.*, 2010 and Elsevier) [20]

1.1.3 HIV-1 Diagnosis

After HIV-1 exposure, HIV antibody presence may be absent for weeks or months during the so-called window period [21]. Nucleic acid tests are recommended in presence of high risk of acute infection. [9]. HIV RNA assays are characterized by 100% sensitivity and 97.4% specificity [22]. The US Centers for Disease Control and Prevention suggests an antigen antibody assay for the rapid detection of the virus during acute infection. Rapid HIV testing using blood from a finger stick or collection of oral fluid give results within 30 minutes.

1.1.4 HIV Genome

The genome of HIV-1 is characterized by two linked copies of single stranded RNA, less than 10 kb in length, containing coding and non-coding regions involved in the production of regulatory and accessory proteins and in the regulation of viral expression respectively. The long terminal repeats (LTRs) at the ends of the provirus are characterized by two untranslated regions (U3 and U5) and a repeat element (R). LTRs are constituted by an enhancer/promoter sequence, ATT repeats involved in provirus integration, a primer binding site (PBS), a packaging signal ψ and a polyadenylation signal (polyA). The ψ -site is between the 5'LTR and the gag initiation codon and contains four stem loops (SL1-SL4) important for encapsidation. The enhancer sequence binds the transcription factor kappa-light-chain-enhancer of activated B cells (NF- κ B) and Nuclear factor of activated T-cells (NFAT) [23]. The HIV-1 promoter includes 3 important elements, stimulatory protein 1 (SP1) binding sites [24], a TATA element (TATAAA) [25], and an active initiator sequence [26], that allows the interaction between transcription factor TFIID and TATA binding protein associated factor (TAF) with the TATA element [27].

HIV-1 contains three main structural genes, gag which codes for matrix, capsid, nucleocapsid and p6 proteins, pol encoding for the protease, reverse transcriptase (RT) and integrase and env encoding the envelope proteins gp41 and gp120. Other proteins include Vif, Vpu/Vpx, Vpr and the negative regulatory factor (Nef) [28]

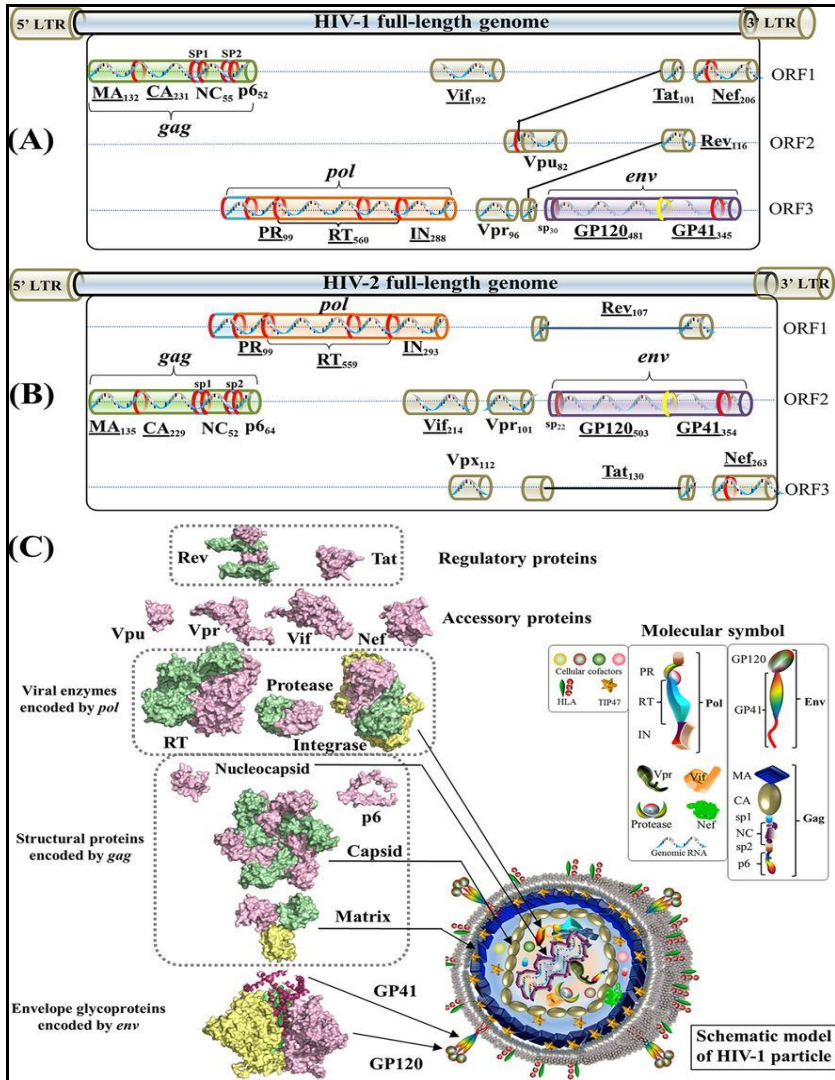


Figure 4: HIV Genome Map and Structural Biology. Representation of the HIV-1 (panel A) and HIV-2 (panel B) full length genomes. Structural representations and a schematic of the HIV-1 viral particle show localization and protein-protein interactions of each viral protein. (Figure reproduced with permission from Li G. *et al.*, 2016 and the American Society of Microbiology) [28]

1.1.5 HIV Structural Biology

The HIV envelope proteins gp41 and gp120 possess spikes decorated with carbohydrates and bind host receptors allowing viral penetration into host cells. The cleavage of the structural Gag polyprotein during the viral maturation results in the production of proteins within the matrix (MA), of the capsid (CA), of the nucleocapsid (NC) and p1, p2 and p6 proteins [28].

The matrix protein (p17) is characterized by five α -helices, a 310 helix and a three-stranded mixed β -sheet. The carboxy-terminal α -helix connects the MA domain with the adjacent CA domain. MA proteins assemble into trimers that interact with the acid inner membrane of the virus, creating a coat of the viral membrane. An important function of these proteins is the transport of P55^{GAG} protein to the cellular membrane, allowing the assembly of gp120 and gp41 into the viral particles [29].

The capsid protein forms stable hexamers which form a cone-shaped coat around the viral RNA. The HIV-1 capsid binds to the cellular proline isomerase cyclophilin A in the viral particle.

The NC protein contains two zinc-finger-like domains and interacts with the viral genome. This protein is involved in the recognition and packaging of reverse transcriptase, the primer tRNA_{Lys}³ and the viral genome, interacting with almost 120 nucleotides of the unspliced RNA ψ -site [30], [31]. After a protease processes the Gag precursor, NC creates a ribonucleoprotein complex and allows the tRNA_{Lys}³ primer to anneal to the viral RNA initiating reverse transcription. Likewise, NC facilitates the elongation of viral DNA and is involved in viral particle formation. Mutations in conserved regions of the NC gene can alter RNA packaging specificity [32], [33].

HIV-1 protease is a homodimer containing an active site at the interface of the two subunits, formed by a catalytic triad (Asp25- Thr26-Gly27)

responsible for cleavage. Mutations of this protein can alter cleavage efficiency resulting in the production of dysfunctional cores [34].

HIV-1 reverse transcriptase is the protein involved in the retro-transcription of viral RNA into DNA. This protein is introduced in the viral particles as part of Gag Pol precursor and later processed as a mature p66-p51 RT heterodimer containing polymerase and an RNase H domain. The first domain can copy either DNA or RNA templates, while the RNase H domain cleaves RNA of RNA/DNA duplexes. For the synthesis of viral DNA, RT requires a host tRNA_{lys3} primer containing an 18-nucleotide sequence at the 3' end, complementary to the primer binding sequence at 5' end of the viral genome. RT synthesizes the negative RNA strand using the positive strand as a template, creating a RNA/DNA hybrid. The minus strand DNA hybridizes with the 3' end of one of the two viral RNAs present in the viral particle, first jump, allowing the rest of synthesis of the minus strand DNA followed by the degradation of the RNA strand. The polypurine tract at the 3' extremity of the RNA is not damaged by the RNase H activity and is used like a primer for positive DNA strand synthesis. After initial synthesis RT copies the first 18 nucleotides of the tRNA and RNase H remove one nucleotide from the tRNA/DNA junction, leaving a ribo-A on the 3' end of the viral negative strand DNA. The elimination of the tRNA allows the exposure of a single strand portion of the positive DNA strand, which contains a complementary sequence to the PBS site. After the synthesis of this region on the negative DNA strand, the 5' end is transferred to the positive strand (second jump) allowing the extension of both strands. The produced DNA has the same sequences at both ends and is longer than the initial RNA. The viral DNA, after integration, serves as stamp for viral replication using host enzyme DNA-dependent RNA polymerase [35].

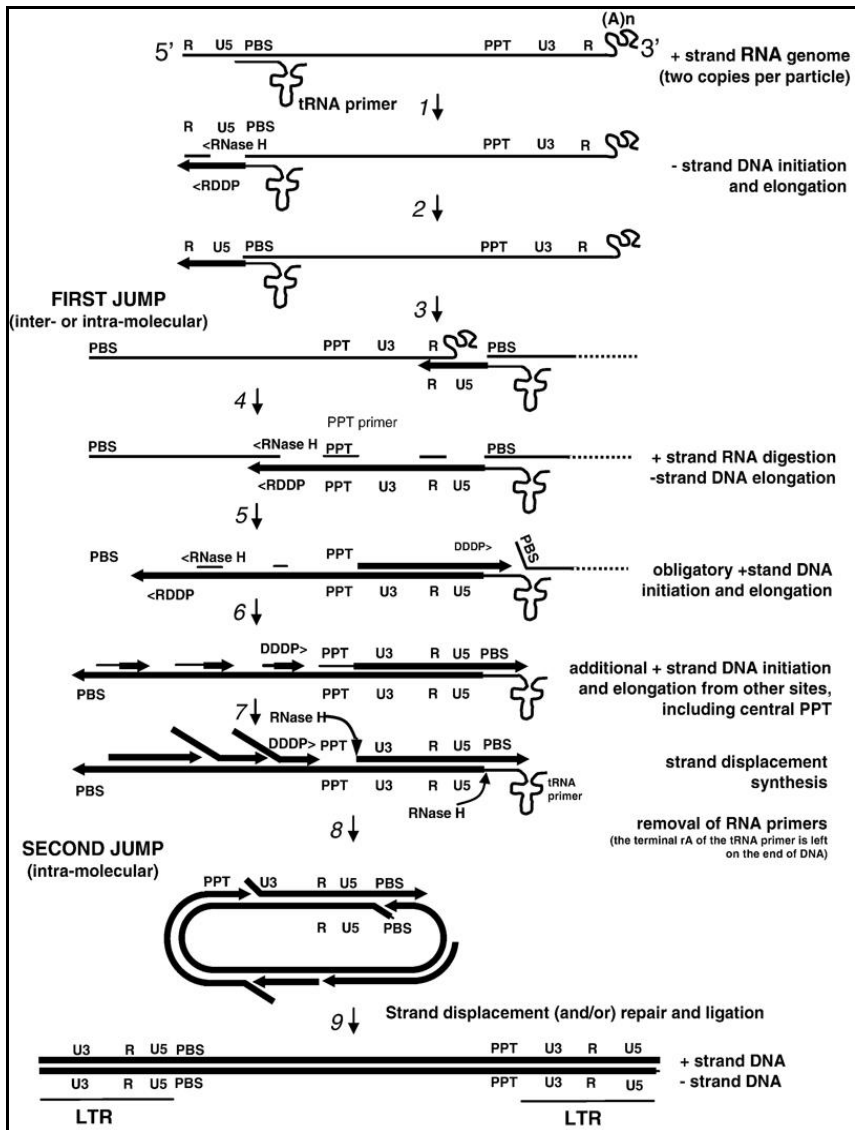


Figure 5: Reverse Transcription of HIV-1 RNA. Model of HIV-1 reverse transcription into positive and negative strands of viral DNA. (Figure reproduced by permission from Sarafinos SG. *et al.*, 2009 and Elsevier) [35]

HIV-1 integrase (IN) is a viral enzyme consisting of 3 functional domains, a N-terminal zinc binding domain, a C-terminal DNA-binding domain and a central catalytic domain. IN is part of the pre-integration complex (PIC) and

recognizes the 3' LTRs of the viral DNA complex, cutting two or three nucleotides at the 3' end. The enzyme ligates the 3'-hydroxyl group of the end of the 3' viral DNA to a pair of phosphodiester bonds in the host DNA.

Cellular enzymes remove the two unpaired nucleotides at the 5' end of the viral DNA and the DNA polymerase extends the unligated 3' end of the human DNA, resulting in the incorporation of proviral DNA into the cellular genome. Analysis of the integration sites used by HIV-1 in the cellular genome revealed a low degree of specificity [36].

Nef is a 27 kDa accessory protein abundantly produced during the early phase of viral expression (37). A majority of Nef proteins are incorporated into the virions and are cleaved by the viral protease resulting in association with the viral core (38). Nef is involved in the downregulation of the CD4 receptor by linking the tail of CD4 to the clathrin adapter protein complex 2 (AP-2), resulting in the internalization and degradation of the receptor, preventing reinfection by new viral particles [39]. Nef is also involved in the downregulation of major histocompatibility complex class I (MHC-I), mature MHC-II, CD28, CCR5 and CXCR4 receptors on the surface of infected CD4⁺ T-lymphocytes [40], [41]. The regulation of MHC-I involves clathrin adapter protein complex 1 (AP-1) or sarcoma (SRC) family kinase-ZAP70/Syk-PI3K cascade recruited by phosphofurin acidic cluster sorting protein 1 (PACS2). The decrease of MHC-I expression from CD4⁺ cells and the consequent upregulation of Fas ligand (FasL) molecules results in the apoptosis of infected CD8⁺ T cells. Nef down-regulates host antiviral proteins serine incorporator 3 and 5 (SERINC3 and SERINC5), which decreases the incorporation of env proteins into the virions, allowing the spread of infection. NF also alters several functions of dendritic cells, monocytes/macrophages and NK cells [42], [43].

Rev is a 116 amino acids protein composed of two domains, an amino-terminal domain, harboring the nuclear localization signal (NLS), and a RNA-binding domain, carrying the nuclear export signal (NES) [44]. The major role of Rev is the regulation of HIV-1 protein expression and the export rate of mRNA. HIV-1 gene expression can be classified into early stage (Rev-independent) for the expression of the regulatory proteins Tat, Rev and Nef and late stage (Rev-dependent) for the expression of the remaining proteins [45], [46]. HIV-1 mRNA is subjected to three different splicings, the ~9 kb unspliced mRNA (genomic and gag and pol mRNA), the ~4 kb single spliced (encoding a truncated 72 amino acids form of Tat, Env, Vpu, Vif and Vpr) and the ~1.8 kb doubly spliced (early transcripts that encoding Tat, Rev and Nef). Doubly spliced mRNAs are small and immediately exported to the cytoplasm and translated into proteins. The other transcripts require the action of Rev for cytoplasmic transport as Rev recognizes and interacts with the Rev responsive element (RRE), present in unspliced and single spliced transcripts. The Rev NLS sequence binds directly to KPNB1/Importin beta-1 complex, and KPNB1 binds Ran-GDP form, allowing the transport of Rev into the nucleus, where Ran GDP is converted in Ran-GTP and Rev dissociated from KPNB1 and associates with the region RRE of the immature transcripts. This binding exposes the NES site of Rev allowing the binding of this protein with exportin XPO1/CRM1 complex and Ran-GTP and the nuclear export of the complex. Rev can regulate expression of viral proteins like Tat, keeping a correct equilibrium between early and late viral gene expression. Without Rev the transcripts are not translated into viral proteins [47].

Viral protein U (Vpu) is a 16 kDa protein translated from vpu-env bicistronic mRNA. The N terminal domain is characterized by a transmembrane (TM) domain involved in the regulation of viral release. The phosphorylation of serine residues within the C-terminal cytoplasmic domain is critical for CD4

degradation in the endoplasmic reticulum [48]. Vpu induces ubiquitination and the proteosomal degradation of BST2, an interferon (IFN)-inducible cell surface protein that interferes with the release of the viral particles in absence of Vpu [49].

Vif is a 23 kDa protein essential for viral replication. Vif inhibits the antiviral activity of the cellular apolipoproteins B mRNA editing enzyme catalytic subunits 3F and 3G (APOBEC3F and APOBEC3G) via proteosomal degradation and inhibition of the mRNA translation respectively, preventing the incorporation of these enzymes into new virions. In the absence of Vif, these proteins cause hypermutation of the viral genome influencing the stability of the viral nucleoprotein core and contributing to the G2 cell cycle arrest in HIV infected cells [50].

Vpr (viral protein r) is a 14 kDa protein involved in the transport of the PIC complex to the nucleus. It can associate with DNA damage-binding protein 1 (DDB1) as part of E3 ubiquitin ligase complex targeting specific host proteins for proteosomal degradation. The association of Vpr with the cellular CUL4A-DDB1 E3 ligase complex may result in cell cycle arrest or apoptosis of the infected cells [51]. Vpr carried into the virions can arrest cell cycle in G2 phase within hours of infection, increasing viral expression and can induce apoptosis by interacting with mitochondrial permeability transition pore complex (PTPC). This interaction results in a loss of the mitochondrial transmembrane potential and in a mitochondrial release of apoptogenic proteins such as cytochrome C or apoptosis inducing factors. Vpr can regulate the tumor suppressor p53-induced transcription [52].

1.1.6 Regulatory Tat protein

Tat is a 14-kDa regulatory protein important for the expression of HIV-1 genes. In presence of Tat, the activity of RNA polymerase is stabilized

allowing increased elongation of the viral transcripts [53]. The binding of Tat to a transactivation response region (TAR) at 3' region of the initiation site of transcription of the mRNA originates a stem loop complex, nuclease resistant, and a conformation change of the RNA structure [54]. Mutations present in the TAR RNA loop, but not specifically to the region recognized by Tat, interfere with transactivation [55], which suggests the presence of a cellular cofactor involved in the mechanism of regulation of gene expression [56]. Herrmann *et al.* described the presence of a protein kinase complex binding Tat, Tat-associated kinase (TAK) [57], [58]. Tat and TAR RNA interact with the two components, CDK9 and cyclin CycT1, of the positive transcription elongation factor pTEFb, a cofactor of HIV-1 elongation. The interaction between Tat and CycT1 yield conformational changes, resulting in CDK9 activation [59]. P-TEFb activated by Tat regulates elongation via phosphorylation of different elongation factors. In absence of Tat, the negative elongation factor (NELF) blocks the transcription via interaction of its subunit E with TAR region [60]. After activation by Tat, p-TEFb phosphorylates NELF-E, which dissociates from TAR and this release stops transcription elongation complexes. In absence of Tat, inactive p-TEFb molecules are sequestered by a 7SK RNP complex formed by 7SK RNA and RNA-binding proteins. During the elongation process the Tat/PTEFb complex phosphorylates RNAPII CTD and a subunit of the DRB sensitivity inducing factor (DSIF), [47] increasing elongation efficiency. Interaction of human transcription factors FF4, ENL, AF9, ELL2 with the Tat P-TEFb complex increases the elongation process [61]. Tat mediates the nuclear translocation of NF-kappa-B via oxidative stress-induced cell signaling pathway like the PI3K/Akt signaling pathway to increase the transcriptional elongation [62]. In absence of Tat, RNA Pol II generates non-processive transcripts that terminate at approximately 60 bases from the initiation site. Circulating Tat acts like a chemokine or

growth factor-like molecule and interferes with many cellular pathways. The recruitment of histone acetyltransferases (HATs) Cyclic-AMP response element binding protein B (CREBBP), E1A binding protein p300(EP300) and acetyl-CoA acetyltransferase (PCAF) by Tat to the chromatin increases proviral transcription especially in latently infected cells transactivating LTR promoter [63]. Tat can be endocytosed by surrounding uninfected cells, like neurons, leading to apoptosis and the progression of HIV-Associated Neurocognitive Disorders (HAND) [64].

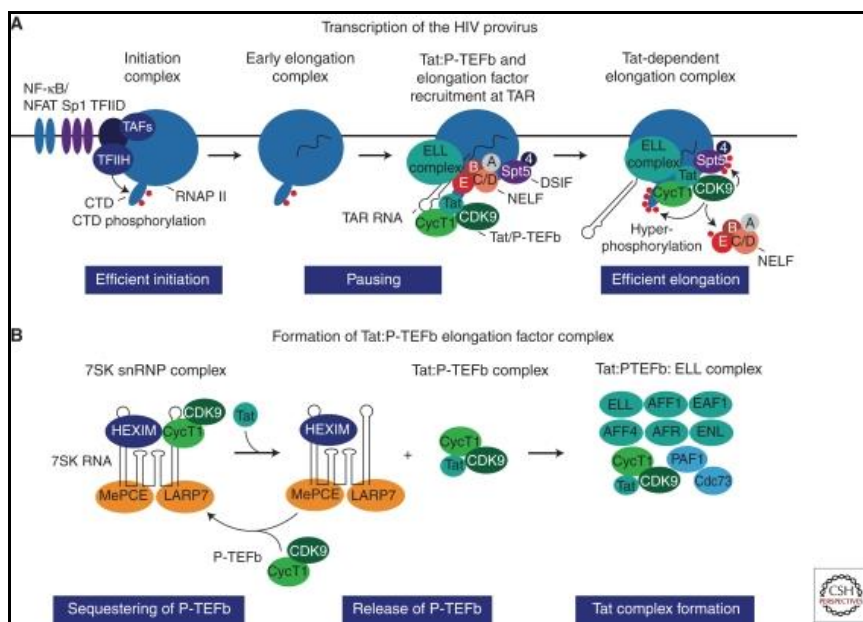


Figure 6: Interaction of Tat with NF- κ B and P-TEFb. NF- κ B promotes the initiation of viral transcription, then the Tat/P-TEFb complex interacts with the TAR region to create the elongation factor complex and the phosphorylation of RNAP and efficient elongation. (Figure reproduced with permission from Karn J. *et al.*, 2012 and Cold Spring Harbor Perspective in Medicine) [47].

1.1.7 HIV-1 replication cycle

The HIV-1 replication cycle is divided into early and late phases. The first period is characterized by the binding of HIV with the host cellular

receptors to viral integration into the human DNA. The second stage encompasses the events from the protein translation to the release of the mature virions. Initially, viral particles bind to various cell surface binding effectors, such as heparin, sulfate proteoglycane, integrin subunit beta 2 (ITGB2) and nucleolin. This binding facilitates HIV-1 interactions with viral receptor on the cells [65]. HIV entry into cells involves viral binding to CD4, a receptor expressed on the surface of T lymphocytes (activated T lymphocytes represent the main target of HIV-1), monocytes, macrophages and dendritic cells [9] and interactions with co-receptors, CCR5 or CXCR4, which are both chemokine receptors. HIV-1 variants use either CCR5 or CXCR4 and are denoted R5 and X4, likewise some variants use both, denoted R5X4. CCR5 is expressed in memory T lymphocytes, macrophages and dendritic cells, and is not expressed in naïve T lymphocytes. HIV-1 infection of dendritic cells relies on the capture of the virus, resulting in the spread of T lymphocyte infection [66]. Infected follicular dendritic cells retain HIV-1 within B cell follicles of lymph nodes [9]. For viral entry, the envelope glycoprotein gp120, which form gp41/gp120 trimers, binds to CD4 [67]. Viral binding induced conformational changes in CD4 and gp120, and additional conformational changes occur after the recognition of gp120 by one of the HIV-1 coreceptors, inducing to the dissociation of gp120 from gp41, and the insertion of gp41 into the cellular membrane. This event results in the release of the viral core, from viral particles into the target cells after the fusion of viral and cellular membranes into the cytoplasm [65]. In the cytoplasm, the viral particle is uncoated and RT converts viral RNA into linear viral DNA double stranded molecules. Viral DNA associates with viral proteins forming PIC complexes of 56 nm diameter composed of PR, RT, IN, Vpr, CA, NC and MA proteins [68], [69]. PIC complexes are then transported through small channels of the nuclear pore (25 nm of

diameter), a process facilitated by mediators. HIV-1 Nef and Vif protein, associated with the viral core, and the cellular protein cyclophilin A, modulate early events of HIV-1 replication [65]. An early production of viral proteins was described even before viral integration [70], [71], [72], [73], [74]. Viral replication and viral transcripts production depend on integration of HIV-1 DNA into the host DNA resulting in a productive infection [65]. Different RNAs include unspliced full-length transcripts, singly spliced mRNAs and fully spliced mRNAs. During the late phase of HIV-1, transcripts are translated in the cytoplasm, producing both Gag precursor (55kDa) protein and GagPol (160 kDa) polyprotein precursor (resulting from a ribosomal frameshift events). Gag precursor protein contains MA, CA, NC and p66 domains and two spacer peptides SP1 and SP2, while the GagPol polyprotein precursor contains the viral protease, reverse transcriptase and integrase. The MA domain interacts with phosphoinositide phosphatidylinositol-4,5-bisphosphate, a protein in the plasma membrane, to drive the Gag domain into the inner leaflet of the plasma membrane and to stimulate the incorporation of the Env protein into viral particles [75]. The CA induces the multimerization of Gag protein during its assembly. NC is critical for the packaging of the viral genome into virions. The p6 protein regulates the budding of nascent virions from the cell membrane, through a PTAP motif by recruiting Tsg101 and ALIX, components of the endosomal sorting complex required for transport (ESCRT) apparatus. P6 mediates the incorporation of Vpr protein into budding virions. In the cytoplasm, two copies of viral genome are packaged into HIV-1 virion core [76]. RNA dimerization occurs in the presence of a dimer initiation signal (DIS), present within the 5' UTR sequence. Different conformational changes of the 5' end of the viral genome may favor translation or promote packaging [77]. In the plasma membrane the Gag protein, full-length RNA and the GagPol precursor assemble into immature

viral particle. After the multimerization of Gag molecules, nascent virions are released from the membrane of infected cells, budding process, which is mediated by the endosomal sorting complexes required for transport (*ESCRT*) machinery. Simultaneously with viral budding, Gag precursor and Gag Pol polyproteins are cleaved by the viral protease allowing the maturation of the virions and the formation of infective particles.

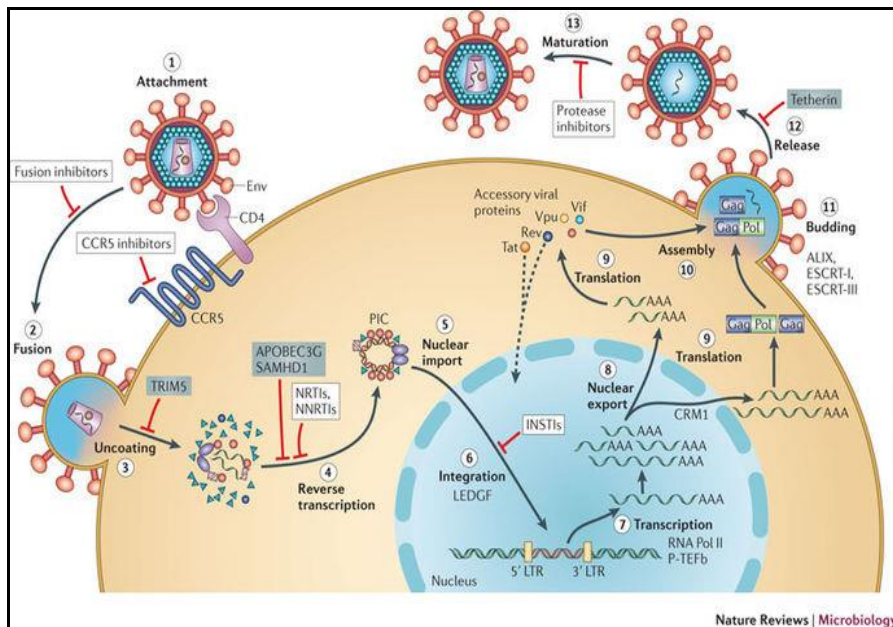


Figure 7: HIV-1 Life Cycle. After the interaction between Env, CD4 and the co-receptors during the fusion of the virus with the cell membrane, the virus enters into the cells, where is subjected to uncoated process, reverse transcription, PIC complex formation, transcription and protein translation with final assembly, budding and release of the new viral particles. (Figure reproduced with permission from Engelman A. *et al.*, 2012 and Nature Publishing group) [78]

1.1.8 Latency

Viral latency can be classified into pre-integration and post-integration latency [79], [80]. Pre-integration latency results from incomplete reverse

transcription, decreased entry of the PIC into the nucleus or incomplete integration [81], [82]. Pre-integration latency is not involved in the formation of long-term latent reservoirs [83]. Post-integration latency results from transcriptional silencing, a condition that is influenced by the cellular environment at the site of the integration; sequestration of host transcription factors like NF-kappaB or NFAT in the cytoplasm, presence of repressors of transcription like COUPTF Interacting Protein 2 (CTIP2), Negative Elongation Factor (NELF), DRB-Sensitivity Inducing Factor (DSIF), T cell factor 4 (TCF-4) associated with beta-catenin molecule and the family of tripartite motif-containing (*TRIM*) proteins, the presence of nucleosome (nuc-0 and nuc-1) on the LTR promoter, epigenetic silencing of HIV transcription, the sequestration of P-TEFb and the concentration of Tat [84], [85]. Histone deacetylation contributes to transcriptional suppression, an inhibitor of the histone deacetylase HDAC6 decreases HIV latency by increasing the acetylation of histones H3 and H4 in the nuc-1 region of the HIV LTR [86]. Histone modification is important for HIV-1 transcription, with histone acetylation resulting in transcriptional activation, histone methylation of H3K9, H3K27 and H4K20, is associated with transcriptional activation while the methylation of lysine residue 4 H3K4, is associated with activation [87]. During latency, the transcription start site of the LTR promoter is hyper-methylated at two CpG islands [88]. A defective transport of transcripts in the cytoplasm can be correlated with insufficient levels of Tat and Rev proteins [89]. Post-transcriptional modification of Tat residues influences HIV-1 regulation, with lysine 28 acetylation inducing a strong affinity for binding to P-TEFb [90], [91], while lys50/51 acetylation dissociates Tat from TAR. HIV-1 produces viral interference RNAs (viRNAs) that can target viral mRNAs (inducing virus latency), cellular mRNAs, like CD28, and cellular miRNAs. During HIV-1 infection, Tat and Vpr modulate cellular miRNA expression levels in infected cells [92].

In ART patients, there exists a low level of viremia derived from low viral replication in anatomic sanctuaries inaccessible to the drugs or from viral reactivation in resting T cells. Viral reservoirs develop when the transcriptionally silent virus persists in some cells or tissues without active replication. The main reservoirs are resting central memory T cells (TCM), CD45RA⁻ CCR7⁺ CD27⁺, (half-life of ~44 months) and translational memory T cells (TTM), CD45RA⁻ CCR7⁻CD27⁺ [93] [94]. Infected TCM cells can originate from infected active T cells that live enough long to differentiate to TEM [95], or they can be directly infected or infected prior to differentiate in resting T cells. Another source of reservoirs came from monocytes and macrophages, naïve T cells and hematopoietic progenitor cells (HPC) [96]. Reservoir in the central nervous system (CNS) and the gut associated lymphoid tissues (GALT) possesses viral RNA at 5-10 times higher levels than found in peripheral blood mononuclear cells [97]. In the brain, is possible find infected macrophages after differentiation of monocytes that cross the blood brain barrier. Also proviral DNA is present in astrocytes and is associated to dementia [98]. The integration of HIV-1 in the host is preferentially into introns of active cellular genes. In actively infected cells the sense orientation to actively genes comparing to the position of viral integrated DNA, may have a repressive role in viral transcription comparing than antisense orientation. Substances like phorbol, prostatin or methamphetamine, inhibitor of Wnt, histone deacetylase inhibitors (HDACI, valproic acid or SAHA) and IL-7 can activate HIV-1 expression [99].

1.2 HIV-1 treatment

1.2.1 Antiretroviral Therapy

Antiretroviral therapy was developed in the late 1990s and changed the outcome of the HIV-1 epidemic. Highly active anti-retroviral therapy (HAART) became available in 1995. US and European regulatory agencies recommend 25 unique antiretroviral drugs specific against different steps of the HIV-1 life cycle. Antiretroviral therapy decreases the level of the viral load below the limit of detection within the initiation of the treatments [3]. Only a small percentage of HIV-infected patients in the world have access to HAART. Patients showing a decreased viral load and an achievement of normal CD4+ count have an expectancy of life close to normal life [100], but interruption of ART leads to viral rebound, active replication and progression towards AIDS. During HAART there is the potential for the emergence of HIV-1 variants which are resistant to anti-retroviral drugs [3]. Different classes of drugs used in ART therapy include nucleoside reverse transcriptase inhibitors (NRTIs), non-nucleoside reverse transcriptase inhibitors (NNRTIs), integrase strand transfer inhibitors, protease inhibitors and entry inhibitors. NRTIs are analogues of natural nucleosides and nucleotides blocking HIV-1 reverse transcriptase activity, but are preferentially incorporated into HIV-1 DNA and determine the termination of HIV synthesis. Drugs recommended in this class are tenofovir, abacavir, lamivudine, emtricitabine. Integrase strand transfer inhibitors avoid viral integration and are well tolerated and safe. NNRTIs inhibit reverse transcriptase binding to a pocket near the active site of the enzyme. Protease inhibitors block the activity of the protease in the late state of HIV-1 replication, avoiding the maturation of the virus, these drugs are usually administered with two nucleoside analogues. Entry inhibitors prevent the entry of the virus into the cells, by binding to CCR5 or the virus.

HIV-1 reservoirs are resistant to the action of antiretroviral drugs, thus providing a source for viral reactivation after ART interruption (viral rebound). The use of other strategies for the control the HIV-1 viral load and of the progression towards AIDS in absence of antiretroviral therapy (functional cure) has been proposed. One such proposed mechanism is a sterilizing cure, in when the aim is to eradicate the virus from all cells in the body, either actively or latently infected. Currently, no sterilizing cure method has proven successful.

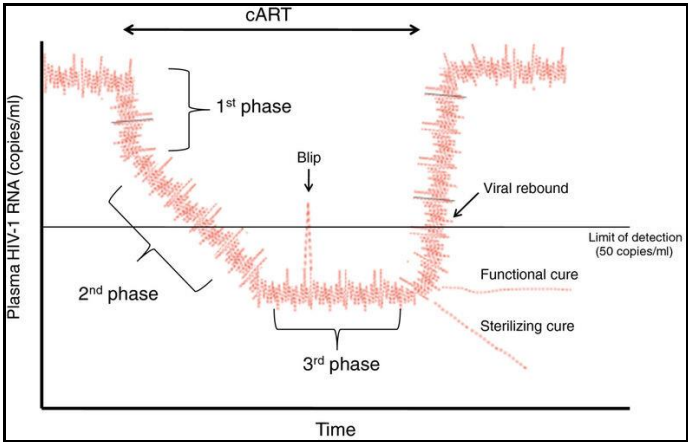


Figure 8: HIV-1 RNA copies/ml in the plasma in patients treated with antiretroviral therapy. The first phase is characterized by a rapid decline of viral load due to the short half life of the infected CD4+ T cells. The second phase is characterized by the loss of infected CD4+T cells, macrophages and dendritic cells. In the third phase a low level of viremia, under the limit of detection is maintained by HIV-1 reservoirs. Viral rebound is observed after antiretroviral therapy interruption. (Figure reproduced with permission from Van Lint C. et al., 2013 and open access Retrovirology Journal) [99]

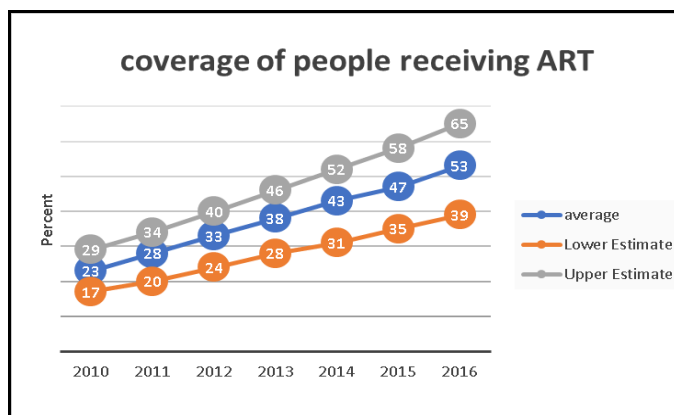


Figure 9: Global Incidence of HIV-1 infected patients under ART therapy between 2010-2015 (Figure created using the official data from UNAIDS, special analysis, 2017) [7]

1.2.2 Vaccines

The genetic diversity of the HIV-1 genome and the difficulty to develop highly immunogenic antigens decreases the probability of developing a candidate vaccine with high efficacy. Numerous neutralizing antibodies act against a conserved region of HIV envelope in 90 % of the HIV strains when administered as passive immunoprophylaxis. A previous trial used an adenovirus vector for vaccine strategy, however this strategy resulted in an increased rate of HIV infection in people with pre-existing antibodies to the adenovirus used [101]. The RV144 trial completed in Thailand in 2013 involved 16402 people with a high risk for HIV. The vaccination series used four immunizations with ALVAC Vcp1521, which express Gag/Pro and Env antigens. This treatment was followed by two booster injections with a recombinant gp120 formulated with alum and is the only clinical trial showing positive results with a 31 % reduction in HIV acquisition [103].

1.2.3 Transplantation of Hematopoietic Stem Cells

Latently infected cells constitute a viral reservoir in circulating blood, CNS, bone marrow and gut associated lymphoid tissue [103]. New strategies for

a sterilizing cure were developed after the case of the “Berlin patient”, an HIV-1 patient that received an allogenic stem cells transplant to treat acute myeloid leukemia from a donor with a mutated CCR5 gene. The donor mutation was CCR5 Δ 32 homozygous, a deletion of a 32-base pair region in the receptor gene that confers HIV-1 resistance due the production of an inactive CCR5 receptor. Homozygous patients with this mutation are completely protected by HIV-1 infection, while heterozygous patients present a slower progression of the disease [104]. After transplantation, the Berlin patient presented with an undetectable viremia level for more than 9 years without ART therapy. Later, two other HIV-1 patients with Hodgkin’s lymphoma who were heterozygotes for CCR5 Δ 32 received transplantation of hematopoietic stem cells from donors with wild type CCR5, but viral rebound was observed after 12 and 32 weeks of interruption of ART therapy [105].

1.2.4 Shock and Kill Therapy Approach

One strategy proposed to eradicate HIV-1 reservoirs is the “purging strategy” [106] or shock and kill therapy. The use of latency reversing agents (LRA) which reactivate viral transcription in latent cells to increase viral production (shock), is followed by infected cell death and recognition by the immune system (kill) in combination of ART to prevent new infection. Different LRA molecules have been used *in vitro* and *ex vivo*. Most commonly HDAC inhibitors such as valproic acid (VPA), an antiepileptic agent that acts against HDAC I and II, trichostatin A (TSA), suberoylanilide hydroxamic acid (SAHA), Panobinostat (LBH-589), Benzamides, and cyclic tetrapeptides. Other molecules including histone methyltransferase (HKMT) inhibitors, PKC agonists or NF-KB are used to promote transcription [103]. This approach has limitations; such as low

efficiency to induce latency cells, no specificity effects and toxicity [107]. Due to these limitations, other strategies are required to eradicate HIV-1, including proposed gene editing strategy.

1.2.5 Gene Therapy Strategies

Different approaches for gene editing involve either RNA based strategies, such as ribozymes, antisense RNA, small interfering RNA, or protein-based strategies, such as meganucleases, zinc finger nuclease (ZFN), transcription activator like effector nuclease (TALEN), clustered regular interspaced repeats (CRISPR system).

1.2.6 Cre recombinase

The first gene editing approach used was Cre recombinase from the P1 bacteriophage, which induces events of recombination between 2 LoxP sites [108]. Through substrate-linked protein evolution (SLiPE) it is possible to place a region of interest adjacent to the recombinase coding region [109]. This system was used to target the LTR region in latently infected cells, obtaining efficient excision of the integrated HIV proviral DNA [110]. Mariyanna et al. [111] describes Tre-recombinases expressed in bacteria targeting the protein transduction domain (PTD) of HIV-1 Tat. These recombinases can induce recombination activity of HIV-1 LTR sequences in human HeLa cells and induce proviral DNA excision from chromosomal integration sites. Hauber *et al.* [112] used a self-inactivating lentivirus to deliver a Tre-recombinase in primary CD4⁺ or CD34⁺ cells engrafted in humanized Rag2^{-/-}, γ ^{-/-} mice inducing HIV-1 provirus excision. A limitation of the Tre-recombinase system is limited specificity, currently only targeting HIV-1 subtype A isolates. Further studies by Karpinski [113], developed a new recombinase (Brec1) effective against 34 base pair of LTR sequences of multiple HIV-1 strains and subtypes. The Brec1

recombinase resulted in excision of integrated HIV-1 provirus *in vitro* and *in vivo*, including in humanized mice engrafted with patient cells.

1.2.7 Homing endonucleases

Homing endonucleases are sequence-specific endonucleases of the meganuclease family that target a DNA sequence of 16-30 base pairs [114]. The DNA binding site and the nuclease site are confined to the same domain. Homing endonucleases were used in lentiviral vectors to target the integrated HIV-1 provirus DNA. An important limitation of this approach is the large size and the low degree of specificity [115].

1.2.8 The Zinc-Finger Nuclease (ZFN)

Zinc-finger nucleases (ZFN) are engineered nucleases containing specific transcription factors that recognize target DNA through zinc finger motifs and a non-specific endonuclease domain Fok1. The binding of the paired zinc finger protein with the Fok1 domain induces activation of the ZFN, leading to double stranded DNA breaks in the target sequence [116]. Each finger of this protein recognizes a specific sequence of three nucleotides. ZFNs technology have been used to modify the genome of plants, animals and humans. Different laboratories used ZFNs protein to target the cellular CCR5 and CXCR4 receptors in infected CD4+ T cells [117], [118], [119], to target M tropic HIV-1 strains (R5 viruses), and T tropic HIV-1 strains (X4 viruses). Holt *et al.* [120] engineered CCR5 knockout human cells and engrafted them into immunodeficient mice. These mice showed a rapid selection of CCR5^{-/-} cells and a consequent reduction of HIV-1 level compared to the negative control. Maier *et al.* used an adenoviral vector encoding CCR5-specific ZFN to express the modified CCR5 in stimulated CD4+ T cells [121]. Tebas *et al.* used this technology to infuse in HIV-1 patients autologous CD4+ T cells after disruption of CCR5. Six of the

twelve patients that suspended ART showed later viral rebound suggesting that this technology delays disease progression yet isn't a permanent cure [122]. Li et al. [123] used a recombinant adenoviral vector for CCR5-ZFN to engineer CD34+ hematopoietic stem/progenitor cells and engraft them into a humanized mouse model, supporting the idea that this strategy allows the selection of the mutated cells by the same virus. Yi et al. [124] reported suppressed viral replication in CD4+ cells of HIV-1 positive patients engrafted in mice and transduced with a non-integrated lentivirus vector inducing expression of CCR5-ZFN. Yao et al. [125] showed the capacity of ZFN engineered CCR5 pluripotent stem cells (hiPSCs) to differentiate into CD34+ cells in vitro, suggesting the possibility of modifying patient-specific stem cells to treat of HIV infection. Yuan et al. [126] engrafted ZFN-modified CXCR4 CD4+ T cells in HIV-1-infected NSG mice, resulting in resistance to HIV-1 CXCR4 strain. Didigu [127] used ZFNs to modify CCR5 and CXCR4 in human CD4+ T cells and infuse them into a humanized mouse model of HIV-1 infection, resulting in resistance to HIV-1 CCR5 and CXCR4 tropic strains.

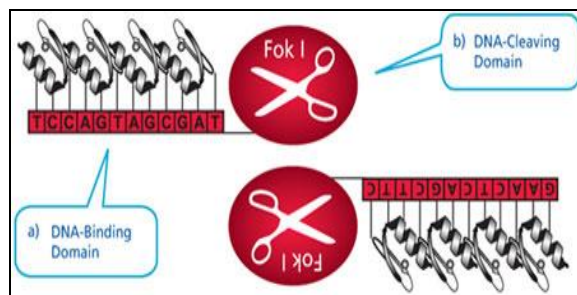


Figure 10: Zinc Finger Nuclease Model. This model is characterized by two domains; a DNA binding domain and a DNA cleaving domain [128]

1.2.9 Transcription Activator-Like Effector Nucleases (TALEN)

Transcription like effector nucleases (TALEN) are produced by the bacteria *Xanthomonas* spp. to modify the transcription of the host plant cells. This system contains a FokI specific nuclease domain and a TALE-derived DNA binding domain with a conserved 33-35 amino acid repeats [129]. The number of repeats determines the length of the DNA target. Each repeat of the TALE domain binds a specific single nucleotide. The DNA specificity depends on two hypervariable residues in position 12 and 13 of each repeat. The presence of Asn/Asp is specific for cytosine, Asn/Gly is specific for thymine, Asn/Asn for guanine and His/Asp for cytosine. TALENs have been used for the therapy of HIV-1, to target the CCR5 gene, the epithelium-derived growth factor and LEDGF/p75 [130]. TALENs and zinc fingers both induce a 45 % disruption of the CCR5 gene, but TALENs are less cytotoxic, more specific (each repeat recognizes one nucleotide instead three for ZFN), possess less off target effects and can target methylated DNA, resulting in specific targeting HIV-1 provirus [131]. Limitations of TALENs include the large size of the construct which constitutes an issue for efficient delivery [130]. Ru *et al.* [132] created a Tat-TALEN protein, complex delivered by a cell penetrating peptide that induced a 5% modification rate in the CCR5 gene of human-induced pluripotent stem cells. Mock *et al.* [133] used non-integrated lentivirus to deliver CCR5-specific TALENs in different cell lines and in T cells, obtaining >50% CCR5 knockout and low off-target activity. Fadel *et al.* [134] used the TALEN technique to target the human PSIP1 gene, which encodes the cellular protein LEDGF/p75, an HIV-1 integration cofactor. Knockout of PSIP1 gene was due to made by deletion of the whole gene or by deletion of the integrase binding domain, resulting in inhibition of HIV-1 integration and viral replication in Jurkat and HEK293 T cells. Ebina *et al.* [135] used a lentiviral vector to deliver HIV LTR TALEN protein in a T

cellular line obtaining an excision of >80% of HIV-1 proviral DNA. Strong *et al.* [136] used HIV TAR TALEN protein to induce indel mutations in HIV-infected cells, resulting in a loss of Gag production.

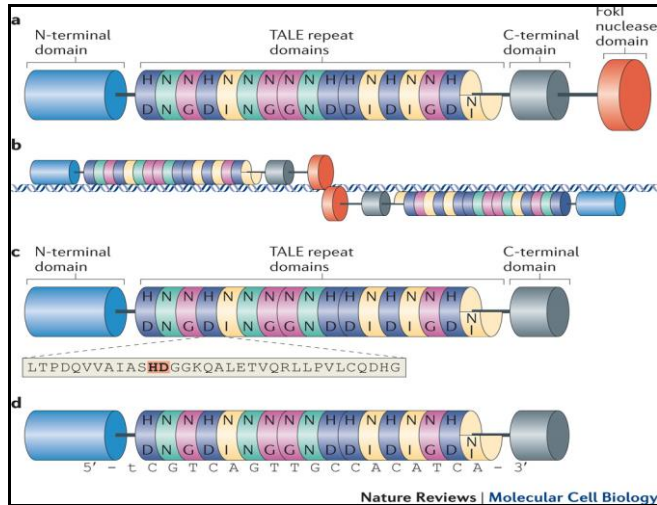


Figure 11: TALEN Model System. Schematic representation of the TALEN model system, showing the presence of TALE repeat domains and the Fok1 nuclease domain, which provides the gene editing capability (Figure reproduced with permission from Joung JK *et al.*, 2013 and Nature Publishing Group) [137]

1.2.10 Double Strand Break (DSB)

The excessive time and cost for production of engineered ZFNs and TALENs protein resulted in the development of an easier and more powerful strategy of gene editing called clustered regulatory interspaced short palindromic repeat system (CRISPR). This mechanism utilizes the adaptive immune system of archaea and of bacteria and was adapted to mammalian genome editing. CRISPR loci contain a clustered set of CRISPR-associated (Cas) genes and a CRISPR array consisting of a series of direct repeats interspaced by specific sequences, called spacers, that recognize foreign sequences, a protospacer, via Watson-Crick base pairing [138]. Generally, genome engineering strategies have been used to

induce double stranded breaks (DSB) at a DNA target site. The DSBs produced by these gene editing molecules are repaired by homology-directed repair (HDR) or non-homologous end joining (NHEJ) system. HDR can utilize a donor template, allowing the introduction of specific point mutations or the insertion of specific sequences through recombination between the donor template and the DNA target. The system NHEJ can introduce mutations like deletions and insertions (indels) that may result in frameshifts or production of stop codons disrupting the open reading frame (ORF) of the target gene and the excision of the section of the DNA between the DSB when multiple gRNAs are employed, resulting in a loss of gene function. The frequencies of these mutations is generally between 1% - 50 %, yet can be higher depending on the system. Unlike the use of monoclonal antibody or RNA interference systems, NHEJ-mediated system induces permanent modification on genome avoiding periods of repeated treatments [139].

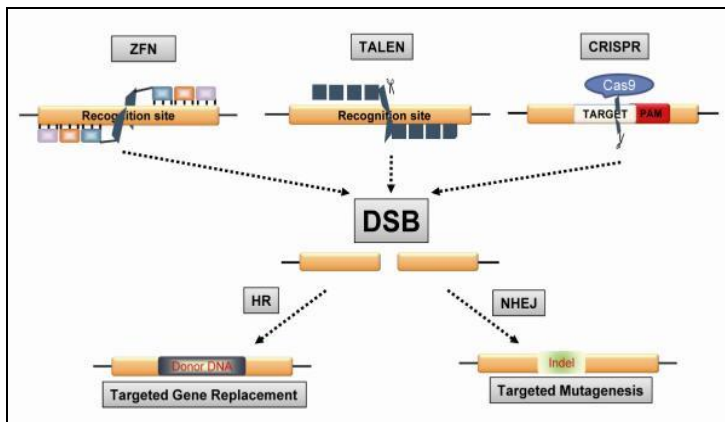


Figure 12: Induction of Double Strand Breaks after gene editing. Gene editing through either zinc finger nucleases, TALEN or CRISPR treatments results in double-stranded DNA breaks, which is repaired by either cellular homologous recombination or non-homologous end joining DNA repair. Generally, homologous recombination is preferred when the goal is gene replacement while non-homologous end-joining is preferred when the goal is

mutagenesis of a target gene (Figure reproduced with permission from Khalili K. *et al.*, 2015 and Springer) [139]

1.2.11 CRISPR SYSTEM

In 1987 Nakata *et al.*, [140] described the presence of 29 nucleotide repeats between five 32 nucleotides non-repetitive sequences in *Escherichia coli*. These repeats were classified belonging to a unique category of clustered repeat elements found in the >40 % of bacteria and 90 % of archaea [141]. In 2002 Jansen and Mojica [142], [143] denoted CRISPR to describe all microbial genomic loci containing interspaced repeat elements. In the same year, Jansen described the presence of cas genes adjacent to the interspaced repeats. The CRISPR system is classified into three types based on difference in the cas genes [144], [145]. Type I and III contain more Cas genes compared to type II and form complexes with crRNA called CASCADE complexes and Cmr or Csm RAMP complexes. CRISPR arrays are transcribed in crRNAs containing spacers that direct the activity of the nuclease to the target, containing by RNA and DNA for CRISPR type III [138], or DNA for types I and II. In type II, the processing of crRNA into mature crRNAs depends on the presence of a trans-activating crRNA (tracrRNA) that hybridizes with the crRNA, together with Cas9 and the endogenous RNase III, the crRNA processes the pre-crRNA into mature RNA [146]. Type II CRISPR, is present only in bacteria and can be classified into three subtypes (IIA-IIIC) based on different Cas genes. Type IIC contains cas9, cas1 and cas2 genes. Types IIA and IIB contain two additional genes, csn2 or cas4 genes respectively [147]. In the latest classification, CRISPR can be divided in two classes, class 1 (that includes the type I and III) which uses several Cas proteins and crRNAs and class II (CRISPR type II and of type V), which employs a single component Cas protein and crRNAs [148]. CRISPR type II uses the Cas9 protein, while the

type V uses another protein of 1300 amino acid called CRISPR from *Prevotella* and *Francisella 1* (Cpf1). Cpf1-associated CRISPR arrays differ from the type II by three important characteristics: pre-crRNA is processed into mature crRNAs without the action of the tracrRNA, the presence of a T rich PAM sequence preceding the target sequences is required instead of a G rich PAM sequence following the DNA target in the type II, and this protein induces DSB with four or five nucleotides 5' overhang [149]. Moineau *et al* discovered that in *Streptococcus thermophilus*, Cas9 (also called Cas5, Csn1 or Csx12) is the only Cas gene able to induce DNA editing [150]. Cas9 protein contains two nuclease domains, RuvC (divided in 3 domains, RuvC I close the N terminal of Cas9 protein and RuvCII/III close to the HNH domain) and HNH (single nuclease domain), each of which nicks a strand of DNA to generate a blunt-ended DSB. The structure of *Streptococcus pyogenes* Cas9 (spCas9) was deeply characterized, revealing the presence of a central channel that houses the RNA-DNA target hetero-duplex after rearrangements of Cas9 binding crRNA and tracrRNA [151]. Cas9 structure analysis revealed the presence of two lobes, an alpha helical recognition (REC) lobe that facilitates binding with the target sequence and a nuclease lobe that contains HNC and RuvC domains and a PAM interacting (PI) C terminal region. When Cas9 is unbound, the active site of HNH domain is blocked by the RuvC domain and the binding RNA-DNA is inhibited by the C-terminal domain. The SpCas9 REC2 domain is poorly conserved in orthologs, allowing the production of Cas9 mutants that are highly compact with increased efficiency [152]. Different bacteria are characterized by several Cas9 with similar structure but different size ranging from 900 to 1600 amino [145]. Type II CRISPR requires the presence of protospacer adjacent motifs region (PAMs) at the 3' end of the target region, sequence specific of each Cas9 ortholog for DNA cleavage [153]. SpCas9 recognizes both 5'NGG

PAM and 5'NAG PAM sequences, with the complexity of the PAM regions determining the DNA targeting space of Cas9 [138]. The choice of the promoter, either U6 or T7, to express gRNAs influences the target sequence by requiring a G or GG at 5' end of the spacer respectively. The Cas9-crRNA-trRNA complex first associates with the PAM sequence, then Cas9 initiates the separation of DNA strand with unknown mechanism and edit the DNA target. CRISPR types I and III require the presence of mismatches at the 5' end of the crRNA and the target sequence to initiate gene editing [154]. In 2012, a study demonstrated the ability of purified Cas9 from *Streptococcus thermophilus* or *Streptococcus pyogenes* (Sp) to edit DNA targets in the presence of crRNAs [155]. CRISPR type II utilizes the combination of SpCas9 and guide RNA (gRNA), which is the fusion of a crRNA and a tracrRNA.

Cas9 is a universal nuclear which has been adapted for gene editing in many organisms, including bacteria, yeast, fruit flies, zebrafish, mice, rats, monkeys, and human cell lines [138]. Following administration of Cas9, target DNA is cleaved, resulting in a DSB three to four nucleotides upstream of the PAM sequence. In mammalian cells, CRISPR-mediated gene editing requires the use of engineered gRNAs, which fuse a crRNA and a tracrRNA containing a roughly 20 nucleotide guide sequence to ensure DSB at specific genomic sites. Likewise, a dual gRNA system can be utilized, containing a second stem loop which increases the stability of the gRNA compared to single gRNAs.

The use of Cas9 as a gene editing strategy for human patients has unlimited potential as both a therapeutic agent and a genome editing agent. Cas9 gene editing has been proposed for the treatment of multiple monogenic recessive disorders resulting from loss-of-function mutations, such as cystic fibrosis, sickle-cell anemia, or Duchenne's muscular dystrophy. Likewise, Cas9 has been proposed to treat polygenic disorders

and dominant-negative disorders, including diabetes, heart disease, schizophrenia, autism, transthyretin-related hereditary amyloidosis and dominant-negative forms of retinitis pigmentosum [138].

However, the therapeutic potential of CRISPR is still in its infancy. The first clinical trial using CRISPR technology was in 2016 at Sichuan University in Chengdu, China. In this trial, peripheral blood lymphocytes were collected and programmed cell death protein 1 (PD-1) was knocked out by CRISPR-Cas9 *in vitro*, after which knockout cells were clonally expanded and infused into the patient. This trial remains underway, with completion and publication being expected in April 2018 [156]. Various studies have demonstrated off-target Cas9 binding, however, this binding does not necessarily induce cleavage at all off-target sites. Currently, several software programs, including DNA2.0 CRISPR gRNA design tool, E-CRISP, sgRNAs9 software package, CasOFFinder, and CasOT, are offered to assist with gRNA design to limit off-target binding [139]. Generally, mismatches in the target sequence are better tolerated at the 5' end of the 20-nucleotide gRNA spacer region than at the 3' end [157], [158], [159]. Experimental analysis of gRNA specificity, off-target DNA binding sites, and the presence of indel mutations can be assessed through multiple assays, including the T7 endonuclease I mutation mismatch assay and deep sequencing analysis. To limit off-target binding, gRNAs can be designed to target GC-rich domains, thus increasing binding specificity. Other methods to decrease off-target binding include reducing gRNA concentration and Cas9 expression, using Cas9 variants or modified gRNAs with truncated 3'-ends or with two extra 5'-guanines, or by using gRNAs with a shortened 5'-end for the complementary region [160]. Another method to reduce off-target effects is to use nickase variants, produced by inactivating one of the two Cas9 nuclease domains via the induction of point mutations, which results in the stronger stimulation of

high fidelity homology directed repair. To improve on this method, a paired nickase system was recently developed which inactivates one of the two nuclease domains of SpCas9 [161]. This system utilizes two gRNAs and two monomeric nickases, resulting in single-strand DNA breaks on opposite DNA strands, which increases the editing specificity by up to 1500-fold [162]. Wild-type Cas9 can be catalytically inactivated (dCas9) and subsequently directed by gRNAs to a targeted DNA sequence, resulting in transcriptional suppression due to Cas9-mediated steric hindrance of the RNA polymerase machinery [163]. This method is called CRISPR-based interference, CRISPRi, in which direct tethering of the catalytically inactivated Cas9 to a transcriptional repressor domain induces epigenetic silencing [164], [165]. The fusion of inactive Cas9 to either transcription activation domains, such as VP16/VP64 or the p65 subunit, or to transcriptional repressor domains allows targeting of endogenous transcription. For transcriptional regulation to occur, two RNA-guided Cas9 monomers must bind targets on opposite DNA strands that are separated by 14-17 base pairs or by 25 base pairs, depending on the system being used. The necessity of both Cas9 monomers binding to a specific sequence serves to significantly increase targeting specificity. This transcriptional regulation can be modified by altering the presence of multiple sgRNAs and has been shown to function in bacteria, mice cells, and human cells [165], [166], [167].

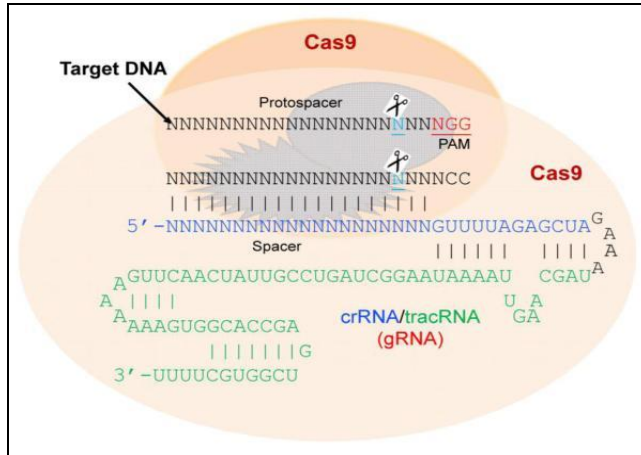


Figure 13: Cas9-gRNAs Interactions. The gRNA is characterized by a CRISPR RNA and a trans activating crRNA. (Figure reproduced with permission from Khalili K. *et al.*, 2015 and Springer)) [139]

1.2.12 CRISPR/Cas9 Delivery

Currently, delivery of CRISPR/Cas9 into cells can be accomplished by a wide variety of mechanisms, including both viral and non-viral delivery methods, which deliver the CRISPR complex into cells in the form of DNA, RNA, or as a protein/RNA complex. Viral delivery methods include lentiviruses, baculoviruses, and recombinant adeno-associated viruses (rAAV). AAV-based vectors are advantageous due to low immunogenicity and multiple administration routes, including intranasal and intratracheal administration and by stereotactic, intravenous, intraperitoneal, and intramuscular injections. AAVs can transduce both dividing and non-dividing cells without host-genome integration. However, the major limitation of AAVs is the limited packaging capacity of 4.7 kilobases. Due to this property, many AAV-based delivery systems utilize Cas9 from *Staphylococcus aureus* (saCas9) as opposed to the traditional *Streptococcus pyogenes* due to the small size of saCas9. While SaCas9 is smaller than SpCas9, it requires a longer PAM sequence for specific

targeting [168]. There are two types of safe lentiviruses vectors that can be used for CRISPR delivery, which are self-inactivating replication incompetent or integrase defective lentiviruses. This delivery system allows for transient CRISPR expression and can be used to transduce both dividing and non-dividing cells. The major advantage of lentiviruses is their high capacity for packaging, allowing for the use of large inserts [139].

There are many options in terms of non-viral delivery mechanisms, including cationic polymer polyethyleneimine (PEI), liposomes, lipid nanoparticles, virus-like particles, bacteriophages, and self-assembled DNA nanoparticles. Recently, the use of ligand functionalized nanoparticles has been prominent due to their ability to bind endothelial cell receptors, allowing efficient transmigration across the blood-brain barrier (BBB) from the periphery into the central nervous system. Another recent advancement has been the use of electric nanoparticles to mediate crossing of the BBB in combination with a magnetic field gradient [169], [170].

1.2.13 CRISPR/Cas9 system for HIV-1 Genome Editing

CRISPR/Cas9 gene editing can be used to impact either host cells to inhibit viral infection, either through cellular entry or other mechanisms, or to directly affect the virus through various mechanisms. The first application of the CRISPR/Cas9 system against HIV was in 2013 by Elbina *et al*, [171] in which it was used to eliminate the HIV provirus from T-cells by targeting the TAR region in the R region and the NF- κ B binding sequence in the U3 region. This study revealed that indel mutations can inhibit active provirus expression and decrease latent virus reactivation. One study in which CRISPR/Cas9 gene editing was used to target host cells was completed by Hou *et al*, in which they showed that targeting the HIV coreceptor CXCR4 induced the receptor expression by 30% on human

T-cells by treatments with Cas9, thus inducing HIV-1 resistance by blocking cellular entry [172]. Another follow up study utilized Cas9/sgRNA ribonucleoproteins (Cas9 RNPs) treatments to decrease CXCR4 expression by 40% in human primary T cells to induce HIV resistance [173]. After the Berlin patient results demonstrated that CCR5 Δ 32 mutation conferred HIV-1 resistance, CRISPR/Cas9 gene editing was used to target the CCR5 coreceptor to inhibit HIV infection. Ye *et al* treated pluripotent stem cells (PSCs) with CRISPR/Cas9 constructs to induce CCR5 Δ 32 deletion, obtaining roughly 100% efficiency for one allele and up to 33% efficient for the deletion of both alleles, obtaining HIV-resistance in cells derived from the treated induced PSCs [174]. Wang *et al* used a lentiviral vector approach, targeting three sites of the CCR5 gene in a human CD4+ T-cell line, obtaining cells which were resistant to HIV R5 infection, yet this gene disruption approach failed in human primary T-cells [175]. Li *et al* used an adenoviral approach to target and destroy CCR5 in TZM-bl cells and CD4+ T-cells [176].

In addition to modifying host cells to resist HIV infection, CRISPR/Cas9 can be used to directly target HIV. Zhu *et al* targeted three sites in the HIV LTR, five sites in *pol*, and two sites in *rev* to eradicate HIV provirus in Jurkat cells, resulting in a 20-fold reduction of HIV production [177]. Additionally, CRISPR/Cas9 has been used in combination with the “shock and kill” approach to potentially eradicate the virus from latent sites of infection. Zhang *et al* used catalytically inactivated Cas9 transcription activator fusion protein complexed with sgRNA to activate HIV latent reservoirs in multiple cell lines such as TZM-bl epithelial, Jurkat T cells and CHME5 microglial cells. The sgRNA targeted twenty different sites within the U3 LTR region, resulting in accumulation of viral proteins and cell death [178]. The results from this study resulted in the NF- κ B binding site being identified as the most highly efficient target site to target when activating HIV in latent cells,

which was bolstered by results from Saayman *et al.* [179]. Hu *et al.* used lentiviruses vectors containing Cas9 or gRNAs A/B targeting the U3 region in both LTRs sequences. This technology assesses the ability of the gRNAs to excise a 9709-base pair region of the integrated virus from the genome of latently infected microglia, promonocytes and T cells obtaining a decrease of viral expression. This study showed that the presence of multiple gRNAs and Cas9 in the cells can prevent new HIV-1 infection through a rapid elimination of viral DNA. This approach can be used like a gene editing based vaccine, likewise further investigation is necessary to assess this system in latent reservoirs cells and analyze in animal model the presence of off target and the ability to eradicate viral reservoir *in vivo* [180]. When CRISPR/Cas9 gene editing was proposed for the treatment of HIV, one potential outcome was the mutation of variants resistant to targeting, called escape variants. The presence of HIV-1 escape variants was shown by Wang *et al.* [181]. These variants, produced by NHEJ repair, contained mutations close to the Cas9 cleavage site, rendering the viral variants immune to gene editing using that system, data that was confirmed by Yorder *et al.* [182]. A proposed method to bypass the creation of escape variants is the use of several gRNAs which direct Cas9 to different regions of the HIV genome. This mechanism creates several excision points in the proviral genome, allowing for the cleavage of escape variants at one cleavage site by targeting a secondary or tertiary cleavage site, thus eliminating the development of HIV escape variants following CRISPR/Cas9 treatment.

Region of interest	Target	Delivery	Reference
LTR (R and U3)	T cells	transfection	[171]
LTR (U3)	TZM-bi/U1/J-Lat	Transfection	[180]
CCR5	HEK 293 T, HeLa, NCCIT, human embryonic stem cell	transfection	[183]
CCR5	Induced PSCs	transfection	[174]
LTR (U3)	TZM- Bi/Jurkat/CHME5 microglia cells	lentivirus	[178]
LTR/POL/REV	Jurkat cells	transfection	[177]
CCR5	TZM-Bi/ CD4+T	Adenovirus	[176]
CXCR4	Human CD4+T cells	lentivirus	[172]
CXCR4	T cells	transfection	[173]
5'LTR	Tcells	transfection	[179]
LTRs	Human CD4+T cells,2D10	lentivirus	[184]
LTR	TZM-Bi/Jurkat cells	lentivirus	[185]
LTR/GAG	Tg26 mice	AAV	[186]
CCR5	HUMAN CD4+ T cells	lentivirus	[181]
CXCR4	B cells	transfection	[187]
LTR/GAG/POL	Tg26/humanized mice	AAV	[188]

Table 2: CRISPR/Cas9 Studies Related to HIV-1 Treatment. Table shows various studies utilizing CRISPR thereapies for HIV-1 treatment and potential eradication. The target gene is described in the region of interest and the tested model, either animal models or human cells, is denoted. Additionally, the delivery system, either adenoviruses, adeno-associated viruses, lentiviruses, or transfection methods, is denoted.

2. Aim of the Study

Throughout the world, HIV-1 infects more than 36.9 million people, including 2.6 million children [7]. Currently, the primary therapeutic regimen is treatment with antiretroviral agents, called antiretroviral therapy (ART). During ART, HIV persists in the body as a provirus in latently infected cells, resulting in a chronic latent condition. As treatment with ART does not eliminate HIV it is not considered a curative strategy [3]. Current studies have focused on developing treatments which can target both actively and latently infected cells to eradicate the virus. Recently, CRISPR-Cas9 has become the predominant strategy for gene editing and elimination of integrated proviral DNA. The CRISPR/Cas9 system consists of a nuclease (Cas9) and a guide RNA (gRNA) that directs Cas9 activity to specific DNA sequences to induce double strand breaks resulting in replication-defective virus [139]. To deliver the CRISPR/Cas9 system to cells either lentiviruses, adenoviruses or adeno-associated viruses (AAV) can be used. To investigate the potential of therapeutic potential of the CRISPR/Cas9 system, our laboratory utilized *in vitro* and *in vivo* approaches:

- a) Studies *in vitro* of an inducible system of spCas9 activated by Tat, targeting LTRs HIV-1 regions and delivered by lentiviral vectors
- b) Studies *in vivo* with the shorter saCas9 targeting LTR and Gag HIV-1 regions and delivered by AAV₉ vectors in transgenic mice and rats
- c) Studies *in vivo* with the shorter saCas9 targeting LTR and Gag HIV-1 regions and delivered by AAV₉ vectors in humanized mice

3 Materials and Methods

3.1 Plasmid Preparation

The vectors px260-LTR-Cas9 containing the full length LTR (-456/+66) and the truncated LTR promoter sequences (-120/+66 or -80/+66) were cloned by PCR using pNL4-3 HIV vector (NIH AIDS Reagent Program #114) as the template and the primers described in Table 6. The PCR products were subcloned into the pCR™2.1-TOPO® TA vector (Life Technologies, CA) and high copies of plasmid DNA were obtained after transformation of the ligation product into the DH5α strain of *Escherichia coli* (Invitrogen, USA). Plasmid DNA was extracted from bacteria using the Qiagen Plasmid Minikit (Qiagen, Germany). Purified DNA was digested with KpnI or XbaI and NcoI restriction enzymes and ligated into pX260-U6-DR-BB-DR-Cbh-NLS-hSpCas9-NLS-H1-shorttracr-PGK-puro plasmid (Addgene #42229) replacing the Cbh promoter with LTR promoters.

In the LentiCas9-Blast plasmid (Addgene #52962) the EFS promoter was replaced with the LTR promoter. Briefly, LTR promoter regions were amplified using the primers listed in table 6, subsequently subcloned into the TA vector and digested with NheI and XbaI restriction enzymes, finally ligated with Nhe I and XbaI digested lentiCas9Blast. The correct replacement of the promoter sequence was confirmed by DNA sequence analysis (Genewiz, USA) using BLAST from the NCBI.

pKLV-U6-LTR A/B-PGKpuro2ABFP and pCMVtat86 plasmids were previously described [184, 189]. pKLV-U6-LTR A and B-PGKpuro2ABFP plasmids contain a gRNA expression cassette under the control of U6

promoter. PcDNA3.1 (#V79020) was bought from Invitrogen (Carlsbad, USA).

px601-AAV-CMV:NLS-saCas9-NLS-3xHA-bGHpA:U6:Bsa1-SgRNA (Addgene #61591). Briefly pX601 was donated by Feng Zhang and was used for cloning the gRNAs LTR1 and GagD sequences. px601 was digested with BsaI, treated with calf intestinal alkaline phosphatase (CIP) and gel purified using QIAquick Gel Extraction kit (Qiagen, Germany). A pair of oligonucleotides specific for LTR and Gag regions (Table 6) were annealed, phosphorylated, and ligated with the linearized vector. To clone the GagD sequence into the pX601 vector containing the LTR1 gRNA, the vector was digested with EcoRI and KpnI and the linearized product was purified and ligated with the PCR product of Gag region using px601 containing GagD gRNA as template and T795 and T796 primers containing the restriction site for EcoRI and KpnI.

T795: ATTACGCTTAAGAATTCCTAGAGC

T796: ggaaataggccctcagACTAGGGGTTCTGCGGCCGCAAA

Clones were tested using BamHI or EcoRI +NotI and sequenced. 80 ug of a positive clone was sent to the Penn Vector Core, (Perelman School of Medicine, University of Pennsylvania) for the packaging in AAV 9 serotype.

3.2 Cell Culture

TZM-bl cells are HeLa cells stably expressing CD4, CCR5, CXCR4 and luciferase and b-galactosidase reporter genes under the control of the HIV-1 LTR promoter. The TZM-bl cell line, obtained from the National Institutes of Health (NIH), was maintained with Dulbecco's Modified Eagle Medium (DMEM), (Thermo fischer scientific, USA), supplemented

with 10% heat inactivated Fetal Bovine Serum (FBS), (Thermo fisher scientific, USA) and gentamicin (10 µg/ml).

Jurkat Clone E6-1 cells were obtained from ATCC (TIB-152™) and the Jurkat 2D10 reporter cell line was previously described [184]. These cells lines were cultured with Roswell Park Memorial Institute (RPMI) medium in presence of 10% FBS and gentamicin (10 µg/ml).

Mouse embryonic fibroblasts (MEFs) from HIV-1 transgene Tg26 mice were obtained from 17-day-gestation embryos after mechanical dissociation [190]. MEFs were cultured in DMEM with 10% FBS.

3.3 Co-Transfection of TZM-bl with pX260-LTR-Cas9 and pCMV-Tat

2.5 x 10⁵ TZM-bl cells were plated in a 6 well tissues culture plate. At 24 hours, the cells were transfected with 0.5 µg of pX260-LTR plus 0.5 µg of pCMV (pcDNA3.1) for control cells and 0.5 µg of pX260LTR + 0.5 µg pCMV-Tat plasmid for Tat treated cells using the lipofectamine 2000 transfection reagent (Invitrogen, USA); un-transfected cells were used as negative control. A total of 1 µg of DNA was added in 50 µl of opti-MEM medium. 50 µl of opti-MEM was mixed with 5 µl of lipofectamine in a second eppendorf and incubated for 5' at RT, after which the diluted DNA was added to the lipofectamine 2000 mixture (1:1 ratio) and incubated for 20'. During this incubation, cellular growth medium was replaced with 750 µl of opti-MEM per well and 150 µl of the reaction mix was added dropwise onto the cells. At 4 hours, the transfection mixture was removed from cells and fresh 10% FBS DMEM was added. Cells were harvested at 2 days post-transfection to analyze the ability of Tat to activate LTR promoter by western blot.

3.4 Lentiviral Packaging

2.5x10⁶ HEK 293 cells were plated in a 100mm dish and transduced to package Cas9 or gRNAs A/B into lentiviral vectors using the calcium orthophosphates (CaPO₄) precipitation method. Briefly, DNA is mixed with calcium chloride in a phosphate solution, resulting in the formation of a calcium-phosphate-DNA precipitate. This precipitate was then added onto HEK293 cells. pMDLg/pRRE (Addgene 12251), pRSV-Rev (Addgene 12253) and pCMV-VSV-G vectors (Addgene 8454) were used for the packaging of pKLV-U6-LTR A/B-PGKpuro2ABFP, while Lenti-LTR- 80/+ 66-Cas9-Blast, psPAX2 (Addgene 12260) and pCMV-VSV-G (Addgene 8454) vectors were used for Cas9 packaging. At 24 and 48 hours, the supernatants were collected and centrifuged at 3000 RPM for 10 minutes and filtered using 0.45 µm filter to remove cellular debris. Lentiviruses were then concentrated by ultracentrifugation (2h, 25000 RPMI, with 20% sucrose cushion) and the pellets were resuspended overnight (O/N) in Hanks Balanced Salt Solution (HBSS) (Lonza, USA). Viral titer was determined after resuspension.

3.5 Viral Titer

1x10⁶ HEK 293 cells were plated in a 24-well plate and transduced at 24 hours with five serial dilutions of viral stock (25 µl of lentivirus stock was diluted in 250 µl of serum free medium in the presence of 8 µg of polybrene). At 24 hours, growth medium was replaced with fresh 10% FBS DMEM and at 1 day the cells were treated with TSA/PMA (250 nM/16 nM) to induce LTR promoter and Cas9 expression. Cas9 Flag was detected with an immunohistochemistry assay while the lentiviruses harboring the gRNAs were quantified with microscopy using blue fluorescent protein as the marker.

3.6 Immunocytochemistry for Cas9

HEK 293 cells were fixed with 4% paraformaldehyde in PBS for 10 minutes at RT, washed with 250 μ l of PBS and permeabilized with 0.25% Triton 100X in PBS. The primary antibody, mouse anti Flag, was diluted at 1:200 in PBS containing 0.05% Triton 100X and 1% BSA and was incubated for 2 hours at 37° C. After incubation, the cells were washed 3 times in PBS containing 0.05% Triton 100X for 5 minutes and incubated with the secondary antibody, anti mouse FITC conjugated diluted 1:200 in PBS with 0.05% Triton 100X and 1% BSA for 2h at 37C. Later, cells were washed 3 times for 5 minutes each in PBS containing 0.05% Triton 100X and were imaged using fluorescent microscopy.

3.7 TZM-bl Transduction with pLENTI-LTR-Cas9

1×10^6 TZM-bl cells were plated in a 12-well plate for 24 hours prior to adenoviral vector transduction. 4 wells were transduced with human adenovirus type 5 (De1/e3) Ad-GFP (catalog # SL100708, Signa Gen Laboratories, MD) at an MOI of 15, 4 wells were transduced with Ad-GFP at an MOI of 12, 4 wells were transduced with Ad-CMVtat at an MOI of 3, and 4 wells were transduced with Ad-Tat at an MOI of 15. Adenoviral stocks were diluted in opti-MEM medium and 500 μ l of mixture was added per well. Fresh 10% FBS DMEM was added to the cells after 1h of incubation. 24 hours later the cells were treated with lentiviral particles containing SaCas9, gRNAs A/B or empty vector to test the ability of spCas9 to induce gene editing on LTR promoter of TZM-bl cells in presence of gRNAs and different amounts of Tat. pLENTI-LTR-Cas9 containing LTR -80/+66 (MOI1), pKLV-gRNA-empty (MOI 8,6,4 and 0) and pKLV-gRNA LTR A and B (MOI 0/0, 1/1, 2/2 and 4/4) were used for the three different MOIs of Tat. The proper amount of virus was transferred to a new eppendorf tube containing opti-MEM (500 μ l final

volume) and polybrene (8 µg/ml) and 500 µl of viral mix was added in each well. Normal 10% FBS DMEM and 1% penicillin/streptomycin was added after 24 hours. Cells were harvested at 48 and 96 hours and processed for PCR, Western Blot, and Luciferase assays.

	Adeno null/GFP	Adeno Tat	Cell number
	3x10 ⁶ IU/µl	3x10 ⁶ IU/ul	
1	MOI 15	-	10 ⁶ /12 well
2	MOI 12	MOI 3	10 ⁶ /12 well
3	-	MOI 15	10 ⁶ /12 well

Table 3: Transduction Conditions for TZM-bl Cells with Adenoviral Vectors

	Lenti pKLV-gRNA-empty	Lenti pKLV-LTRA	Lenti pKLV-LTRB	Lenti LTR-Cas9	Cell number
	3x10 ⁴ IU/µl	1.4x10 ⁶ IU/µl	1.8x10 ⁶ IU/µl	1.3x10 ³ IU/µl	
1	MOI 8	-	-	1/4	2x10 ⁶
2	MOI 6	MOI 1	MOI 1	1/4	2x10 ⁶
3	MOI 4	MOI 2	MOI 2	1/4	2x10 ⁶
4	-	MOI 4	MOI 4	1/4	2x10 ⁶

Table 4: Transduction Conditions for TZM-bl Cells with Lentiviral Vectors

3.8 Stable Cell Lines

1x10⁵ TZM-bl cells per well were plated in a six-well tissue culture dish and transfected with 1 µg of pX260-LTR (-80/+66)-Cas9 using Lipofectamine 2000 reagent (Invitrogen, USA) to induce puromycin resistance. At 24 h cells were transferred into a 100-mm dish and treated with 1µg/ml puromycin (Sigma, USA) for the selection of Cas9 expressing clones. After two weeks, the clones were visualized in an inverted phase contrast microscope and the selection of the positive clones was performed using cloning cylinders (Corning, MA). Briefly after, cells were washed, and the bottom of the cloning cylinder was dipped into a sterile silicone grease creating an isolated well around the colony

of interest. Then, the clones were treated with 200 μ l of 0.25 % trypsin for 3 minutes at 37°C and transferred into a 6-well dish.

The TZM-bl Cas9 stable cell line was transduced with pKLV-gRNA-empty (MOIs of 8,6,4 and 0) and pKLV-gRNA LTR A and B (MOIs of 0/0, 1/1, 2/2 and 4/4) as previously described. At 24 hours, cells were infected with HIV-1_{JRFL} or HIV-1_{SF162} and harvested at 48 and 96 hours post-infection for PCR, western blot and luciferase analysis.

3 μ g of pX260-LTR (-80/+66)-Cas9 was used to electroporate 5×10^5 Jurkat 2D10 cells to create a Cas9 stable line. Electroporation was completed using a Neon System machine (Invitrogen, USA) with the 3 applications of voltage for 10 ms at 1350 V. Cells were plated in a 6-well dish and new medium containing 0.5 μ g/ml of puromycin was added at 48 hours. The following week, cells were diluted to 10 cells/ml and 50 μ l of the dilution was plated in 96 well plate for 2 weeks in presence of 10 % FBS RPMI medium.

Jurkat 2D10 pX260-LTR (-80/+66)-Cas9 stable cell line was transfected with pKLV-gRNA-empty and pKLV-gRNA LTR A/B alone or together with pCMV-empty (pcDNA3.1) and pCMV-Tat plasmids. PCR, qPCR, western blot and flow cytometry assays were performed after 48h.

3.9 Infection of TZM-bl with HIV-1_{JRFL} or HIV-1_{SF162}

1×10^7 freshly isolated peripheral blood mononuclear cells (PBMCs) were activated for 24 hours with Phytohemagglutinins (PHA) (5 μ g/ml) and subsequently infected by spinoculation with 100ng of Gag p24/ 10^6 cells (total 1 μ g) for 3 h (2700 RPMI, 32°C) in Opti-MEM in the presence of 8 μ g/ml polybrene. Supernatants of infected PBMCs were collected at 6 days post-infection and centrifuged at 3000 rpm for 10 minutes and

filtered with 0.45 μm filters to prepare HIV-1_{JRFL} and HIV-1_{SF162} stocks. The purified supernatants were lysed with 1 % Triton X-100 (v/v) and viral titer was determined using p24 ELISA, following the manufacturer's instructions.

Stable Cas9/gRNA T2M-bl cells were pre-seeded into a 24-well plate and infected by spinoculation for 4 hours with 100ng of Gag p24 per well in the presence of polybrene (8 $\mu\text{g}/\text{ml}$), after which they were washed three times with PBS. The activity of the LTR promoter, which is induced by Tat protein, was verified by a luciferase assay using a Modulus II Microplate Multimode Reader (Promega, USA).

3.10 Electroporation of 2D10 Cell Line with LTR (-80/+66)-Cas9

4x10⁶ cells of the 2D10 LTR (-80/+66)-Cas9 stable line were electroporated using Neon Transfection system (Invitrogen, CA) with pKLV-gRNA LTR A and B (3 μg of each) and the control plasmid, pKLV-gRNA-empty (6 μg), alone or together with varying amounts of pCMV-Tat86 (0 μg , 1 μg , 2 μg , 6 μg). The total DNA used during the transfection was normalized to 12 μg for all conditions with the empty pCMV vector (pcDNA3.1). This transfection system uses an electronic pipette tip as an electronic chamber and has the advantage to improve cellular viability and transfection efficiency. 4X10⁶ cells were electroporated 3 times for 10 ms at 1350V with 12 μg of total DNA in 80 μl of buffer T using 10 μl tips. DNA and whole cell protein extracts were collected after 48 hours of electroporation, and 1/10 of the total cells (around 5*10⁵cells) were fixed and analyzed for GFP expression. Electroporation conditions per 100 mm dish are found in Table 5.

	pCMV (pcDNA3.1)	pCMV- Tat86	pKLV- gRNA- empty	pKLV- LTRA	pKLV- LTRB	PDS Red1-N1			
µg/ul	0.92	1.39	1.77	1.28	2.18	1.34			
1	6ug/6.6µl	-	6ug/3.4µl	-	-	-	cells	Buff er T	medi um
2	5.33ug/5.8µl	0.66ug/0.5µl	6ug/3.4µl	-	-	-	4*10 ⁶	80 µl	8ml
3	4ug/4.4µl	2ug/1.5l	6ug/3.4µl	-	-	-	4*10 ⁶	80 µl	8ml
4	-	6ug/4.5µl	6ug/3.4µl	-	-	-	4*10 ⁶	80 µl	8ml
5	6ug/6.6µl	-	-	3ug/2.3µl	3ug/1.4µl	-	4*10 ⁶	80 µl	8ml
6	5.33ug/5.8µl	0.66ug/0.5µl	-	3ug/2.3µl	3ug/1.4µl	-	4*10 ⁶	80 µl	8ml
7	4ug/4.4µl	2ug/1.5µl	-	3ug/2.3µl	3ug/1.4µl	-	4*10 ⁶	80 µl	8ml
8	-	6ug/4.5µl	-	3ug/2.3µl	3ug/1.4µl	-	4*10 ⁶	80 µl	8ml
9	-	-	-	-	3ug/1.4µl	12ug/10µl	4*10 ⁶	80 ul	8ml

Table 5: Electroporation Conditions for the Jurkat 2D10 Stable Cell Line with Lentiviral Vectors Expressing gRNAs and a Tat Plasmid

3.11 Viral Stocks

HIV-1NL4-3-EGFP-P2A-Nef plasmid was donated by the School of Medicine at the University of Pittsburgh. After transfection of HEK 293T cells using CaPO₄ precipitation, HIV-1NL4-3-EGFP-P2A-Nef reporter virus was obtained by processing the plasmid as a lentiviral stock as described before. At 48 hours, viral titer was determined in Jurkat cell line using EGFP as marker. HIV-1_{SF162} and HIV-1_{JRFL} were gifts from Dr. Jay Levy, and Dr. Irvin Chen respectively

3.12 Jurkat HIV-1 Infection

2x10⁶ Jurkat 2D10 cells were transduced with pLENTI-LTR-Cas9 (-80/+66)-Cas9 (MOI 1), pKLV-gRNA LTR A and B (MOI1/1) and pKLV-gRNA-empty (MOI2). Briefly cells were spinoculated for 30 minutes (2700

rpm, 32°C) in Opti-MEM in the presence of 8µg/ml polybrene. At 24 hours, cells were infected with HIV-1NL4-3-EGFP-P2A-Nef reporter virus (MOI 0,01) by spinoculation for 2 hours at 2700 rpm at 32° C in 500 µl inoculum containing 8 µg/ml polybrene. Cell pellets were resuspended and 500 µl of medium was added after 4 hours. The next day, cells were washed in PBS and resuspended in RPMI medium. Flow cytometry, PCR and qPCR analysis were performed at 3 and 5 days post-infection.

3.13 Cellular Viability Assay

200 µl of living 2D10 Jurkat cells were quantified for GFP expression using Guava EasyCyte Mini flow cytometer (Guava Technologies, Germany). Cells were incubated with propidium iodide (10 µg/ml) for 5 minutes to assess cellular viability. Before GFP quantification in HIV-1NL4-3-GFP-P2A-Nef infected Jurkat cells, a fixation step in 2% paraformaldehyde was performed followed by 3 washes in PBS.

3.14 Luciferase Assay

After transfection and transduction of TZM-bl cells and the TZM-bl Cas9 stable cell line with px260-LTR-Cas9 vectors (LTR -456/+66 or -120/+66 or -80/+66) and LV-gRNAs A/B, whole cell protein extracts were analyzed using a Luciferase Reporter Gene Assay kit (Promega, USA). Briefly, cell lysates obtained after lysis with Passive Lysis buffer 1X (Promega, USA) were centrifuged at 13,000 rpm for 10 minutes at 4°C and supernatants were transferred to a new eppendorf. Luciferase activity was assessed by recording luminescence activity with a Modulus II Microplate Multimode Reader (Promega, USA). 50 µl of supernatant was mixed with 50 µl of freshly made 1X luciferase assay reagent substrate. Luminescence activity was corrected for protein concentration.

3.15 Western Blot

Cells were trypsinized and collected and harvested via centrifugation. Cell pellets were lysed with 350 µl of Triton X-100-based lysis buffer supplemented with 1X nuclear extraction proteinase inhibitor mixture (Cayman Chemical, USA) and the lysate was incubated for 30 minutes at 4°C. Following lysis, cells were centrifuged at 14000 rpm for 10 minutes at 4°C to remove cellular debris. 100 µg of protein was separated by SDS-polyacrylamide gel electrophoresis and transferred to nitrocellulose membrane (BioRad, USA). Anti-flag M2 monoclonal antibody and mouse anti α -tubulin monoclonal antibody were used for the detection of Cas9 and for loading control. Living Colors® Full-Length GFP Polyclonal Antibody rabbit and anti-HIV1 tat antibody were used for the detection of GFP and Tat proteins respectively.

3.16 DNA and RNA Isolation

DNA and total RNA were isolated using the NucleoSpin DNA virus kit (Macherey Nagel, Germany) and RNeasy Kit (Qiagen, USA) how described in appendix D1-2. DNA and total RNA was subjected to qualitative and quantitative analysis through PCR and qPCR analysis.

3.17 HIV-1 DNA Detection and Quantification

200 ng of DNA was analyzed using Fail Safe PCR kit (Epicentre, USA) and Buffer D. Specific PCRs for HIV-1 LTR A/B, 5'UTR, env, LTR gag and β -actin (primers listed in table 6) were performed and resolved through a 2% agarose gel. After gel purification of the PCR products, the DNA sequence was cloned to the TA vector and analyzed by Sanger sequencing (Genewiz, USA). 50 ng of DNA and cDNA was quantified using Real time polymerase chain reaction (Real Time PCR), performed in a LightCycler480 (Roche, Germany). The reaction was based on the

use of one Taq man hydrolysis probe specific for HIV-1 5'-UTR, env and gag genes and cellular human beta-globin gene as a reference (table 6). Simplified protocol was modified from a previously published protocol [191]. Genomic DNA of infected HIV-1 U1 cells containing only two copies of provirus per diploid genome was used to prepare a standard curve. The conditions of the qPCR were the following: 98 °C 5 minutes, 45 cycles (98 °C 15 s, 62 °C 30 s, 72 °C 1 minute).

3.18 Selection of gRNAs

The choice of the gRNAs LTR A/B was determined through previously obtained results [180, 184] using Jack Lin's CRISPR/Cas9 gRNA finder tool ([http:// spot.colorado.edu/~slin/cas9.html](http://spot.colorado.edu/~slin/cas9.html)). The same tool was used to search for sense and antisense sequences targeting the LTR-Gag sequence of HIV-1 genome for saCas9/gRNA target sites containing 20 bp gRNA targeting sequence plus the PAM sequence (5'NNGRRT3')

3.19 Transduction of Tg26 MEFs

1.4×10^5 cells were plated in a 6-well dish and incubated overnight at 37°C. To improve transduction efficiency of transduction, ViraDuctin™ AAV Transduction Kit (Cell biolabs, USA) was utilized. Briefly, after warming the ViraDuctin™ at RT for 10 minutes, 100 µl of ViraDuctin™ AAV Transduction Reagent A (20X) was mixed with 20 µl of AAV Transduction Reagent B (100X) and incubated for 5 minutes at RT. After 1.88 ml of growth medium was added to the mix and incubated for 5 minutes, then added to the cells after aspiration of the old cell medium. 24 hours later the medium was replaced, and the cells were washed 2 times with complete culture medium. 10^5 and 10^6 viral inoculums were prepared in 1 ml Opti-Mem, and 500 µl of mix was added to each well and incubated at 37°C, gently shaking every 30 minutes. 1 ml of DMEM

was added after 1 hour of incubation. The next day, the inoculum was aspirated, and cells were washed with PBS. Cells were harvested 1 week later and analyzed for the presence of viral excision by PCR.

3.20 *In vivo* rAAV9:saCas9/gRNA administration

Transgenic mice Tg26 mice carry a transgene derived from the genome of HIV-1NL4-3 [192] and rats were used to test the ability of the rAAV9 saCas9/gRNA construct to perform gene editing *in vivo*. Experiments on animals were performed in our laboratory by Dr. Jennifer Gordon. Briefly 100 μ l of AAV9 (2.73×10^{12}) or 100 μ l of PBS for control animals was injected via the tail vein in 4 transgenic mice at day 0 and day 5. At 5 days, a blood sample of 2 animals (treated and PBS) was harvested and the animals were then sacrificed. The second pair of animals were subjected to a second tail vein injection of AAV9 or PBS after 5 days, and blood and tissues were collected one week later. The tissues collected include the brain, heart, lung, liver, kidney, spleen and peripheral blood. A similar approach was used to treat rats (2 female and 2 male) with 2 injections at 5 days intervals. Tissues were collected after 10 days following the 1st injection for DNA and RNA analysis.

3.21 *Analysis of DNA in Animal Models*

For the analysis of DNA from MEFs and from tissues of animal models, 300 ng of DNA underwent PCR or nested PCR (for tissue samples) using the Fail-Safe Kit, buffer D and the primers listed in Table 6. The first step of amplification used the following conditions: 94 °C for 5 min, 30 cycles (94 °C for 30 s, 55 °C for 30s, 72 C for 30s), 72 °C for 5 min. The PCR products were resolved in a 1% agarose gel. 3 μ l of the first PCR reaction was used to perform nested PCR under the same conditions of the first step. DNA obtained from rat samples was subjected to PCR (one step) using LTR Fw 1 step and Gag Rev 2 step primers. DNA extracted

from tissues of humanized mice underwent other sets of PCRs to detect the presence of viral excision from GagD to 3' LTR and from the 5'-LTR to the 3'-LTR of HIV-1 regions using the primers listed in table 6. Nested PCR was performed to detect the excision from GagD to 3'LTR using 300 ng of DNA and Fail-Safe kit, buffer D in 50 µl of reaction processed under the following condition: 94 °C for 5 min, 30 cycles (94 °C for 30 s, 57 °C for 30s, 72 C for 40s), 72 °C for 5 min. 1µl of the first step of PCR was used for the second step following the same protocol. Detection of excision from 5' to 3'LTR 300 ng of DNA was assessed by standard PCR conditions, 94 °C for 5 min, 30 cycles (94 °C for 30 s, 55 °C for 30s, 72 C for 30s), 72 °C for 5 min. After gel purification of PCR products and cloning into the TA vector, the DNA was sent for sequencing (Genewiz, USA) and aligned in Clustal Omega software (Cambridgeshire, UK) using HIV-1 NL4-3 sequence served as a reference. Human beta globin and mouse beta globin PCRs were performed as a loading control (94 °C for 5 min, 30 cycles at 94 °C for 30 s, 55 °C for 30s, 72 C for 30s, 72 °C for 5 min). 50 ng of DNA from spleen of humanized mice was subjected to absolute quantification (qPCR) for Gag and Pol gene presence as previously described.

3.22 RNA Analysis of Rats and Humanized Mice Samples

RNA isolation was performed on rat and humanized mice tissues using Trizol reagent (Ambion, Foster City, CA, USA) and subjected to DNAase I treatment. 1µg of RNA was retro-transcribed into cDNA using M-MLV reverse transcription (Invitrogen, USA) as described in appendix D3. qPCRs specific for gag and env were performed in a LightCycler480 (Roche, Basel, Switzerland) using 50 ng of rat cDNA and data were normalized to the rat beta actin gene (table 6). qPCR reactions were

performed as follows: 98 °C 3 min, 45 cycles (98 °C 15 s, 60 30s, 72 1min).

50 ng of humanized cDNA from spleen was used for PCR analysis to assess Cas9 and gRNA expression, using beta actin as a loading control.

3.23 Statistical Analysis

qPCR and luminometric assay results were analyzed as means \pm standard deviation. $p < 0.05$ was considered statically significant for student T test.

primer	sequence
Cloning pX260-LTR-Cas9 constructs	
Kpn1-LTR (-454)-S	5'-GGTACCTGGAAGGGCTAATTTGG-3'
Kpn1-LTR (-120)-S	5'-GGTACCTCGAGCTTTCTACAAGG-3'
Xba1-LTR (-80)-S	5'-TCTAGAGGAGGTGTGGCCTGGGC-3'
LTR (+66)-Nco1-AS	5'-CCATGGTAAGCAGTGGGTTCC-3'
Cloning lentiLTR(-80/+66)-Cas9-Blast construct	
Nhe1-LTR(-80)-S	5'-GCTAGCGGAGGTGTGGCCTGGGC-3'
LTR(+66)-Xba1-AS	5'-TCTAGATAAGCAGTGGGTTCC-3'
Cloning px601SaCa9LTR1GagD construct	
LTR1 T708 F	5'-CACCGCAGAACTACACACCAGGGCC-3'
LTR1 T709 R	5'-AAACGGCCCTGGTGTGTAGTTCTGC-3'
Gag D 760 F	5'-CACCGGATAGATGTAAAAGACACCA-3'
Gag D 761 R	5'-AAACTGGTGTCTTTTACATCTATCC-3'
LTR PCRs	
LTR -417/S 2step	5'-GATCTGTGGATCTACCACACACA-3'
LTR -19/AS 2step	5'-GCTGCTTATATGTAGCATCTGAG-3'

LTR -374/S 1 step	5'-TTAGCAGAACTACACACCAGGGCC-3'
LTR +43/AS 1 step	5'-CCGAGAGCTCCCAGGCTCAGATCT-3'
b- actin Fw	5'-CTACAATGAGCTGCGTGTGGC-3'
b-actin Rev	5'-CAGGTCCAGACGCAGGATGGC-3'
5'UTR fw	5'GTTCTGGGCGCCACTGCTAGA3'
5UTR rev	5'TTAAGCCTCAAAGCTTGCC3'
Taqman qPCRs	
HIV-1 Gag Fw	5'-AAGTAGTGTGTGCCCGTCTG-3'
HIV-1 Gag Rev	5'-TCGAGAGATCTCCTCTGGCT-3'
HIV-1 Gag Probe	5'-FAM-CTGTTCTGGGCGCCACTGCTA-ZEN- IowaBlackFQ-3'
Hs b-globin Fw	5'-CCCTTGGACCCAGAGTTCT-3'
Hs b-globin Rev	5'-CGAGCACTTTCTTGCCATGA-3'
Hs b-globin probe:	5'-FAM-GCGAGCATCTGTCCACTCCTGATGCTGTTA TGGGCGCTCGC-ZEN-IowaBlackFQ-3'
Hs b-actin F	5'-TGGACTTCGAGCAAGAGATG-3'
Hs b-actin R	5'-GAAGGAAGGCTGGAAGAGTG-3'
Hs b-actin probe:	5'-FAM-CGGCTGCTTCCAGCTCCTCC-ZEN- IowaBlackFQ-3'

primer	sequence
LTR1 GagD PCR	
LTR fw 1 step	5'-AATTGCGGCCGCTGGAAGGGCTAATTTGGTCCC-3'
Gag rev 1 step	5'-TGTCACCTCCCTTGGTTCTCTC-3'
LTR fw 2 step	5'-AAAAGAATTCGTGGATCTACCACACACAAGGC-3'
Gag rev 2 step	5'-AAAAGGATCCACCATTTGCCCTGGAGGTT-3
Gag-3'LTR PCR	
Gag fw 1 step	5'- GAAAGCGAAAGTAAAGCCAGAGGAGAT-3
3'LTR rev 1 step	5'-ACACAACAGACGGGCACACACTACTT -3'
Gag fw 2 step	5'AAAAGAATTCGACAGCTACAACCATCCCTTCAGACAG-3'
3'LTR rev 2 step	5'-AAAAGGATCCAGCAGTGGGTTCCCTAGTTAGCCAG-3'
5'LTR-3'LTR	
LTR -417	5'-GATCTGTGGATCTACCACACACA-3'
LTR -19	5'-GCTGCTTATATGTAGCATCTGAG-3'
Reference	
Mouse beta globin fw	5'-CCCTTGGACCCAGCGGTACT-3'
Mouse beta globin rev	5'-GTTATCACCTTCTTGCCATG-3'
Hs b-actin F	5'-TGGACTTCGAGCAAGAGATG-3'
Hs b-actin R	5'-GAAGGAAGGCTGGAAGAGTG-3'
Taqman qPCRs	
HIV-1 pol/int F	5'-TCCAGCAGAGACAGGGCAAG-3'
HIV-1 pol/int R	5'-TGCCAAATTCCTGCTTGATCCC-3'
HIV-1 pol/int probe	5'-HEX-CGCCCACCAACAGGCGGCCTTAAGT-ZEN-lowaBlackFQ-3'
HIV-1 Env F	5'- TCCTTGGGATGTTGATGATCT-3'
HIV-1 Env R	5'- TGGCCCAAACATTATGTACC-3'
HIV-1 Env probe	5'-FAM-TGGTGGTTGCTTCTTTCCACACA-ZEN-lowaBlackFQ-3'
Beta actin rat fw	5' AGCGCAAGTACTCTGTGTGG3'
Beta actin rat rev	5' AACAGTCCGCCTAGAAGCAT 3'
Beta actin rat probe	5'-FAM-CCTCCATGGTGCACCGCAA -ZEN-lowaBlackFQ-3'

RT-PCRs	
LTR 1 fw	5'-GCAGAACTACACACCAGGGCC-3'
Gag D fw	5'-GGATAGATGTAAAAGACACCA-3'
pX601gRNAscaffold/R	5'-CGCCAACAAGTTGACGAGAT-3'
SaCas9/263/F	5'-TCGACTACAACCTGCTGACC-3'
SaCas9/SEQ1	5'-GGTGGGCTTCTTCTGCTT-3'
b- actin fw	5'-CTACAATGAGCTGCGTGTGGC-3'
b- actin rev	5'-CAGGTCCAGACGCAGGATGGC-3'

Table 6: Primer Sequences for PCR and qPCR Assays

4. Results

4.1 Determination of the minimal promoter region activated by Tat

To test the ability of Tat to activate different regions of the LTR promoter, TZM-bl cells were co-transfected with pCMVTat or pCMV and px260 LTRCas9 (-456/+66, or 120/+66 or (-80/+66). At 48 hours, cells were harvested and processed for DNA and total protein extraction. Western blot analysis showed that Tat induces Cas9 expression (160KDa) in all three LTR constructs tested. A low level of Cas9 expression is detected in the absence of pCMVTat, suggesting a basal activation of LTR promoter by cellular transcriptional factors. Tubulin serves as the loading control (Figure14).

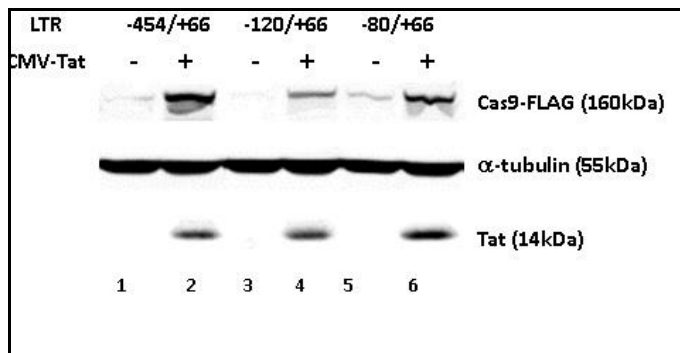


Figure 14: Determination of the minimal promoter region activated by Tat. Western blot was performed on TZM-bl protein lysates co-transfected with pCMVTat/ pCMV and three different px260 constructs harboring three regions spanning the HIV-1LTR Promoter (-456/+66)/ (-120/+66) or (-80/+66) for the detection of Cas9FLAG (160 KDa), α -tubulin (55kDa) and Tat (14 kDa). Lane 1-2: transfection with px260LTR -456/+66, lanes 3-4: transfection with px260LTR -120/+66, lanes 5-6: transfection with px260LTR -80/+66. (Figure reproduced with permission from Kaminski R. *et al.*, 2016 and a Creative Commons CC-BY license) [185].

After showing the ability of Tat to activate the minimal promoter LTR -80/+66, further studies were designed to evaluate the efficiency of delivery of LTR (-80/+66) spCas9 system in TZM-bl and Jurkat 2D10 cells using a

lentiviral delivery system. After this result, we evaluated the ability of Tat to activate integrated copies of spCas9 gene and induce the excision of viral DNA in HIV-1 infected TZM-bl LTRSaCas9 stable cell line and in latently infected Jurkat 2D10 LTRSaCas9 stable cell line. At the end we analyze the capacity of spCas9 system in Jurkat cells to induce gene editing in the early stage of HIV-1 infection investigating the possibility to produce a vaccine able to prevent HIV-1 reinfection.

Studies *in vivo* were also performed to test the efficiency of AAV9 delivery and gene editing strategy in animal models using a shorter version of Cas9, saCas9.

4.2 Increase of Cas9 expression in the presence of Tat

After developing a lentiviral vector carrying SpCas9 gene under the control of LTR (-80/+66) promoter, TZM-bl cells were transduced with adGFP MOI 15 and adTat MOI 3 and 15. At 24 hours, cells were treated with a lentiviral vector containing SpCas9, gRNAs A/B or empty vector to test lentiviral delivery of spCas9 to cells and to induce gene editing. Analysis by western blot at 48 hours assessed the production of Cas9 after transduction. Results showed increased production of Cas9 in the presence of Tat (lane 5-12) and a homogenous level of tubulin expression (figure 15). These results suggest that Tat transduction induces Cas9 expression in the model system.

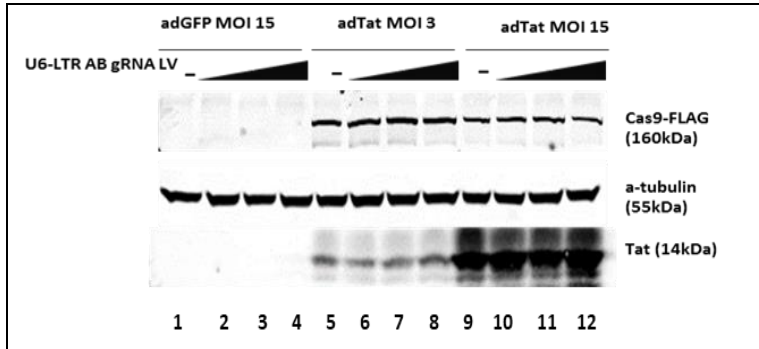


Figure 15: Cas9 expression is activated by Tat. Western Blot of TZM-bl protein lysates transduced with adGFP MOI 15 and adTat MOI 3 and 15 and treated with pKLV-gRNA-empty (MOI 8,6,4 and 0) and pKLV-gRNA LTR A and B (MOI 0/0, 1/1, 2/2 and 4/4) and lenti LTRCas9. Lane 1-4: transduction with adGFP MOI 15, lanes 5-8: transduction with adGFP MOI 12 and adTat MOI 3, lanes 9-12: transduction with adTat MOI 15. A-tubulin was used like loading control. Cas9 production is activated by Tat (lanes 5-12). (Figure reproduced with permission from Kaminski R. *et al.*, 2016 and Creative Commons CC-BY license) [185].

4.3 Viral excision increases in presence of Tat and gRNAs

DNA was extracted from the same cells at 48 and 96h, and analyzed with PCR specific for the LTR region. PCR products of 395 base pairs and 205 base pairs, corresponding to the full length LTR and the truncated LTR, were detected in presence of Tat and gRNAs A/B (lane 6-8, 10-12) at 48 and 96h, likewise in the absence of Tat at 96h (lane 4). The truncated LTR product, indicating viral promoter excision, is not visible in the negative control (absence of gRNAs, lane 1/5/9), (figure 16). The sequence of truncated LTR promoter was analyzed in BLAST using the HIV-1 NL4-3 sequence as reference. Results revealed the presence of editing of a190 bp region in the LTR promoter region. Full length and truncated LTR sequences of one sample (lane 6) are shown in figure 17.

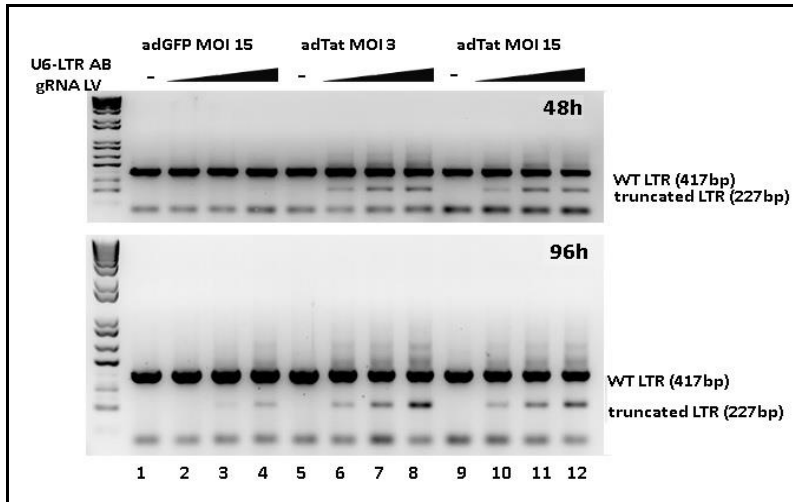


Figure 16: Increased viral excision in presence of Tat and gRNAs. TZM-bl Cells were transduced adGFP MOI 15 and adTat MOI 3 and 15 and treated with pKLV-gRNA-empty (MOI 8,6,4 and 0) and pKLV-gRNA LTR A and B (MOI 0/0, 1/1, 2/2 and 4/4) and lenti LTRCas9. PCR analysis was performed at 48 H (top) and 96 H (bottom). Lane 1-4: transduction with adGFP MOI 15, lanes 5-8: transduction with adGFP MOI 12 and adTat MOI 3, lanes 9-12: transduction with adTat MOI 15. (Figure reproduced from Kaminski R. *et al.*, 2016 and Creative Commons CC-BY license) [185].

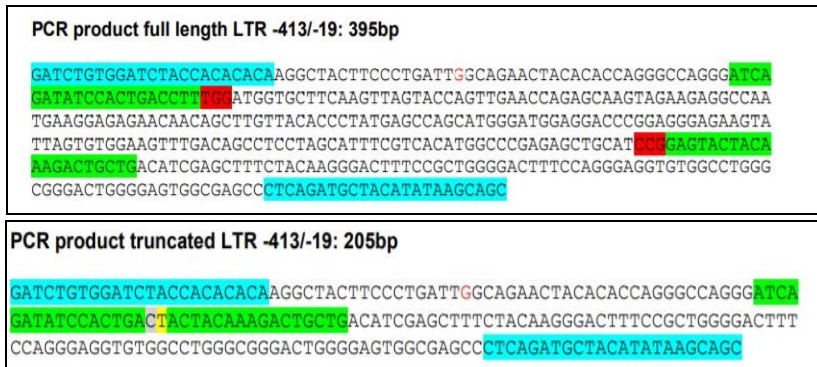
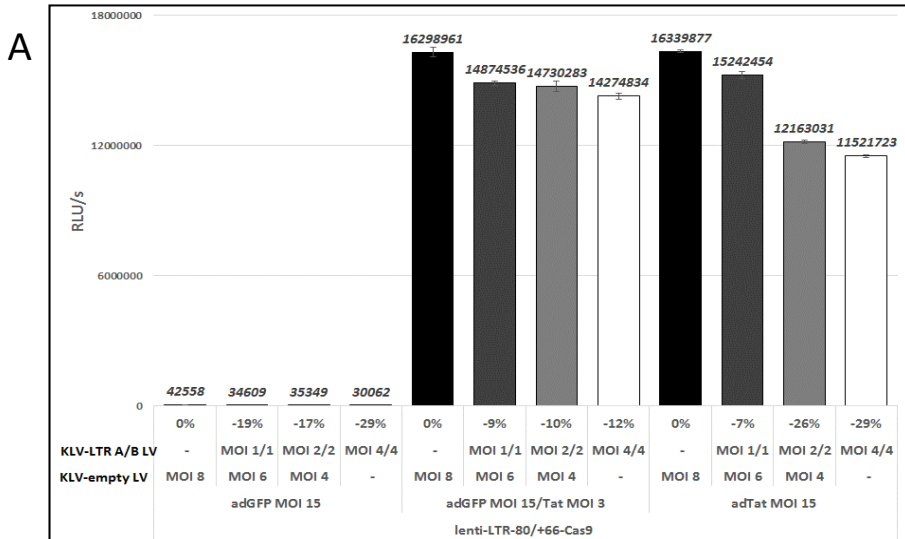


Figure 17: DNA analysis of truncated LTR confirms viral excision: After gel purification of PCR on TZM-bl cells transduced with adGFP MOI 15 and adTat MOI 3 and 15 and treated with pKLV-gRNA-empty (MOI 8,6,4 and 0) and pKLV-gRNA LTR A and B (MOI 0/0, 1/1, 2/2 and 4/4) and lenti LTRCas9 the DNA was cloned in TA and sent for sequencing. Sequences were aligned to the reference LTR region of the HIV-1_{NL4-3} sequence. Sequences

of gRNA A and B are Highlighted in Green, Primers in Blue, and the PAM Sequence in Red. (Figure reproduced from Kaminski R. *et al.*, 2016 and Creative Commons CC-BY license) [185].

4.4 Decreased LTR promoter activity in presence of Tat

LTR promoter excision was assessed through a luciferase assay of transduced TZM-bl cells. At 48 and 96 hours, supernatants of the transduced cells were collected and processed to determine luciferase activity. As shown in figure 18a (48h) and 18b (96h), the transcriptional activity of the LTR promoter decreased in the presence of Tat and gRNAs A/B. A basal activity of the LTR promoter is observed in the presence of adGFP MOI 15, which likewise decreased in the presence of gRNAs. Cells treated with increasing concentrations of gRNAs showed the higher level of viral DNA excision after 48h of incubation. These results corroborate with data obtained from PCR assays.



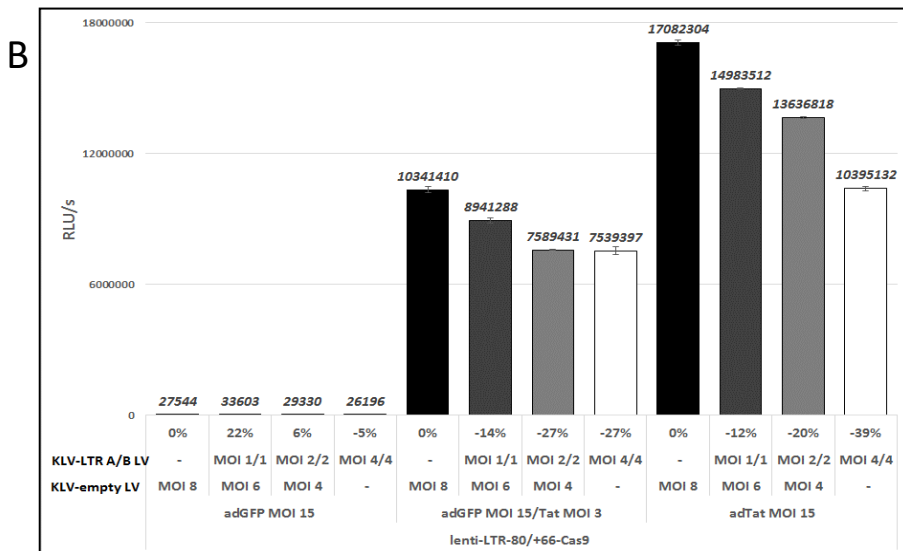


Figure 18 A/B: Decrease of LTR promoter activity in presence of Tat. Luciferase Assays on TZM-bl cells transduced with adGFP MOI 15 and adTat MOI 3 and 15 and treated with pKLV-gRNA-empty (MOI 8,6,4 and 0) and pKLV-gRNA LTR A and B (MOI 0/0, 1/1, 2/2 and 4/4) and lenti LTRCas9 at 48 Hours (18A) and 96 Hours (18B) post-Lentiviral transduction. (Figure reproduced from Kaminski R. *et al.*, 2016 and Creative Commons CC-BY license) [185].

4.5 Cas9 expression is activated during HIV-1 infection

To investigate the efficacy of excision of viral DNA during the early stages of HIV-1 infection, new experiments were conducted on TZM-bl pX260-LTR (-80/+66)-Cas9 stable line. 24 hours after transduction with different MOIs of LV-gRNAs A/B (MOI 0/0, 1/1, 2/2 and 4/4) and pKLV-gRNA-empty (MOI 8,6,4 and 0), the cells were infected with HIV-1_{JRFL} or HIV-1_{SF162}. Analysis of WB showed activation of Cas9 protein in presence of Tat produced during HIV-infection. Equal amounts of the house keeping gene α -tubulin were detected (Figure 19).

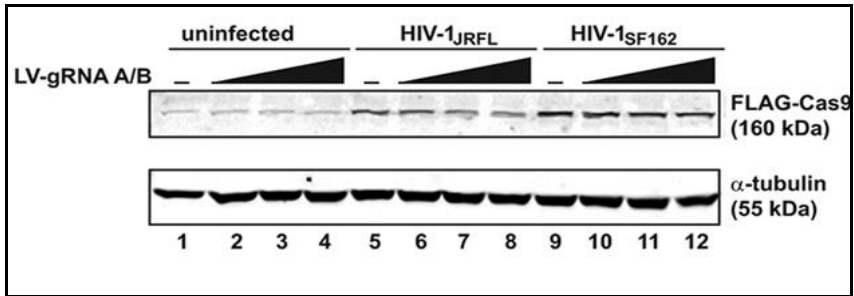


Figure 19: Cas9 expression during HIV-1 infection. Western Blot was performed on protein lysates from the pX260-LTR (-80/+66)-Cas9 Stable Cell Line transduced with pKLV-gRNA-empty (MOI 8,6,4 and 0) and pKLV-gRNA LTR A and B (MOI 0/0, 1/1, 2/2 and 4/4) and Infected with HIV-1_{JRFL} or HIV-1_{SF162}. (Figure reproduced from Kaminski R. *et al.*, 2016 and Creative Commons CC-BY license) [185].

4.6 Tat protein expression drives viral excision.

PCR assay analyzed the presence of viral editing after Tat-mediated Cas9 activation. A truncated LTR fragment (205 bp) was detected in the presence of HIV-1_{JRFL} infection with gRNAs A/B (lane 6-8, figure 20). The different results obtained between the two HIV-1 viral strains may be the result of a differential ability of these viruses to infect TZM-bl cells. A higher level of infectivity by HIV-1_{SF162} virus may explain the higher level of Cas9 protein detected in western blot (figure 19). However, it must be noted that a high production of viral DNA may reduce the final total amount of edited product which is not easily detected by PCR.

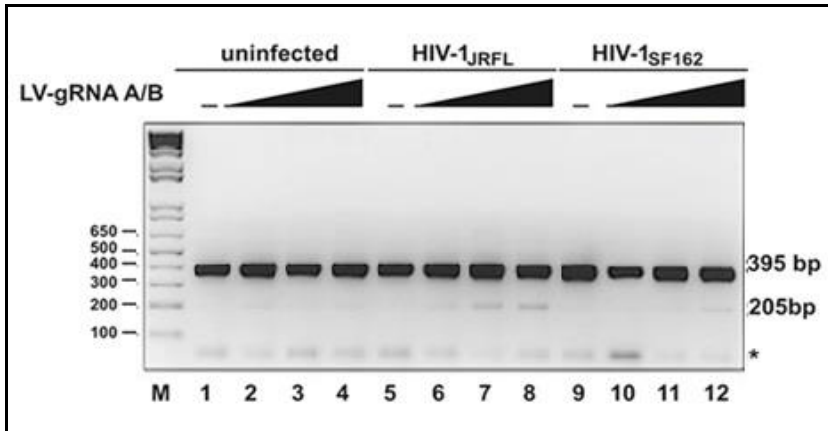


Figure 20: Tat protein production drives viral excision: PCR Analysis of the pX260-LTR (-80/+66)-Cas9 Stable Cell Line Transduced with pKLV-gRNA-empty (MOI 8,6,4 and 0) and pKLV-gRNA LTR A and B (MOI 0/0, 1/1, 2/2 and 4/4) and Subsequently Infected with HIV-1_{JRFL} or HIV-1_{SF162}. Lanes 1-4 uninfected cells, lanes 5-8 cells infected with HIV-1 JRFL, lanes 9-12 cells infected with HIV-1 SF162. LTR full length is detected at 395 bp, truncated LTR at 205 bp. (Figure reproduced from Kaminski R. *et al.*, 2016 and Creative Commons CC-BY license) [185].

4.7 Decreased LTR promoter activity during HIV-1 infection

At 48 hours post-infection, cells were harvested and processed for analysis with a luciferase assay to assess the ability of Cas9 to interfere with the transcriptional activity of the LTR promoter in the TZM-bl pX260-LTR (-80/+66)-Cas9 stable line. Luciferase activity decreased in the presence of both HIV-1 strains, and was directly correlated to the amounts of gRNAs used (higher decrease for MOI 4/4, figure 21).

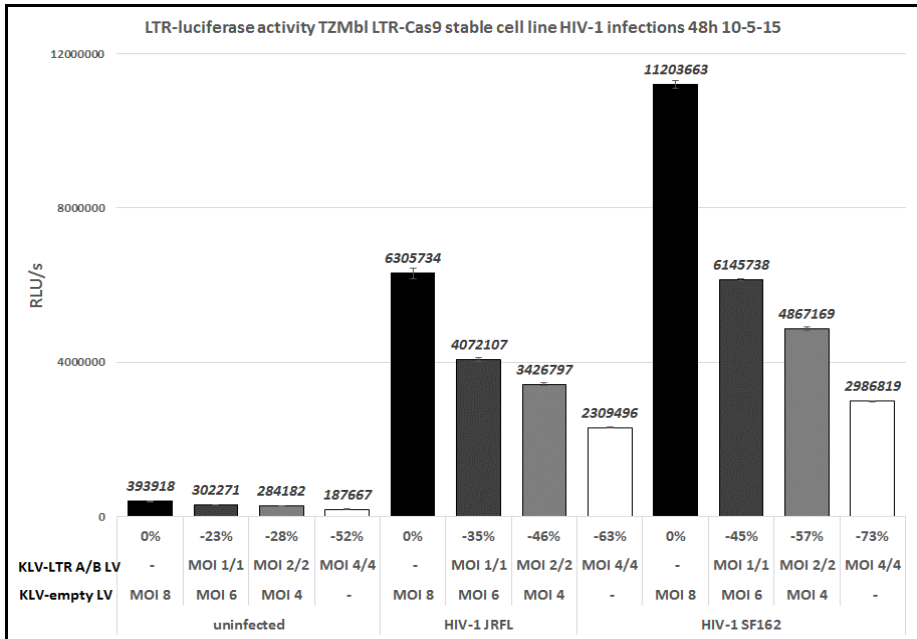


Figure 21: Decreased LTR promoter activity in presence of Tat Detection of the transcriptional activity of the pX260-LTR (-80/+66)-Cas9 stable cell line transduced with pKLV-gRNA-empty (MOI 8,6,4 and 0) and pKLV-gRNA LTR A and B (MOI 0/0, 1/1, 2/2 and 4/4) and subsequently infected with HIV-1_{JRFL} or HIV-1_{SF162}. On the left side uninfected cells, in the middle HIV-1 JR-FL infected cells, on the left side HIV-1 SF162 infected cells. (Figure reproduced from Kaminski R. *et al.*, 2016 and Creative Commons CC-BY license) [185].

4.8 Cas9 expression in Jurkat 2D10 cells as model of latently infected cells

Next, the ability of our system to excise the virus from latently infected cells was assessed. A similar experiment to the previously described experiments was conducted using Jurkat 2D10 cells; a cell line that harbors integrated copies of HIV-1 NL4-3, whose genome lacks a portion of the Gag and Pol genes, as well as possessing the reporter green fluorescent protein (GFP) replacing the Nef gene. The 2D10 cells were transduced with lenti-SpCas9 LTR -80/+66 plasmid to generate a stable cell line with integrated copies of LTR -80/+66-Cas9 gene. The 2D10 stable

cell line was transduced with pKLV (6 μ g) or pKLV -gRNAs A/B (3 μ g of each) and with pCMV or pCMV-Tat plasmid (0 μ g, 1 μ g, 2 μ g, 6 μ g). Western blot analysis at 48 hours revealed an increased level of Cas9 and GFP expression in the presence of Tat. The level of GFP protein decreased in presence of higher concentration of gRNAs A/B and Tat, suggesting that HIV transcription was decreased. The basal level of Cas9 expression may be attribute to the low constitutive level of Tat expression in 2D10 cells line (figure 22).

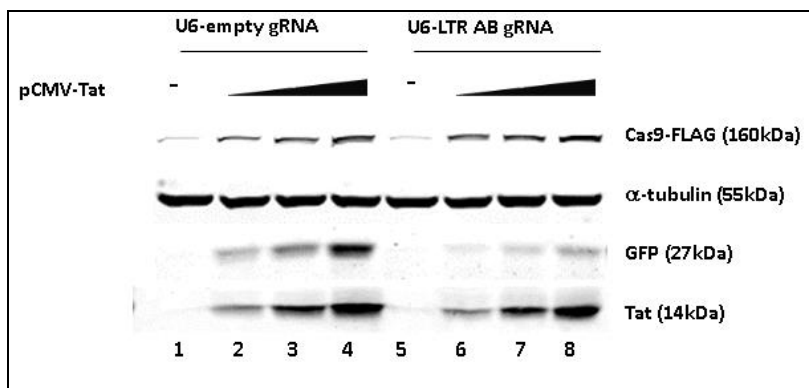


Figure 22: Cas9 expression in Jurkat 2D10 cells. Western Blot analysis for the detection of Cas9, GFP and Tat in the Jurkat 2D10-LTR (-80/+66)-Cas9 stable cell line transduced with pKLV-gRNA-empty (6 μ g) and pKLV-gRNA LTR A and B (3 μ g of each) in presence of pCMV-Tat86 (0,1,2,6 ug) and pcDNA3.1. α -tubulin was used like loading control. Lanes 1-4 cells transduced with pKLV-gRNA-empty, lanes 5-8 cells transduced with and pKLV-gRNA LTR A and B. (Figure reproduced from Kaminski R. *et al.*, 2016 and Creative Commons CC-BY license) [185].

4.9 Viral excision in the Jurkat 2D10 cell model of latently infected cells

Specific PCR for the detection of the LTR promoter showed the presence of a truncated LTR region (227 base pairs) in presence of gRNAs and Tat (Figure 23 lanes 5-8). Analysis of the truncated LTR sequences confirmed the excision of 190 bp fragment between gRNA A and B in LTR promoter

(Figure 24). Excision efficiency was determined as a percentage of the ratios between truncated versus full length LTR and quantified by qPCR assay. Results were expressed in percentage of cut efficiency of treated cells versus untreated (figure 25).

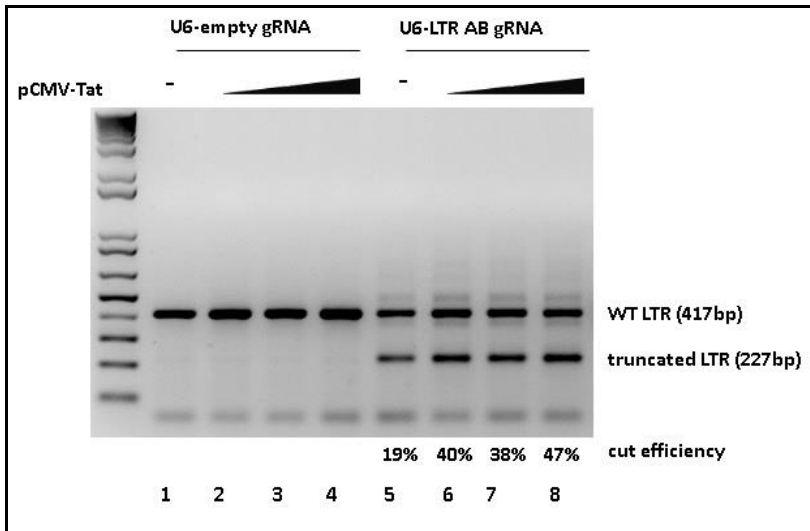


Figure 23: Viral excision in a model of HIV-latent infection. PCR Assay of the Jurkat 2D10-LTR (-80/+66)-Cas9 stable cell line transduced with pKLV-gRNA-empty (6 ug) and pKLV-gRNA LTR A and B (3ug for each) in presence of pCMV-Tat86 (0,1,2,6 ug) and pcDNA3.1. Lanes 1-4 cells transduced with pKLV-gRNA-empty, lanes 5-8 cells transduced with and pKLV-gRNA LTR A and B. Percent of viral excision is showed on the bottom after qPCR quantification of LTR region. (Figure reproduced from Kaminski R. *et al.*, 2016 and Creative Commons CC-BY license) [185].

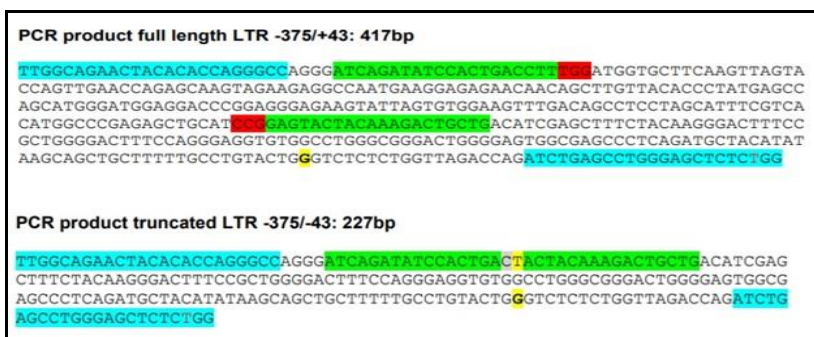


Figure 24: Sequence analysis of the truncated LTR Fragment. Sanger sequencing was performed to analyse the sequence of LTR truncated fragment after PCR in the Jurkat 2D10-LTR (-80/+66)-Cas9 stable cell line following transduction with pKLV-gRNA LTR A and B (3ug for each) in the presence of Tat (6ug). (Figure reproduced from Kaminski R. *et al.*, 2016 and Creative Commons CC-BY license) [185].

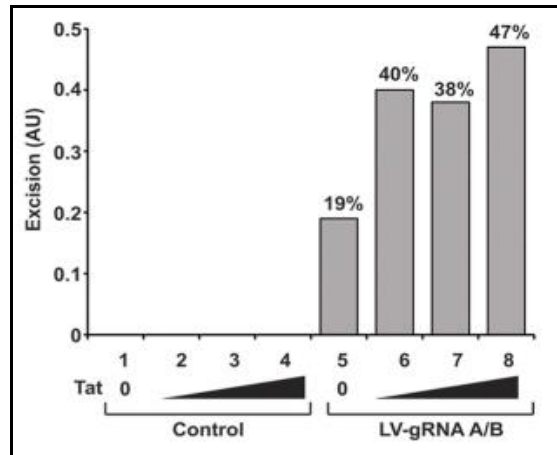


Figure 25: Excision Percentage of the LTR Promoter region. qPCR was performed in Jurkat 2D10-LTR (-80/+66)-Cas9 Stable Cell Line transduced with pKLV-gRNA-empty (6 µg) and pKLV-gRNA LTR A and B (3 µg for each) in presence of pCMV-Tat86 (0,1,2,6 ug) and pcDNA3.1. Data are represented as arbitrary units (AU). (Figure reproduced from Kaminski R. *et al.*, 2016 and Creative Commons CC-BY license) [185].

4.10 GFP reduction in Jurkat 2D10 cells as model of latently infected cells

To investigate the ability of Tat to activate the LTR promoter, flow cytometry analysis was performed to quantify the number of GFP, an index of viral reactivation. An increased percentage of GFP cells was detected in the presence of Tat and in absence of gRNAs. The percentage of viral reactivation drastically decreases when gRNAs are expressed and Cas9 is induced by Tat (figure 26)

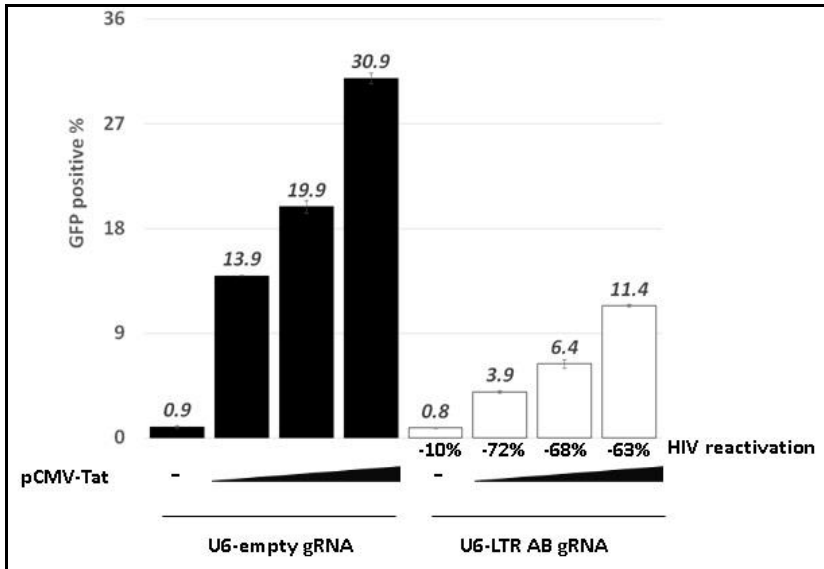


Figure 26: Decrease of viral reactivation. Analysis of flow cytometry was performed on Jurkat 2D10-LTR (-80/+66)-Cas9 stable cell line transduced with pKLV-gRNA-empty and pKLV-gRNA LTR A and B (3 μg of each) in presence of pCMV-Tat86 (0,1,2,6 ug) and pcDNA3.1 to detect GFP expression. (Figure reproduced from Kaminski R. *et al.*, 2016 and Creative Commons CC-BY license) [185].

4.11 Viral excision in Jurkat cells during the early stage of infection

To evaluate the possibility of vaccine generation based on a gene editing strategy, further studies were performed on Jurkat cells to evaluate the presence of Cas9 in the cells as protection from HIV-1 reinfection. Jurkat cells were transduced with pLENTI-LTR-Cas9 (-80/+66) Cas9 (MOI 1), pKLV-gRNA (MOI1/1) or pKLV negative control (MOI2). At 24 hours cells were infected with HIV-1 NL4-3 EGFP-P2APNef.

PCR analysis was performed at 3 and 5 days post-infection, revealing the presence of a truncated LTR fragment (205 bp) whose intensity is higher at day 5, possibly due to increased production of Tat and subsequent Cas9

activation (figure 27). Indel mutations were detected by analysis of 10 clones (trunc LTR 1-10) of the truncated LTR fragment amplified at day 5 (clones 2/6/8/10, figure 28).

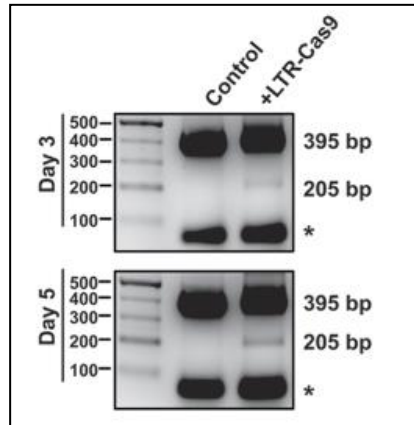


Figure 27: Viral excision in Jurkat Cells at the early stage of infection. Jurkat cells were transduced with pLENTI-LTR-Cas9 (-80/+66) Cas9 (MOI 1) and pKLV-gRNA (MOI1/1) or pKLV Negative Control (MOI2) and infected with HIV-1 NL4-3 EGFP-P2APNef (MOI 0.01). Analysis PCR was performed at 3 and 5 days post infection for the detection of LTR region. (Figure reproduced from Kaminski R. *et al.*, 2016 and Creative Commons CC-BY license) [185].

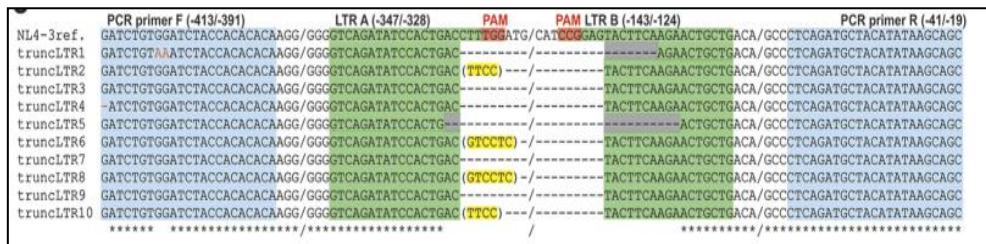


Figure 28: Sequence Analysis of Truncated LTR Fragments. Jurkat cells were transduced with pLENTI-LTR-Cas9 (-80/+66) Cas9 (MOI 1) and pKLV-gRNA (MOI1/1) or pKLV negative control (MOI2) and infected with HIV-1 NL4-3 EGFP-P2APNef (MOI 0.01). After PCR analysis the truncated LTR fragment was gel purified, cloned in TA vector and sent for Sanger sequencing. Sequence of HIV-1NL4-3 was used as reference. Yellow highlights the presence of indel mutations. (Figure reproduced from Kaminski R. *et al.*, 2016 and Creative Commons CC-BY license) [185].

To investigate if gene editing occurs between the 5’LTR and 3’LTR, PCRs specific for genes positioned in the middle of HIV-1 sequence, 5’UTR (+97 to +235) and env (+5828 to +5977)) were performed at 3 and 5 days post-infection. PCRs showed the presence of 139 and 150 bp fragments, respectively, whose intensities decreased at day 5 compared to day 3. Amplification of the housekeeping gene beta actin (270 bp) was used as a loading control (figure 29).

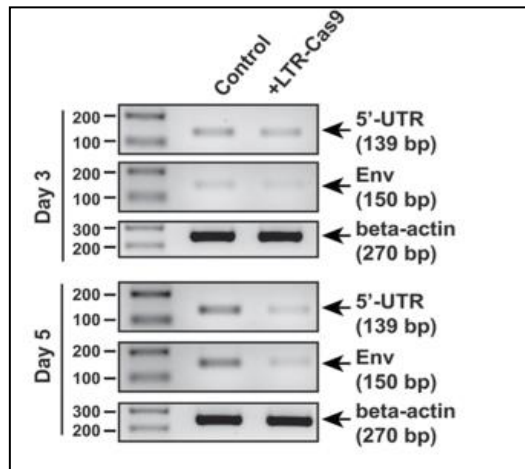


Figure 29: Excision of the viral DNA between LTR regions. PCR Assay was performed on Jurkat Cells transduced with pLENTI-LTR-Cas9 (-80/+66) Cas9 (MOI 1) and pKLV-gRNA (MOI1/1) or pKLV Negative Control (MOI2) and infected with HIV-1 NL4-3 EGFP-P2APNef (MOI 0.01) at 3 and 5 days after infection for the detection of viral DNA region between LTR regions. Beta actin DNA was used as quality control. (Figure reproduced from Kaminski R. *et al.*, 2016 and Creative Commons CC-BY license) [185].

4.12 GFP reduction in Jurkat cells on the early stage of infection

To investigate the ability of Cas9 to protect cells from HIV-1 reinfection, the level of GFP positive cells was calculated as marker of viral expression. A decrease of positive cells was observed at day 3 (-64%), 5 (-84%) and 8 (-88%) post infection, revealing the ability of Cas9 to suppress viral expression at early stages of infection (Figure 30).

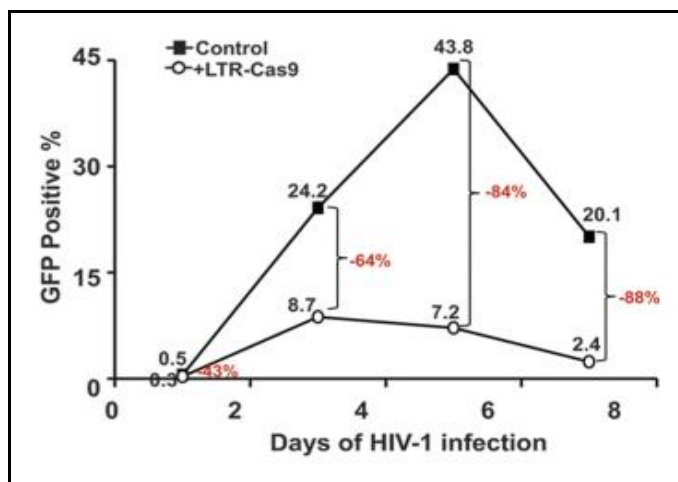


Figure 30: GFP reduction in Jurkat cells on the early stage of infection. Flow cytometry assay detection of GFP positive Jurkat Cells transduced with pLENTI-LTR-Cas9 (-80/+66) Cas9 (MOI 1) and pKLV-gRNA (MOI1/1) or pKLV Negative Control (MOI2) and infected with HIV-1 NL4-3 EGFP-P2APNef (MOI 0.01) at day 3, 5 and 7 post infection. (Figure reproduced from Kaminski R. *et al.*, 2016 and Creative Commons CC-BY license) [185].

4.13 Reduction of GFP protein levels in presence of gRNAs and Cas9 in Jurkat cells

The presence of gRNAs and LTR Cas9 was assessed using fluorescence microscopy with BFP as a marker. The presence of gRNAs and lentiviral vector encompassing Cas9 and gRNAs was visually detected (figure 31 top). Analysis of GFP showed decreased positive cells in the presence of Cas9 and gRNAs compared to gRNAs only (figure 31 middle). Qualitative and quantitative analysis was performed using light microscopy, showing no cytopathic effects and a comparable number of cells. Cells treated with LTR-Cas9/gRNAs appeared healthy and possessed no morphological changes, suggesting a lack of cytotoxicity by gene editing (figure 31 bottom and figure 32).

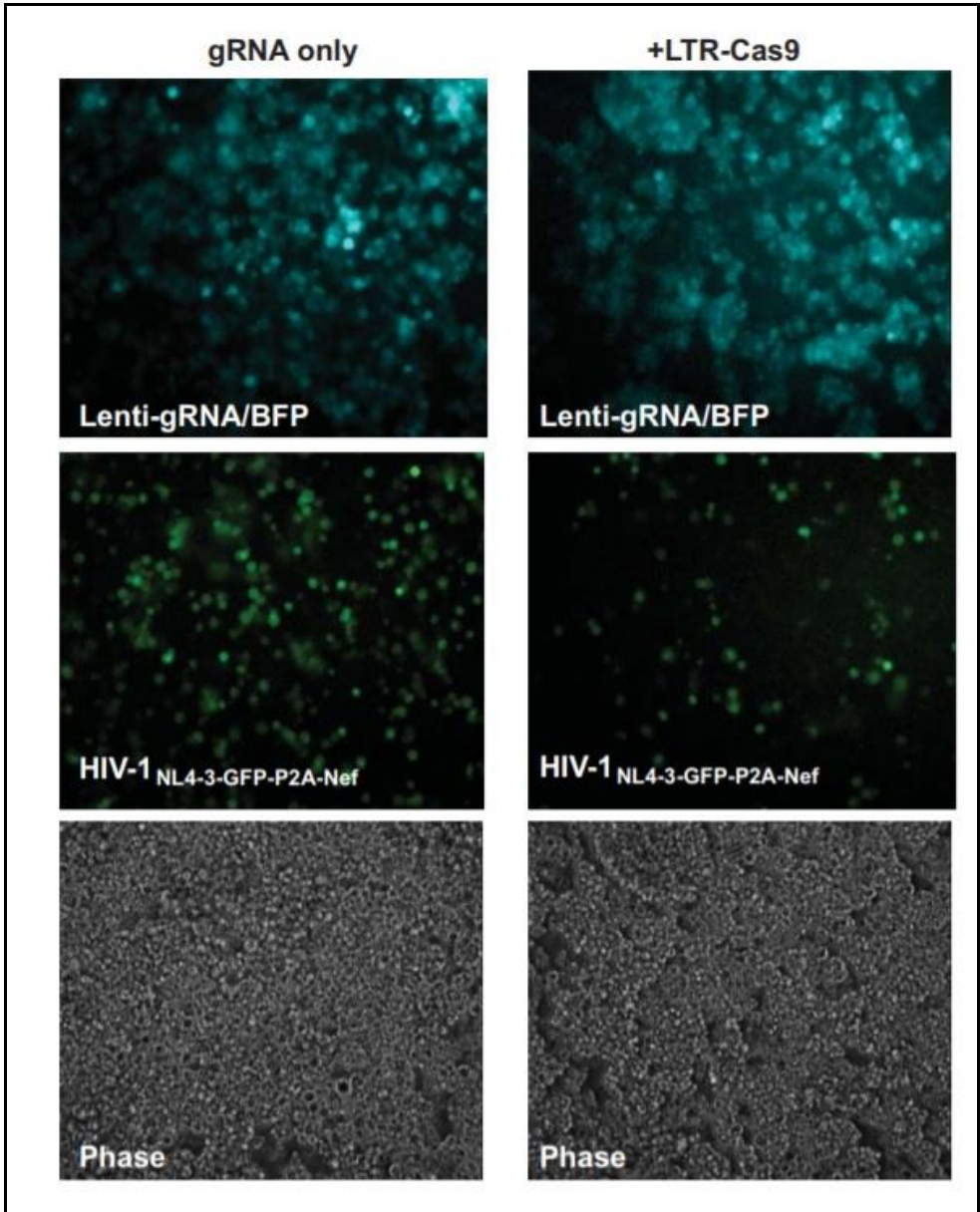


Figure 31: Reduction of GFP protein levels in presence of gRNAs and Cas9. Fluorescent and phase microscopy analysis of Jurkat Cells transduced with pLenti-LTR (-80/+66)-Cas9 and pKLV-gRNA LTR A and B or pKLV-gRNA LTR A and B only and infected with HIV-1 NL4-3 EGFP-P2APNef. On the bottom gRNAs and Cas9 expression using BFP as marker, on the middle GFP levels in presence of gRNAs only and gRNAs plus

Cas9. In the bottom morphological view of the cells. (Figure reproduced from Kaminski R. *et al.*, 2016 and Creative Commons CC-BY license) [185].

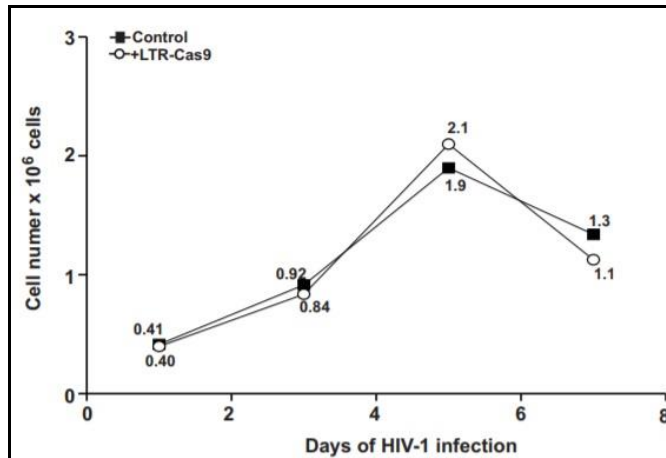


Figure 32: Quantification of Viable Jurkat Cells. Quantification was performed on Jurkat cells after transduction with pLENTI-LTR-Cas9 (-80/+66) Cas9 (MOI 1) and pKLV-gRNA (MOI1/1) or pKLV Negative Control (MOI2) and infected with HIV-1 NL4-3 EGFP-P2APNef (MOI 0.01). (Figure reproduced from Kaminski R. *et al.*, 2016 and Creative Commons CC-BY license) [185].

4.14 Gag DNA and RNA reduction in Cas9 treated Jurkat cells at the early stage on infection

Analyses by qPCR was performed on DNA and RNA extracted from Jurkat cells transduced with pLENTI-LTR-Cas9 (-80/+66) Cas9 (MOI 1), pKLV-gRNA (MOI1/1) or pKLV negative control (MOI2) and infected with HIV-1. Results showed a decrease of Gag gene at days 3 and 5 in treated cells compared to control (figure 33 left side). Analysis of Gag RNA was performed after reverse transcription of RNA into cDNA, with a 91 and 96% decrease detected at 3 and 5 days post-infection, respectively, in treated

cells (figure 33 right side). These results reveal a potential use of gene editing to protect cells from HIV-1 reinfection.

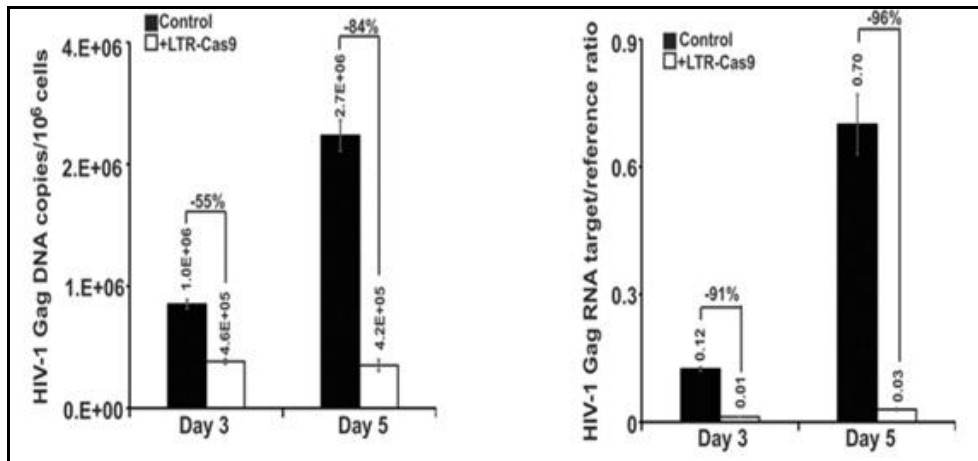


Figure 33: Cas9 DNA and RNA reduction in Jurkat cells. Quantification of Gag copies on DNA and cDNA of Jurkat Cells transduced with pLENTI-LTR (-80/+66)-Cas9 and pKLV-gRNA LTR A and B or negative control (pKLV empty) and Infected with HIV-1 NL4-3 EGFP-P2APNef (MOI 0,01) at 3 and 5 days post infection. (Figure reproduced from Kaminski R. *et al.*, 2016 and Creative Commons CC-BY license) [185].

4.15 Viral Excision in MEF cells treated with rAAV9 SaCas9/gRNAs

Following *in vitro* studies, a construct was created to allow the delivery of the Cas9 system *in vivo* using an innovative AAV9 delivery system. AAV9 requires the use of a smaller Cas9, saCas9, which is 1kb shorter than spCas9. The gRNAs LTR1 and GagD were introduced in the same construct of SaCas9 under the control of two separate U6 promoters.

To test the functionality of this new system studies *in vitro* were performed on MEFs cells, obtained from Tg26 mice. At one-week post-transduction with rAAV9 SaCas9/gRNAs, cells were harvested and subjected to PCR analysis.

Specific PCR was performed to amplify the LTR Gag region of HIV-1 genome, obtaining a full-length fragment of 1323 bp and a truncated fragment of 345 bp, not detected in untreated cells (figure 34).

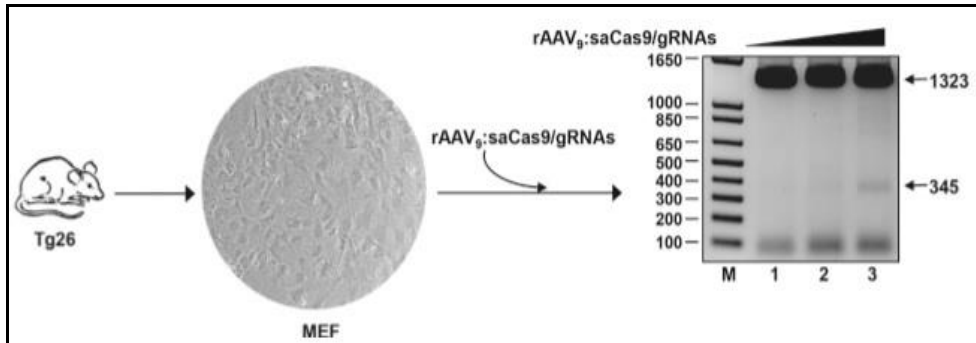


Figure 34: Viral excision on DNA of MEF cells. Mouse embryo fibroblasts (MEFs) were prepared from 17-day-gestation embryos by mechanical and enzymatic dissociation. PCR analysis of MEF cells after transduction with rAAV9 SaCas9/gRNAs. Cells were harvested after one week and DNA extraction was performed for viral excision detection. Lane 1 untransduced cells, lane 2 and 3 transduced cells (MOI 10^5 and 10^6). Full length LTR-Gag region is detected at 1323 bp, truncated LTR region is detected at 345 bp. (Figure reproduced from Kaminski R. *et al.*, 2016 and Nature Publishing group) [186].

4.16 Viral excision *in vivo* in Tg26 mice treated with rAAV9 SaCas9/gRNAs

After verifying the functionality of the AAV9 SaCa9LTR1/GagD construct *in vitro*, studies *in vivo* were performed on Tg26 mice to evaluate the efficiency of delivery and gene editing in animal model tissues. 4 animals were treated with AAV9 virus or PBS (2 mice received one injection while the other two received two injections). Nested-PCRs were performed on blood and tissues including liver, heart, spleen, lung, kidney and brain. One full length fragment was detected in treated and non-treated animals

(1171 bp), while a truncated fragment (160 bp), an index of viral excision, was detected only in treated animals after one and two AAV9 injections (figure 35). Analysis of the truncated LTR1GagD fragment confirmed the excision of 1011 base pair fragment (figure 36).

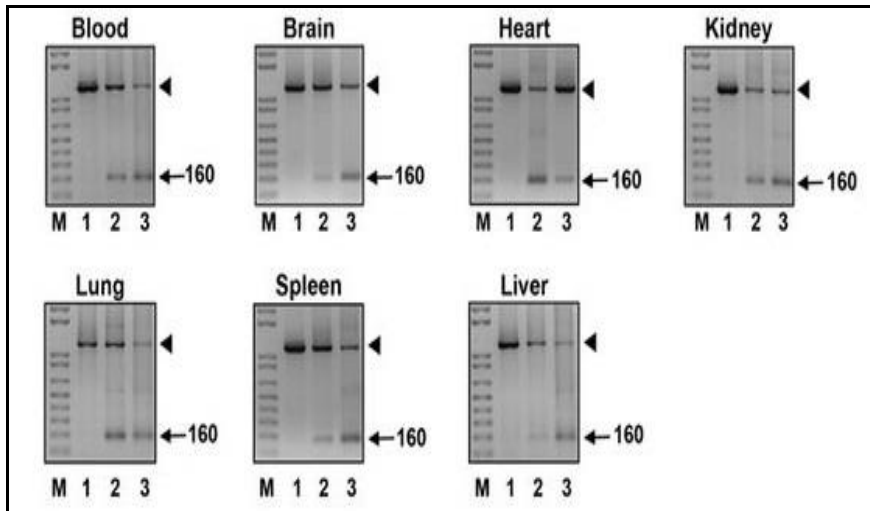


Figure 35: Viral excision in vivo in tissues of Tg26 mice. Nested PCR was performed on DNA of tissues of Tg26 mice treated with rAAV₉saCas9/gRNAs to detect viral excision. Lane 1: tissue from mouse treated with 100 μ l of PBS as negative control, lane 2: tissue from rAAV₉saCas9/gRNAs (2.73×10^{12}) treated mouse, lane 3: MEF with rAAV₉saCas9/gRNAs treatment (MOI 10^6). (Figure reproduced from Kaminski R. *et al.*, 2016 and Nature Publishing group) [186].

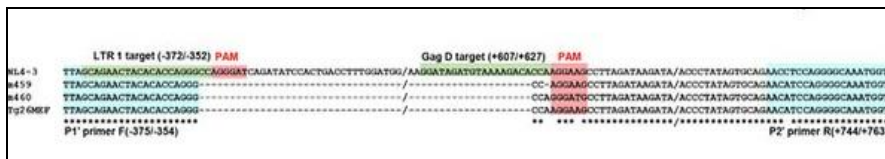


Figure 36: Sequence analysis of truncated fragments from liver DNA. The truncated LTR-GAG fragment detected after PCR on DNA of liver tissue was gel purified, cloned in TA vector and sequenced. The Position of the Primers and the gRNAs are highlighted in the figure in blue and green respectively. (Figure reproduced from Kaminski R. *et al.*, 2016 and Nature Publishing group) [186].

4.17 Viral excision in vivo in Tg26 rats treated with rAAV9 SaCas9/gRNAs

The same set of experiments was then performed on 4 rats (2 treated, 2 untreated). PCR data obtained from blood showed the presence of a truncated LTR1GagD fragment (221 bp) in the treated animals but not in control samples (figure 37). The sequence of the truncated fragments obtained in blood PCR was analyzed with BLAST using HIV-1 NL4-3 as reference sequence, which showed the excision of a 955 bp fragment (figure 38).

Total RNA was extracted by blood samples, converted into cDNA and analyzed by qPCR to check the presence of Gag and Env transcripts. Results showed a decrease of transcript production for both regions in treated animals compared to controls, suggesting a loss of function of the LTR promoter in treated animals (figure 39, left and right side). Data were normalized by the number of rat cells using beta actin as reference. Similar results were obtained from RNA prepared from lymph nodes (data not shown).

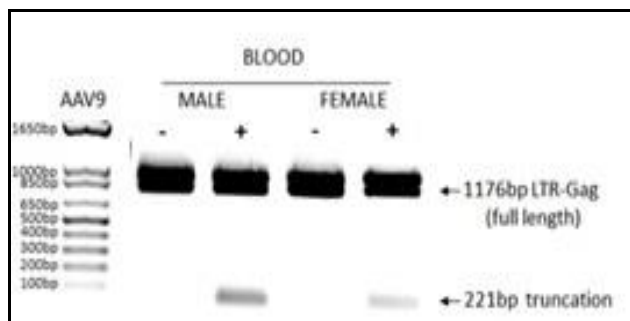


Figure 37: Viral excision in DNA of blood of rats treated with rAAV9SaCa9 gRNAs. Retro-orbital inoculation of rAAV9: Cas9/gRNA or 100 μ l of PBS was injected into 4 mice. PCR was performed on blood DNA of rats with (lanes 2 and 4) and without (lanes 1 and 3) SaCas9 treatment to detect viral excision. (Figure reproduced from Kaminski R. *et al.*, 2016 and Nature Publishing group) [186].

4.18 Viral excision *in vivo* in humanized mice treated with rAAV9 SaCas9/gRNAs

Nod/Cg-Prkdc^{scid} Il2rg^{tm1wjl}/SzJ (NSG) mice were used to test the ability of the AAV9SaCas9LTR1GagD construct to induce gene editing in a humanized animal model. After the injection of human peripheral blood lymphocytes (PBLs) into the mice, they were infected with HIV-1_{NL4-3} and then were divided in three groups, 5 mice received no antiretroviral treatment and one injection of AAV9 construct and 13 were treated with LASER ART therapy. The 13 mice were then divided into a non-treatment group (4 mice) and a Cas9-treated group (9 mice). Tissues were harvested after 5 weeks of CRISPR treatment. Specific PCRs were performed to amplify 5' LTR GagD, GagD 3'LTR and 5'LTR-3'LTR regions of HIV-1 genome (figure 40) on spleen, GALT, kidney, lung, liver and brain tissue to investigate the ability of CRISPR/Cas9 to induce double stranded breaks in the viral DNA as illustrated in figure 40. Excision between 5'LTR and GagD results in the editing of 978 bp fragment and the generation of a truncated/end joined fragment of 193 bp. Excision between GagD and 3'LTR results in the editing of 8.097 bp fragment and the generation of a truncated/end joined fragment of 523 bp. Excision between 5'LTR and 3'LTR consists in the editing of 9.074 bp fragment and the generation of a truncated/end joined fragment of 396 bp.

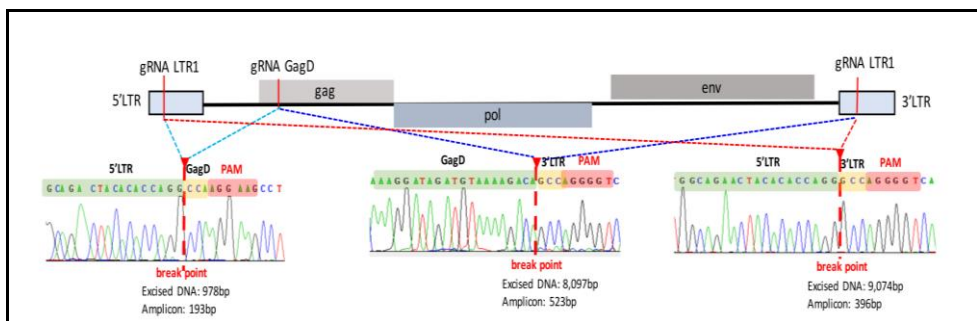


Figure 40: HIV-1 genome map. Illustration of gRNAs positions and the size of truncated amplicons expected after editing of viral DNA in LTRs and GagD regions by CRISPR/Cas9.

Excision between 5'LTR and GagD consists in the editing of 798 bp fragment and the generation of a truncated/end joined fragment of 193 bp. Excision between GagD and 3'LTR consists in the editing of 8.097 bp fragment and the generation of a truncated/end joined fragment of 523 bp. Excision between 5'LTR and 3'LTR consists in the editing of 9.074 bp fragment and the generation of a truncated/end joined fragment of 396 bp.

PCRs performed on tissues of spleen, GALT and kidney of mice AAV9-CRISPR/Cas9 treated and LASER ART/AAV9 CRISPR/Cas9 treated detected the presence of amplicons of 193 and 523 bps resulting from excision between the 5'LTR and GagD and GagD and the 3'LTR. A fragment of 396 bp derived from both full length or truncated LTRs after the excision between the 5' LTR and the 3' LTR was detected by specific PCR (Figure 41).

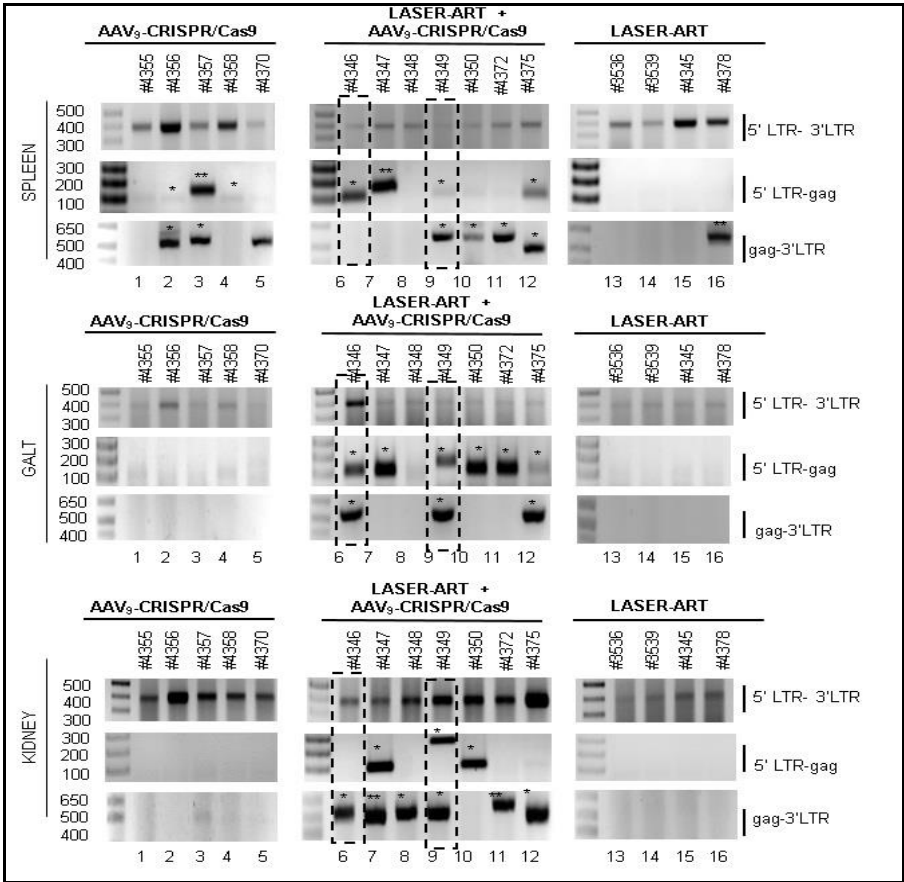


Figure 41: Viral excision in spleen, GALT, and kidney of humanized mice HIV-1 infected. PCRs of Spleen, GALT, and Kidney tissues from CRISPR/Cas9 treated Humanized Mice CRISPR/Cas9 (n:5), LASER+CRISPR/Cas9 Treated (n:9) and only LASER-ART Treated (n:4). Tissues were harvested after 5 weeks from CRISPR treatment and analysis of DNA was performed for the detection of viral excision between 5’LTR and GagD, GagD and 3’LTR, 5’LTR and 3’LTR regions. One asterisk denotes that the highlighted fragment is Cas9 correlated and verified by sequence analysis. Two Asterisks indicate aspecific fragments not Cas9 related.

PCR performed on tissues of lung, liver and brain of mice AAV9-CRISPR/Cas9 treated and LASER ART/AAV9 CRISPR/Cas9 treated detected the presence of amplicons of 193 and 523 bps resulting from excision between the 5’LTR and GagD and GagD and the 3’LTR. (Figure 42).

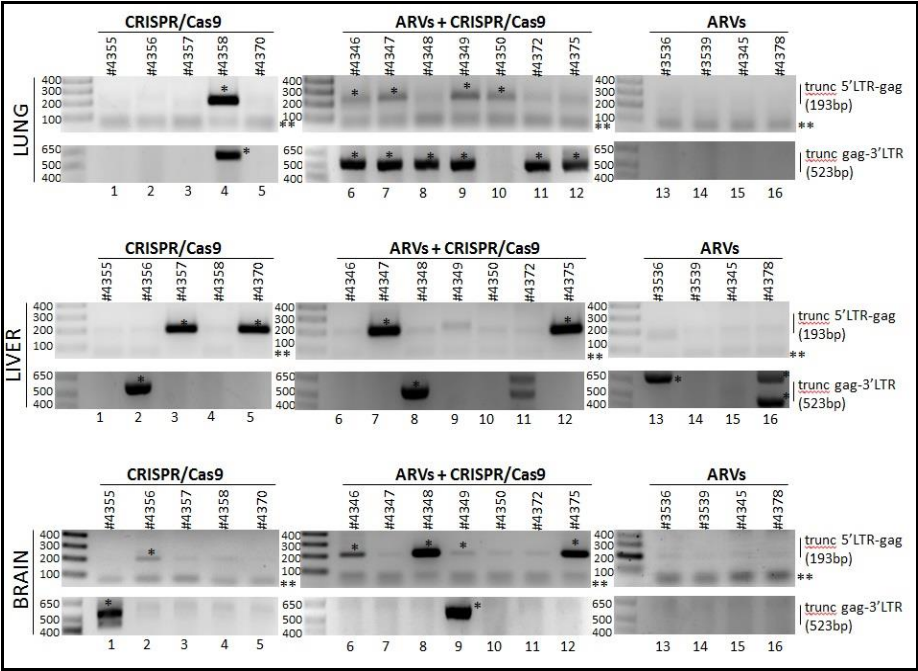


Figure 42: Viral excision in lung, liver and brain of humanized mice HIV-1 infected. PCRs of Spleen, GALT, and Kidney Tissues from CRISPR/Cas9 Treated Humanized Mice CRISPR/Cas9 (n:5), LASER+CRISPR/Cas9 Treated (n:9) and only LASER-ART Treated (n:4). Tissues were harvested after 5 weeks from CRISPR treatment and analysis of DNA

was performed for the detection of viral excision between 5'LTR and GagD, GagD and 3'LTR. One asterisk denotes that the highlighted fragment is Cas9 correlated and verified by sequence analysis. Two Asterisks indicate aspecific fragments not Cas9 related.

The specificity of each truncated/end-joined fragment revealed in these PCRs was gel purified, cloned in TA vector and analyzed using Sanger sequencing that revealed the presence of indel mutations, deletions and insertion, which was CRISPR Cas9 related. In figure 43 sequences obtained from the analysis of the truncated/end joined viral DNA resulting from the excision between 5'LTR/GagD and GagD/3'LTR of spleen, GALT and kidney tissues showed the presence of indel mutations, deletions and insertion CRISPR/Cas9 related.

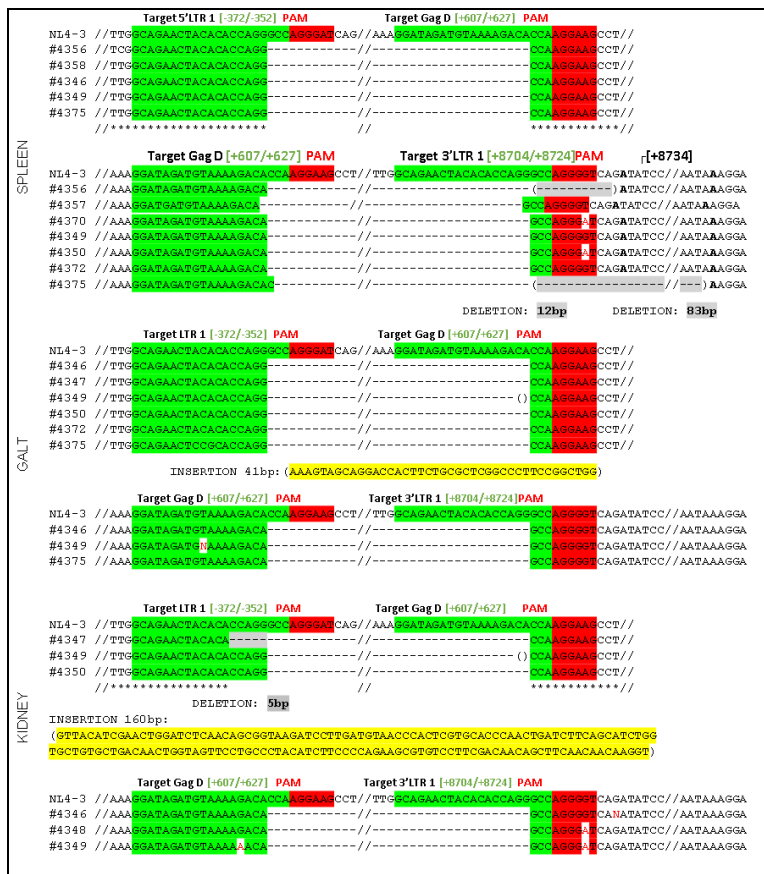


Figure 43: Analysis of truncated/endjoined viral DNA sequence. The truncated/end joined LTR-GAG viral DNA detected after nested PCR for the DNA of each tissue was gel purified, cloned in TA and sent for sequence. In the figure is reported representative DNA sequences obtained from the analysis of DNA from spleen, GALT and Kidney tissues. Pam Sequences are in red, gRNA sequences are in green, and the presence of indel mutations is denoted by arrows

PCR specific for the housekeeping gene human and mouse beta actin was performed on tissues as loading control and control of DNA quality. Figure 44 showed beta actin amplification on spleen, GALT and kidney.

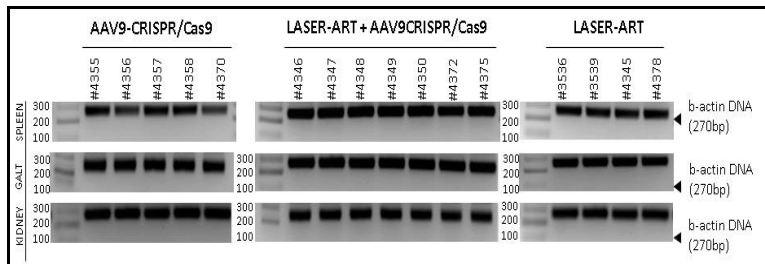


Figure 44: Quality control on spleen, GALT and kidney DNA of humanized mice HIV-1 infected. PCR on human and mouse β -actin gene was performed as quality control of the DNA used to verify viral excision. Mice CRISPR/Cas9 (n:5), LASER+CRISPR/Cas9 Treated (n:9) and only LASER-ART Treated (n:4).

Specific human beta globin and mouse beta globin PCRs were performed on DNA to show the co-presence of human and mice cells in spleen tissue (Figure 45). The presence of human cells was detected in all mice samples, showing the ability of the injected PBLs to reach different tissues in this animal model.

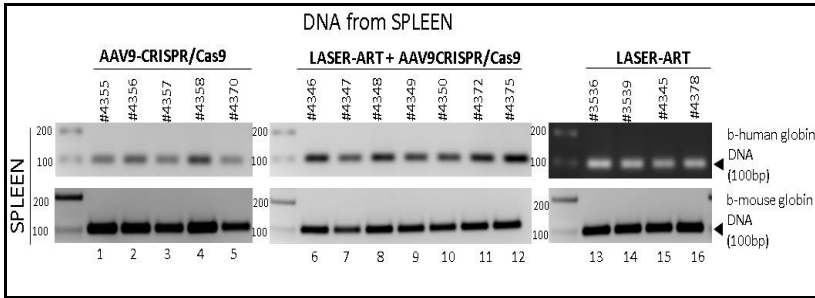


Figure 45: Detection of human beta globin in spleen tissue of humanized mice HIV-1 infected. PCR on human beta globin was performed on spleen DNA as marker of presence of human cells on tissues of humanized mice. Mouse β -Globin PCR was performed as loading control. Mice CRISPR/Cas9 (n:5), LASER+CRISPR/Cas9 Treated (n:9) and only LASER-ART Treated (n:4).

4.19 Cas9 and gRNAs expression in the tissues Humanized mice

Total RNA was extracted by spleen tissues of mice AAV9-CRISPR/Cas9 treated, LASER ART/AAV9 CRISPR/Cas9 treated or only LASER ART treated, converted in cDNA and analyzed for the expression of saCas9, LTR1 and GagD gRNAs, human beta actin was used as quality control (Figure 46). The expression of Cas9 and gRNAs was detected in AAV9-CRISPR/Cas9 treated and LASER ART/AAV9 CRISPR/Cas9 treated mice but no in LASER ART group, who was treated with antiretroviral drugs but without CRISPR/Cas9. The lack of gRNAs expression for some mice in AAV9-CRISPR/Cas9 treated and LASER ART/AAV9 CRISPR/Cas9 treated groups may depends from the long time within the injection of the AAV construct carrying the gRNAs and the time of harvest of the tissues.

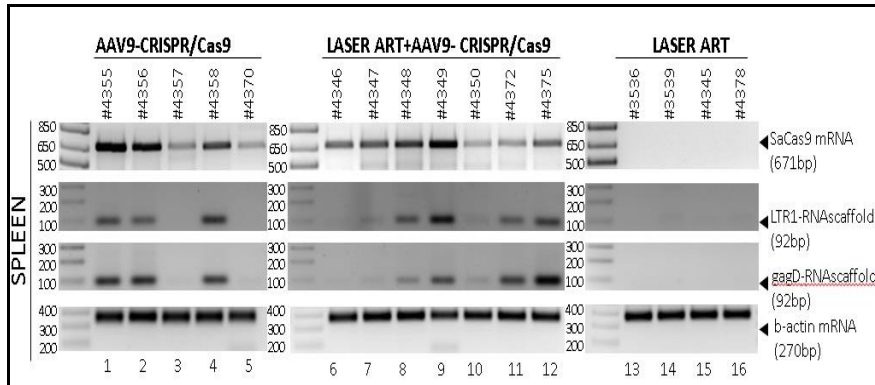


Figure 46: Cas9 and gRNAs expression in spleen tissue of humanized mice HIV-1 infected. PCR was performed on spleen cDNA to detect the expression of Cas9 (on the top) and gRNA (middle row). Human and mouse β -actin was used as the loading control (bottom). Mice CRISPR/Cas9 (n:5), LASER+CRISPR/Cas9 Treated (n:9) and only LASER-ART Treated (n:4).

4.20 No viral DNA was observed in two LASER ART/AAV9 CRISPR/Cas9 treated mice

DNA from spleen of AAV9-CRISPR/Cas9 treated, LASER ART/AAV9 CRISPR/Cas9 treated and only LASER ART treated mice was used for qPCR assay for the quantification of pol and env region to assay the integrity of viral genome. Absence of viral DNA was observed in 2 mice, M#4346 and M#4349, suggesting the presence of viral sterilization (Figure 47) that was also confirmed with RNase scope analysis and ultrasensitive digital droplet PCR performed from collaborators at the University of Nebraska Medical Center (data not shown).

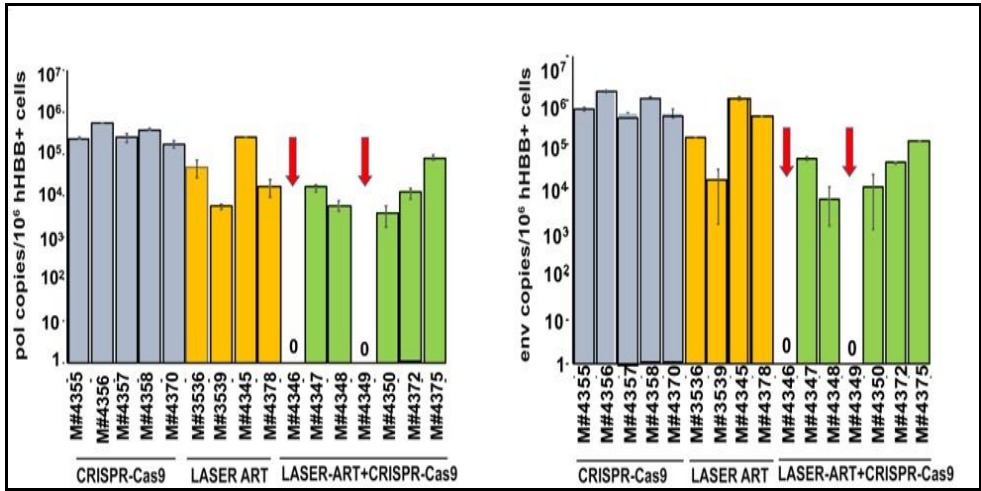


Figure 47: Decreased pol and env copies on DNA spleen tissue of humanized mice HIV-1 infected. qPCR on pol and env viral DNA was performed for experimental Mouse Groups, Note the Absence of Viral DNA Highlighted by Arrows for Mouse #4346 and Mouse #4349 in LASER ART group.

5. Discussion

Human immunodeficiency virus is a member of the *Retroviridae* family that was first detected in France at the Pasteur institute. In 1981, HIV was recognized as causative agent of acquired immune deficiency syndrome [193]. Retroviruses are spherical enveloped viruses characterized by a specific mechanism of replication in which the viral RNA is converted into DNA and integrates in the host genome. HIV-1 belongs to the genus of Lentivirus encompassing the human immunodeficiency virus 1 and 2. The epidemic spread of HIV-1 initiated with zoonotic infection of SIV in the 1900s. HIV-2, transmitted by sooty mangabeys, is diffused in Africa and causes a similar disease to HIV-1 but is less transmissible [4]. HIV-1 contains 4 different groups, characterized by different sources of transmission. The main group derives from chimpanzees and is responsible for the worldwide HIV-1 pandemic. Since 1982, 76.1 million people in the world have become infected with HIV-1 and 35 million people have died of HIV-1 related illnesses. Currently 36.5 million people live with HIV infection while the number of deaths has decreased after the introduction of ART therapy. HIV-1 transmission occurs by sexual, percutaneous, and peritoneal routes, with a 15- 25% risk of transmission during pregnancy and 35-40% risk during the breastfeeding period [13].

HIV-1 infection is characterized by an initial infection of CD4+ T cells in the mucosal tissues, followed by an eclipse phase which is characterized by asymptomatic or associated with minor symptoms where the virus spreads throughout the lymphoid system. After this phase the viral load decreases until reaching a set point due to CD8+ T cell action. This period is not associated with clinical manifestations and can persist up to 15 years. The last stage of HIV-1 is characterized by the point at which the level of CD4

positive cells reaches 100 cells per μl of blood. This stage presents with an increased incidence of opportunistic infections and HIV-1 related diseases.

The HIV-1 genome consists of two copies of linear single stranded positive sense RNA [2] and is characterized by the presence of non-coding regions involved in the regulation of the gene expression and by regions expressing regulatory, accessory, structural and enzymatic proteins.

The target cells of HIV-1 infection are memory and naïve T lymphocytes, macrophages and dendritic cells. Viral replication can be divided in two phases, early and late stages. During the early stage, the virus binds the host cell receptors and integrates its genome in the human DNA. In the late stage, after the expression of viral proteins, the new viral particles are released outside the infected cells to facilitate the infection of new cells. The regulation of viral replication is controlled by HIV-1 proteins, primarily Nef, Rev and Tat that are produced during the early stages of infection and are involved in the downregulation of cellular receptors and in the control of HIV-1 protein expression. Rev regulates the trafficking of the viral transcripts to the cytoplasm and Tat interacts with the TAR region of the viral genome inducing the activation of pTEF and the phosphorylation of RNA pol II resulting in an increased elongation of viral transcripts. The importance of these proteins explains the interest of the scientific community to use molecules able to target the pathways regulated by Tat and Rev [194]. Hamy discovered a new compound, stilbene CGA137053 that binds to Tat and interferes with the viral expression [195]. Balachandran identified three molecules which reduce the levels of both proteins altering the transcripts levels and HIV-1 protein expression [196].

In 1990, the therapy of antiretroviral drugs was discovered, with these molecules targeting different steps of HIV-1 replication to suppress the viral load in treated patients. However, ART is ineffective against latent viral reservoirs, including memory T cells, monocytes, naïve T cells and macrophages [93] or anatomic sanctuaries such as CNS and GALT [97], that become a source of viral reactivation after ART interruption. The limitations of ART to eradicate HIV-1 virus as well as the high cost make the development of an alternative strategy to completely eradicate the virus necessary.

Different vaccine trials had been tested in the past to control the spread of the epidemic, but only one, the RV144 trial, showed a reduction in HIV-1 acquisition. The difficulty to create an efficient vaccine is due to the genomic diversity of different HIV-1 strains and the high frequencies of mutations that occur during viral infection. Recently, the shock and kill therapy provides the use of molecules to induce viral reactivation and lysis of the infected cells combined with antiretroviral drugs that after viral reactivation avoid the spread of new infection. This system is associated with cell toxicity and a low ability to induce viral reactivation. Other strategies involved the use of antibodies against the binding site of CD4 with env viral protein and against the CD3 receptor to induce HIV-1 resistance in infected T cells that are recognized and lysed by CD8 positive cells [197].

Recently, the use of gene editing platforms has been largely assessed for the development of an HIV-1 cure. Different approaches involve small interfering RNAs, meganucleases, ZFNs, TALENs and the CRISPR/Cas9 system. The first example of gene editing targeting HIV-1 DNA was performed with a recombinase of bacteriophages to target Tat and LTR

regions [111]. The application of homing endonucleases for genome editing was limited due the large size of these proteins and the low specificity, instead ZFNs and TALENs molecules were successfully employed to target HIV-1 infected cells. After the initiate case of the Berlin patient, other HIV-1 patients with Hodgkin's lymphoma received transplantation of CCR5 wild type hematopoietic stem cells, resulting in reduction of the viral load, but eventually showed viral rebound. This resulted in the development of new strategies, characterized by the treatment of autologous hematopoietic cells with gene editing molecules targeting CCR5, CXCR4 cellular receptor or viral genes, such as the LTR promoter, and the infusion of the modified cells into patients. A second strategy consists of the direct administration of the gene editing molecules to the patients. Different studies were developed, employing ZFNs targeting the CCR5 receptor to treat autologous T cells [121], [122]. ZFNs showed positive results in animal models where the use of CD4 positive cells T cells against CCR5 induced HIV-1 resistance. This resistance persisted after engraftment of these T cells in NOD-SCID IL2ryc null (NSG) mice [124]. A clinical trial using CCR5 ZFNs (SB-728) to test the specificity of this system in HIV-1 infected patients was performed [198]. TALEN molecules were also employed to target the CCR5 receptor, HIV Tat or HIV LTR region [131], [132], [135]. The limitations of TALENs are the high cost of production, the large size and less specificity comparing to the new strategy of CRISPR/Cas9. Gene editing induces breaks in the DNA strands disrupting opening reading frame or introducing indels mutations or insertions of specific sequences, allowing the utilization of this technique for the treatment of different disease such as cystic fibrosis, sickle-cell anemia, or Duchenne's muscular dystrophy, diabetes, heart disease, schizophrenia, autism, transthyretin-related hereditary amyloidosis and dominant-negative forms of *retinitis pigmentosum* [138]. Different studies

were performed in T cells using CRISPR/Cas9 system to induce viral excision targeting different viral regions or cellular receptors, such as the TAR region [171], the CXCR4 coreceptor [172], [173], the CCR5 coreceptor [181] [176] and the LTR, Pol and Rev regions [177]. The importance to target the U3 region in the LTR promoter, which is the NF-Kb binding site, was recognized by multiple groups [178], [179], [180], [184]. Hu *et al* showed the importance of using a multiplex system of gRNAs delivered by lentiviral vectors to protect the cells from the generation of viral escape mutants. In that study, the presence of Cas9 in the cells was associated with the acquisition of resistance to new HIV-1 infection. To increase the specificity of CRISPR system new Cas9 variants were generated. Examples are the creation of a paired nickase, able to induce a single break in the two opposite DNA strands increasing the specificity by up to 1500-fold [162]. dCas9 was employed to induce transcriptional suppression mediated by steric hindrance of Cas9 in the DNA target using specific gRNAs that direct Cas9 in the region of interest [163].

Cas9 can be delivered to cells with viral and non-viral delivery systems; viral delivery systems include lentiviruses, baculoviruses, AAV viruses while non-viral delivery systems include cationic polymer polyethleimine, liposomes, lipid nanoparticles, virus-like particles, bacteriophages, and nanoparticles [170]. AAVs are low immunogenic viruses which allow the transduction of dividing and non-dividing cells and can be efficiently delivered in a large variety of human tissues. Lentiviral vectors are used to transduce dividing and non-dividing cells but their capacity for packaging allows the introduction of larger inserts than AAV vectors. The use of nanoparticles is a promising strategy that already has important results in animal models. A significant reduction of viral RNA was detected in the plasma of HIV-1 infected immunodeficient NOD-*scid IL-2 γ* ^{-/-} mice that were

engrafted with PBMCs treated with nanoparticles containing molecules targeting the CCR5 receptor compared to the negative control [199]. Different experiments in animal models were performed by Yin et al., using AAV system to deliver saCas9 and a combination of gRNAs, 2 specific for the LTR region, one for Gag and one for Pol in HIV-1 transgenic mice, ecoHIV acutely infected mice, and humanized bone marrow, liver, thymus (BLT) mice harboring chronic viral infection, obtaining viral excision in different tissues of all three animal models [188].

The efficiency of CRISPR/Cas9 in vivo is still a topic that requires more investigation, primarily to optimize the delivery in all tissues, particularly the brain. Additionally, more studies using humanized mice or monkeys are necessary to identify a delivery system able to induce the excision of the viral DNA from all infected cells without toxicity. The presence of a regulated system to be specifically activated by the virus may be an important key in animal models to induce gene editing in an early stage of infection before development of viral latency and without off target effects.

6. Conclusion

Following the initiation of ART therapy in HIV-1 patients, the viral load decreases within two weeks from the beginning of the treatment, resulting in the reduction of free virus and the death of infected macrophages and partially activated T cells, whose half-life is longer than fully activated T cells. Latently infected resting CD4+ T cells represent a source of viral reactivation when ART therapy is discontinued [200]. One study by the Visconti group focused on 14 HIV-1 infected patients who discontinued ART. Viral rebound was observed in these patients, even in those who started ART therapy early, suggesting that the existence of a viral reservoir is more important to viral reactivation than the number of latently infected cells [201]. Recently a child from Mississippi, born from a HIV-1 mother who was not ART treated, underwent antiretroviral treatment for 18 months after her birth, resulting in an undetectable viral load at 23 months, suggesting that early ART initiation serves to reduce the pool of infected cells and can eliminate free viral particles [202]. Currently only 53% of people diagnosed with HIV-1 undergo ART treatment. Statistical analysis reveals that only a long term pharmaceutical intervention (more than 73 years) may completely eradicate the virus from each latently infected cell, suggesting that this approach works as a functional cure, serving to control the viral load, as opposed to functioning as a sterilizing cure [203].

Tat protein has a critical role in the transcriptional regulation of viral genes by binding the TAR region located downstream of the initiation site of transcription of the RNA, resulting in the recruitment of the pre-initiation and initiation complexes to the transcription start site allowing the transcriptional elongation of the RNA [60]. The interaction of Tat with other transcriptional factors such as NF-Kb, p300/CBP and GCN5 [90], [203], [204] may influence viral and cellular transcription. The role of Tat in the

regulation of HIV-1 replication resulted in the interest of the scientific community to develop drugs such as inhibitors of the interaction Tat-Tar to interfere the spreading of infection [194], [195]. Different approaches were used to target viral or cellular genes involved in viral replication, using gene editing strategies. In 2014, ZFNs were used in a clinical trial to target CCR5 receptor in 12 patients after the interruption of ART, which showed slow viral rebound, whose spread was correlated to the degree of gene editing obtained in both alleles [122]. Recently, the CRISPR/Cas9 system appears to be a promising approach for the cure of HIV-1 by targeting cellular receptors, such as CCR5 or CXCR4 [176], [206] or viral genes [171], [177], [178]. Hu *et al* [180] used lentiviral vectors to target HIV-1 LTRs regions obtaining the excision of the integrated provirus in latently infected cells such as microglia, TZM-bl reporter and U1 cell lines. These data corroborate with results obtained by Kaminski targeting the same U3 LTR region in human T lymphocytic cell line 2D10, PBMCs and CD4 positive cells obtained from HIV-1 infected patients [184].

In our first study, published in Scientific Reports, we used lentiviral vectors *in vitro* to target HIV LTRs using the same gRNAs sequence of a previous study published from our laboratory [180], [184] with an innovative Tat-inducible Cas9 system, generating a negative feedback loop in the presence of HIV. During the early stages of infection, Tat regulates viral replication (positive feedback) and simultaneously induces the activation of Cas9 promoter (shown by western blot), which excises the LTR promoter from TZM-bl cells and Jurkat 2D10 cells in the presence of specific gRNAs resulting in reduced transcriptional activity (shown by luciferase assay) and in a reduced GFP production respectively. Viral excision was reported after two days of infection of Jurkat cells previously treated with Cas9, suggesting a pre-exposure prophylactic action. Similar experiments were

performed on human primary astrocytes and microglia, obtaining a reduction of viral expression (data not shown). This inducible system avoids a long term Cas9 expression that may result in off target effects into the genome of human cells, but further investigations must be performed to test the functionality and the specificity of this system *in vivo*.

The second experiment we performed, published in Gene Therapy, was the first proof of HIV-1 excision *in vivo* by using a Cas9 system delivered by the AAV9 vector. In this study, we targeted two different regions of HIV-1, LTR and Gag, obtaining viral excision in different tissues of Tg26 mice and rats. The advantage of AAV vectors is the reduced toxicity and immune response by the host immune system and the high delivery efficiency of these viral vectors in different tissues. Similar results were obtained in a recent study performed by Yin and colleagues targeting different regions of HIV-1 genome using AAV vectors in HIV-1 transgenic mice, Eco HIV acutely infected mice, and BLT mice [188].

The last set of experiments was performed on HIV-1 infected humanized mice. Results showed complete HIV eradication and absence of viral rebound in 29% of the infected animals that were previously subjected to ART treatment. Deep sequencing analysis revealed the absence of CRISPR/Cas9 related off-target effects. This study documented for the first time the presence of viral sterilization *in vivo*, but more studies must be performed to evaluate the functionality of CRISPR/Cas9 system in SIV-infected monkey models. This new approach, combined with antiretroviral therapy, represents a promising strategy for HIV-1 sterilization and a prospect towards clinical trials.

7. References

- 1) Vogt VM, Simon MN. Mass determination of rous sarcoma virus virions by scanning transmission electron microscopy. *Journal of virology*. 1999;73(8):7050–5.
- 2) Hélio A. Tomás, Ana F. Rodrigues, Paula M. Alves and Ana S. Coroadinha. Lentiviral Gene Therapy Vectors: Challenges and Future Directions, *Gene Therapy - Tools and Potential Applications*, Dr. Francisco Martin (Ed.), InTech, 2013: DOI: 10.5772/52534.
- 3) Maartens G, Celum C, Lewin SR. HIV infection: epidemiology, pathogenesis, treatment, and prevention. *Lancet*. 2014 Jul 19;384(9939):258-71.
- 4) Sharp PM, Hahn BH. Origins of HIV and the AIDS pandemic. *Cold Spring Harb Perspect Med* 2011; 1: 006841.
- 5) Hemelaar J, Gouws E, Ghys PD, Osmanov S, for the WHO-UNAIDS Network for HIV Isolation and Characterisation. Global trends in molecular epidemiology of HIV-1 during 2000–2007. *AIDS* 2011; 25: 679–89.
- 6) Centers for Disease Control (CDC). Kaposi's sarcoma and Pneumocystis pneumonia among homosexual men--New York City and California. *MMWR Morb Mortal Wkly Rep*. 1981 Jul 3;30(25):305-8.
- 7) UNAIDS. Report on the global AIDS epidemic 2017. <http://aidsinfo.unaids.org/>
- 8) Ortblad KF, Lozano R, Murray CJ. The burden of HIV: insights from the GBD 2010. *AIDS* 2013; 27: 2003–17.
- 9) Deeks SG, Overbaugh J, Phillips A, Buchbinder S. HIV infection. *Nat Rev DisPrimers*. 2015 Oct 1; 1:15035.
- 10) Levi J, Raymond A, Pozniak A, Vernazza P, Kohler P, Hill A. Can the UNAIDS 90-90-90 target be achieved? A systematic analysis of

- national HIV treatment cascades. *BMJ Glob Health*. 2016 Sep 15;12:e 000010.
- 11) Baeten JM, Kahle E, Lingappa JR, Coombs RW, Delany-Moretlwe S, Nakku-Joloba E, Mugo NR, Wald A, Corey L, Donnell D, Campbell MS, Mullins JI, Celum C; Partners in Prevention HSV/HIV Transmission Study Team. Genital HIV-1 RNA predicts risk of heterosexual HIV-1 transmission. *Sci Transl Med*. 2011 Apr 6;3(77):77ra29.
 - 12) Weiss HA, Quigley MA, Hayes RJ. Male circumcision and risk of HIV infection in sub-Saharan Africa: a systematic review and meta-analysis. *AIDS* 2000; 14: 2361–70
 - 13) Nduati R, Mbori-Ngacha D, John G, Richardson B, Kreiss J. Breastfeeding in women with HIV. *JAMA*. 2000 Aug 23;284(8):956-7.
 - 14) Vanhems P, Dassa C, Lambert J, Cooper DA, Perrin L, Vizzard J, Hirschel B, Kinloch-de Loes S, Carr A, Allard R. Comprehensive classification of symptoms and signs reported among 218 patients with acute HIV-1 infection. *J Acquir Immune Defic Syndr* 1999; 21:99-106
 - 15) Mellors JW, Rinaldo CR Jr, Gupta P, White RM, Todd JA, Kingsley LA. Prognosis in HIV-1 infection predicted by the quantity of virus in plasma. *Science*. 1996 May 24;272(5265):1167-70. Erratum in: *Science* 1997 Jan 3;275(5296):14.
 - 16) Freiberg MS, Chang CC, Kuller LH, Skanderson M, Lowy E, Kraemer KL, Butt AA, Bidwell Goetz M, Leaf D, Oursler KA, Rimland D, Rodriguez Barradas M, Brown S, Gibert C, McGinnis K, Crothers K, Sico J, Crane H, Warner A, Gottlieb S, Gottdiener J, Tracy RP, Budoff M, Watson C, Armah KA, Doebler D, Bryant K, Justice AC. HIV infection and the risk of acute myocardial infarction. *JAMA Intern Med*. 2013 Apr 22;173(8):614-22.

- 17) Joshi D, O'Grady J, Dieterich D, Gazzard B, Agarwal K. Increasing burden of liver disease in patients with HIV infection. *Lancet* 2011; 377: 1198–209
- 18) Cohen T, Murray M, Wallengren K, Alvarez GG, Samuel EY, Wilson D. The prevalence and drug sensitivity of tuberculosis among patients dying in hospital in KwaZulu-Natal, South Africa: a postmortem study. *PLoS Med* 2010; 7: e1000296.
- 19) HIV In Site Knowledge Base Chapter January 2006; Content reviewed December 08, 2009, C. Bradley Hare, MD, University of California San Francisco <http://hivinsite.ucsf.edu/InSite?page=kb-03-01-01>
- 20) An P, Winkler CA. Host genes associated with HIV/AIDS: advances in gene discovery. *Trends Genet.* 2010 Mar;26(3):119-31.
- 21) Busch MP, Lee LL, Satten GA, Henrard DR, Farzadegan H, Nelson KE, Read S, Dodd RY, Petersen LR. Time course of detection of viral and serologic markers preceding human immunodeficiency virus type 1 seroconversion: implications for screening of blood and tissue donors. *Transfusion* 1995; 35:91-7
- 22) Hecht FM, Busch MP, Rawal B, Webb M, Rosenberg E, Swanson M, Chesney M, Anderson J, Levy J, Kahn JO. Use of laboratory tests and clinical symptoms for identification of primary HIV infection. *Aids* 2002; 16:1119-29
- 23) Nabel G, Baltimore D. An inducible transcription factor activates expression of human immunodeficiency virus in T cells. *Nature.* 1987 Apr16-22;326(6114):711-3. Erratum in: *Nature* 1990 Mar 8;344(6262):178.
- 24) Jones KA, Kadonaga JT, Luciw PA, Tjian R. Activation of the AIDS retrovirus promoter by the cellular transcription factor, Sp1. *Science.* 1986 May9;232(4751):755-9.

- 25) Garcia JA, Harrich D, Soultanakis E, Wu F, Mitsuyasu R, Gaynor RB. Human immunodeficiency virus type 1 LTR TATA and TAR region sequences required for transcriptional regulation. *EMBO J.* 1989 Mar;8(3):765-78.
- 26) Zenzie-Gregory B, Sheridan P, Jones KA, Smale ST. HIV-1 core promoter lacks a simple initiator element but contains a bipartite activator at the transcription start site. *J Biol Chem.* 1993 Jul 25;268(21):15823-32.
- 27) Rittner K, Churcher MJ, Gait MJ, Karn J. The human immunodeficiency virus long terminal repeat includes a specialised initiator element which is required for Tat-responsive transcription. *J Mol Biol.* 1995 May 5;248(3):562-80.
- 28) Li G, De Clercq E. HIV Genome-Wide Protein Associations: a Review of 30 Years of Research. *Microbiol Mol Biol Rev.* 2016 Jun 29;80(3):679-731.
- 29) De Francesco MA, Baronio M, Poiesi C. HIV-1 p17 matrix protein interacts with heparan sulfate side chain of CD44v3, syndecan-2, and syndecan-4 proteoglycans expressed on human activated CD4+ T cells affecting tumor necrosis factor alpha and interleukin 2 production. *J Biol Chem.* 2011 Jun 3;286(22):19541-8.
- 30) Dorfman T, Luban J, Goff SP, Haseltine WA, Göttlinger HG. Mapping of functionally important residues of a cysteine-histidine box in the human immunodeficiency virus type 1 nucleocapsid protein. *J Virol.* 1993. Oct;67(10):6159-69.
- 31) Julian N, Demene H, Morellet N, Maigret B, Roques BP. Replacement of His23 by Cys in a zinc finger of HIV-1 NCp7 led to a change in 1H NMR-derived 3D structure and to a loss of biological activity. *FEBS Lett.* 1993 Sep 27;331(1-2):43-8.

- 32) Barat C, Schatz O, Le Grice S, Darlix JL. Analysis of the interactions of HIV1 replication primer tRNA (Lys,3) with nucleocapsid protein and reverse transcriptase. *J Mol Biol.* 1993 May 20;231(2):185-90.
- 33) Zhang Y, Barklis E. Effects of nucleocapsid mutations on human immunodeficiency virus assembly and RNA encapsidation. *J Virol.* 1997 Sep;71(9):6765-76.
- 34) Jaskólski M, Tomasselli AG, Sawyer TK, Staples DG, Henrikson RL, Schneider J, Kent SB, Wlodawer A. Structure at 2.5-Å resolution of chemically synthesized human immunodeficiency virus type 1 protease complexed with a hydroxyethylene-based inhibitor. *Biochemistry.* 1991 Feb 12;30(6):1600-9.
- 35) Sarafianos SG, Marchand B, Das K, Himmel DM, Parniak MA, Hughes SH, Arnold E. Structure and function of HIV-1 reverse transcriptase: molecular mechanisms of polymerization and inhibition. *J Mol Biol.* 2009 Jan 23;385(3):693-713.
- 36) Craigie R. HIV integrase, a brief overview from chemistry to therapeutics. *J Biol Chem.* 2001 Jun 29;276(26):23213-6.
- 37) Guy B, Kieny MP, Riviere Y, Le Peuch C, Dott K, Girard M, Montagnier L, Lecocq JP. HIV F/3' orf encodes a phosphorylated GTP-binding protein resembling an oncogene product. *Nature.* 1987 Nov 19-25;330(6145):266-9.
- 38) Kotov A, Zhou J, Flicker P, Aiken C. Association of Nef with the human immunodeficiency virus type 1 core. *J Virol.* 1999 Oct;73(10):8824-30.
- 39) Ren X, Park SY, Bonifacino JS, Hurley JH. How HIV-1 Nef hijacks the AP-2 clathrin adaptor to downregulate CD4. *Elife.* 2014;3: e01754.
- 40) Michel N, Ganter K, Venzke S, Bitzegeio J, Fackler OT, Keppler OT. The Nef protein of human immunodeficiency virus is a broad-spectrum modulator of chemokine receptor cell surface levels that

- acts independently of classical motifs for receptor endocytosis and Galphai signaling. *Mol Biol Cell*. 2006 Aug;17(8):3578-90.
- 41) Blagoveshchenskaya AD, Thomas L, Feliciangeli SF, Hung CH, Thomas G. HIV-1 Nef downregulates MHC-I by a PACS-1- and PI3K-regulated ARF6 endocytic pathway. *Cell*. 2002 Dec 13;111(6):853-66.
 - 42) daSilva LL, Sougrat R, Burgos PV, Janvier K, Mattera R, Bonifacino JS. Human immunodeficiency virus type 1 Nef protein targets CD4 to the multivesicular body pathway. *J Virol*. 2009 Jul;83(13):6578-90.
 - 43) Geyer M, Fackler OT, Peterlin BM. Structure--function relationships in HIV-1 Nef. *EMBO Rep*. 2001 Jul;2(7):580-5.
 - 44) Pollard VW, Malim MH. The HIV-1 Rev protein. *Annu Rev Microbiol*. 1998;52:491-532.
 - 45) Kim SY, Byrn R, Groopman J, Baltimore D. Temporal aspects of DNA and RNA synthesis during human immunodeficiency virus infection: evidence for differential gene expression. *J Virol*. 1989 Sep;63(9):3708-13.
 - 46) Pomerantz RJ, Trono D, Feinberg MB, Baltimore D. Cells nonproductively infected with HIV-1 exhibit an aberrant pattern of viral RNA expression: a molecular model of latency. *Cell* 1990, 61:1271–76
 - 47) Karn J, Stoltzfus CM. Transcriptional and posttranscriptional regulation of HIV-1 gene expression. *Cold Spring Harb Perspect Med*. 2012 Feb;2(2): a006916.
 - 48) Nomaguchi M, Fujita M, Adachi A. Role of HIV-1 Vpu protein for virus spread and pathogenesis. *Microbes Infect*. 2008 Jul;10(9):960-7.
 - 49) Akari H, Bour S, Kao S, Adachi A, Strebel K. The human immunodeficiency virus type 1 accessory protein Vpu induces apoptosis by suppressing the nuclear factor kappaB-dependent

- expression of antiapoptotic factors. *J Exp Med.* 2001 Nov5;194(9):1299-311.
- 50) Izumi T, Ito K, Matsui M, Shirakawa K, Shinohara M, Nagai Y, Kawahara M, Kobayashi M, Kondoh H, Misawa N, Koyanagi Y, Uchiyama T, Takaori-Kondo A. HIV-1 viral infectivity factor interacts with TP53 to induce G2 cell cycle arrest and positively regulate viral replication. *Proc Natl Acad Sci U S A.* 2010 Nov30;107(48):20798-803.
- 51) Belzile JP, Duisit G, Rougeau N, Mercier J, Finzi A, Cohen EA. HIV-1 Vpr-mediated G2 arrest involves the DDB1-CUL4AVPRBP E3 ubiquitin ligase. *PLoS Pathog.* 2007 Jul;3(7): e85.
- 52) Kim K, Heo K, Choi J, Jackson S, Kim H, Xiong Y, An W. Vpr-binding protein antagonizes p53-mediated transcription via direct interaction with H3 tail. *Mol Cell Biol.* 2012 Feb;32(4):783-96. doi: 10.1128/MCB.06037-11. Epub 2011 Dec 19. Erratum in: *Mol Cell Biol.* 2017 Jul 14;37(15):. PubMed PMID: 22184063; PubMed Central PMCID: PMC3272969.
- 53) Kao SY, Calman AF, Luciw PA, Peterlin BM. Anti-termination of transcription within the long terminal repeat of HIV-1 by tat gene product. *Nature.* 1987 Dec 3-9;330(6147):489-93.
- 54) Puglisi JD, Tan R, Calnan BJ, Frankel AD, Williamson JR. Conformation of the TAR RNA-arginine complex by NMR spectroscopy. *Science.* 1992 Jul 3;257(5066):76-80.
- 55) Feng S, Holland EC. HIV-1 tat trans-activation requires the loop sequence within tar. *Nature.* 1988 Jul 14;334(6178):165-7.
- 56) Dingwall C, Ernberg I, Gait MJ, Green SM, Heaphy S, Karn J, Lowe AD, Singh M, Skinner MA. HIV-1 tat protein stimulates transcription by binding to a U-rich bulge in the stem of the TAR RNA structure. *EMBO J.* 1990 Dec;9(12):4145-53.

- 57) Herrmann, C. H., Rice, A. P. Lentivirus Tat proteins specifically associate with a cellular protein kinase, TAK, that hyperphosphorylates the carboxyl-terminal domain of the large subunit of RNA polymerase II: Candidate for a Tat cofactor. *J. Virol.* 69, 1995, 1612-1620.
- 58) Herrmann CH, Gold MO, Rice AP. Viral transactivators specifically target distinct cellular protein kinases that phosphorylate the RNA polymerase II C-terminal domain. *Nucleic Acids Res.* 1996 Feb 1;24(3):501-8
- 59) Wei, P., Garber, M. E., Fang, S.-M., Fischer, W. H., Jones, K. A. A novel cdk9-associated c-type cyclin interacts directly with HIV-1 Tat and mediates its high-affinity, loop specific binding to TAR RNA. *Cell* 1998, 92, 451-462.
- 60) Zhang, J., Tamilarasu, N., Hwang, S., Garber, M. E., Huq, I., Jones, K. A. & Rana, T. M. HIV-1 TAR RNA enhances the interaction between Tat and cyclin T1. *J. Biol. Chem.* 2000, 34314-34319.
- 61) Sobhian B, Laguette N, Yatim A, Nakamura M, Levy Y, Kiernan R, Benkirane M. HIV-1 Tat assembles a multifunctional transcription elongation complex and stably associates with the 7SK snRNP. *Mol Cell.* 2010 May 14;38(3):439-51.
- 62) Nicoli F, Finessi V, Sicurella M, Rizzotto L, Gallerani E, Destro F, Cafaro A, Marconi P, Caputo A, Ensoli B, Gavioli R. The HIV-1 Tat protein induces the activation of CD8+ T cells and affects in vivo the magnitude and kinetics of antiviral responses. *PLoS One.* 2013 Nov 4;8(11): e77746. doi: 10.1371.
- 63) Mahmoudi T, Parra M, Vries RG, Kauder SE, Verrijzer CP, Ott M, Verdin E. The SWI/SNF chromatin-remodeling complex is a cofactor for Tat transactivation of the HIV promoter. *J Biol Chem.* 2006 Jul

- 21;281(29):19960-8. Epub 2006 May 10. Erratum in: *J Biol Chem*. 2006 Sep 8;281(36):26768.
- 64) Chang JR, Mukerjee R, Bagashev A, Del Valle L, Chabrashvili T, Hawkins BJ, He JJ, Sawaya BE: HIV-1 Tat protein promotes neuronal dysfunction through disruption of MicroRNAs. *J Biol Chem* 2011, 286:41125–41134.
- 65) Nisole S, Saïb A. Early steps of retrovirus replicative cycle. *Retrovirology*.2004 May 14;1:9.
- 66) Wu, L. & KewalRamani, V. N. Dendritic-cell interactions with HIV: infection and viral dissemination. *Nat. Rev. Immunol.* 2006, 6, 859–868.
- 67) Kwong PD, Wyatt R, Robinson J, Sweet RW, Sodroski J, Hendrickson WA. Structure of an HIV gp120 envelope glycoprotein in complex with the CD4 receptor and a neutralizing human antibody. *Nature*. 1998 Jun 18;393(6686):648-59.
- 68) Miller MD, Farnet CM, Bushman FD: Human immunodeficiency virus type 1 preintegration complexes: studies of organization and composition. *J Virol* 1997, 71:5382-5390.
- 69) Bukrinsky MI, Sharova N, McDonald TL, Pushkarskaya T, Tarpley WG, Stevenson M: Association of integrase, matrix, and reverse transcriptase antigens of human immunodeficiency virus type 1 with viral nucleic acids following acute infection. *Proc Natl Acad Sci U S A* 1993, 90:6125-6129.
- 70) Butera ST, Perez VL, Besansky NJ, Chan WC, Wu BY, Nabel GJ, FolksTM: Extrachromosomal human immunodeficiency virus type-1 DNA can initiate a spreading infection of HL-60 cells. *J Cell Biochem* 1991, 45:366-373.
- 71) Stevenson M, Haggerty S, Lamonica CA, Meier CM, Welch SK,Wasiak AJ: Integration is not necessary for expression of human

- immunodeficiency virus type 1 protein products. *J Virol* 1990, 64:2421-2425.
- 72) Teo I, Veryard C, Barnes H, An SF, Jones M, Lantos PL, Luthert P, Shaunak S: Circular forms of unintegrated human immunodeficiency virus type 1 DNA and high levels of viral protein expression: association with dementia and multinucleated giant cells in the brains of patients with AIDS. *J Virol* 1997, 71:2928-2933.
- 73) Cara A, Cereseto A, Lori F, Reitz MS Jr: HIV-1 protein expression from synthetic circles of DNA mimicking the extrachromosomal forms of viral DNA. *J Biol Chem* 1996, 271:5393-5397.
- 74) Wu Y, Marsh JW: Early transcription from nonintegrated DNA in human immunodeficiency virus infection. *J Virol* 2003, 77:10376-10382.
- 75) Ono A, Ablan SD, Lockett SJ, Nagashima K, Freed EO. Phosphatidylinositol (4,5) biphosphate regulates HIV-1 Gag targeting to the plasma membrane. *Proc Natl Acad Sci U S A*. 2004 Oct 12;101(41):14889-94.
- 76) Chen J, Nikolaitchik O, Singh J, Wright A, Bencsics CE, Coffin JM, Ni N, Lockett S, Pathak VK, Hu WS. High efficiency of HIV-1 genomic RNA packaging and heterozygote formation revealed by single virion analysis. *Proc Natl Acad Sci U S A*. 2009 Aug 11;106(32):13535-40.
- 77) Lu K, Heng X, Garyu L, Monti S, Garcia EL, Kharytonchyk S, Dorjsuren B, Kulandaivel G, Jones S, Hiremath A, Divakaruni SS, LaCotti C, Barton S, Tummillo D, Hosic A, Edme K, Albrecht S, Telesnitsky A, Summers MF. NMR detection of structures in the HIV-1 5'-leader RNA that regulate genome packaging. *Science*. 2011 Oct 14;334(6053):242-5.

- 78) Engelman A, Cherepanov P. The structural biology of HIV-1: mechanistic and therapeutic insights. *Nat Rev Microbiol.* 2012 Mar 16;10(4):279-90.
- 79) Colin L, Van Lint C: Molecular control of HIV-1 postintegration latency: implications for the development of new therapeutic strategies. *Retrovirology* 2009, 6:111.
- 80) Marcello A: Latency: the hidden HIV-1 challenge. *Retrovirology* 2006, 3:7.
- 81) Pierson TC, Kieffer TL, Ruff CT, Buck C, Gange SJ, Siliciano RF: Intrinsic stability of episomal circles formed during human immunodeficiency virus type 1 replication. *J Virol* 2002, 76:4138–4144.
- 82) Strebel K, Luban J, Jeang KT: Human cellular restriction factors that target HIV-1 replication. *BMC Med* 2009, 7:48.
- 83) Durand CM, Blankson JN, Siliciano RF: Developing strategies for HIV-1 eradication. *Trends Immunol* 2012, 33:554–562.
- 84) Verdin E: DNase I-hypersensitive sites are associated with both long terminal repeats and with the intragenic enhancer of integrated human immunodeficiency virus type 1. *J Virol* 1991, 65:6790–6799.
- 85) Verdin E, Paras P Jr, Van Lint C: Chromatin disruption in the promoter of human immunodeficiency virus type 1 during transcriptional activation. *EMBO J* 1993, 12:3249–3259.
- 86) Ying H, Zhang Y, Zhou X, Qu X, Wang P, Liu S, Lu D, Zhu H: Selective histone deacetylase inhibitor M344 intervenes in HIV-1 latency through increasing histone acetylation and activation of NF-kappaB. *PLoS One* 2012, 7: e48832.
- 87) Narlikar GJ, Fan HY, Kingston RE: Cooperation between complexes that regulate chromatin structure and transcription. *Cell* 2002, 108:475–487.

- 88) Kauder SE, Bosque A, Lindqvist A, Planelles V, Verdin E: Epigenetic regulation of HIV-1 latency by cytosine methylation. *PLoS Pathog* 2009, 5: e1000495
- 89) Huang J, Wang F, Argyris E, Chen K, Liang Z, Tian H, Huang W, Squires K, Verlinghieri G, Zhang H: Cellular microRNAs contribute to HIV-1 latency in resting primary CD4+ T lymphocytes. *Nat Med* 2007, 13:1241–1247.
- 90) Kiernan RE, Vanhulle C, Schiltz L, Adam E, Xiao H, Maudoux F, Calomme C, Burny A, Nakatani Y, Jeang KT, et al: HIV-1 tat transcriptional activity is regulated by acetylation. *EMBO J* 1999, 18:6106–6118.
- 91) Bres V, Tagami H, Peloponese JM, Loret E, Jeang KT, Nakatani Y, Emiliani S, Benkirane M, Kiernan RE: Differential acetylation of Tat coordinates its interaction with the co-activators cyclin T1 and PCAF. *EMBO J* 2002, 21:6811–6819.
- 92) Coley W, Van Duyne R, Carpio L, Guendel I, Kehn-Hall K, Chevalier S, Narayanan A, Luu T, Lee N, Klase Z, Kashanchi F: Absence of DICER in monocytes and its regulation by HIV-1. *J Biol Chem* 2010, 285:31930–31943.
- 93) Chun TW, Carruth L, Finzi D, Shen X, DiGiuseppe JA, Taylor H, Hermankova M, Chadwick K, Margolick J, Quinn TC, et al: Quantification of latent tissue reservoirs and total body viral load in HIV-1 infection. *Nature* 1997, 387:183–188
- 94) Chun TW, Finzi D, Margolick J, Chadwick K, Schwartz D, Siliciano RF: In vivo fate of HIV-1-infected T cells: quantitative analysis of the transition to stable latency. *Nat Med* 1995, 1:1284–1290.
- 95) Siliciano RF, Greene WC: HIV latency. *Cold Spring Harb Perspect Med* 2011, 1: a007096.

- 96) Saksena NK, Hoy J, Crowe SM, et al: Both CD31(+) and CD31(-) naive CD4 (+) T cells are persistent HIV type 1-infected reservoirs in individuals receiving antiretroviral therapy. *J Infect Dis* 2010, 202:1738–1748
- 97) Chun TW, Nickle DC, Justement JS, Meyers JH, Roby G, Hallahan CW, Kottlil S, Moir S, Mican JM, Mullins JI, et al: Persistence of HIV in gut-associated lymphoid tissue despite long-term antiretroviral therapy. *J Infect Dis* 2008, 197:714–720
- 98) Churchill MJ, Wesselingh SL, Cowley D, Pardo CA, McArthur JC, Brew BJ, Gorry PR: Extensive astrocyte infection is prominent in human immunodeficiency virus-associated dementia. *Ann Neurol* 2009, 66:253–258
- 99) Van Lint C, Bouchat S, Marcello A. HIV-1 transcription and latency: an update. *Retrovirology*. 2013 Jun 26; 10:67.
- 100) Rodger AJ, Lodwick R, Schechter M, Deeks S, Amin J, Gilson R, Paredes R, Bakowska E, Engsig FN, Phillips A; INSIGHT SMART, ESPRIT Study Groups. Mortality in well controlled HIV in the continuous antiretroviral therapy arms of the SMART and ESPRIT trials compared with the general population. *AIDS*. 2013 Mar 27;27(6):973-9.
- 101) Buchbinder SP, Mehrotra DV, Duerr A, Fitzgerald DW, Mogg R, Li D, Gilbert PB, Lama JR, Marmor M, Del Rio C, McElrath MJ, Casimiro DR, Gottesdiener KM, Chodakewitz JA, Corey L, Robertson MN; Step Study Protocol Team. Efficacy assessment of a cell-mediated immunity HIV-1 vaccine (the Step Study): a double-blind, randomised, placebo-controlled, test-of-concept trial. *Lancet*. 2008 Nov 29;372(9653):1881-1893.
- 102) Kenneth L. Rosenthal, Mangalakumari Jeyanathan, Zhou Xing. *Mucosal immunology (fourth immunology), Filling the Immunological*

- Gap: Recombinant Viral Vectors for Mucosal Vaccines, Chapter 66, Elsevier Inc, 2015.
- 103) Datta PK, Kaminski R, Hu W, Pirrone V, Sullivan NT, Nonnemacher MR, Dampier W, Wigdahl B, Khalili K. HIV-1 Latency and Eradication: Past, Present and Future. *Curr HIV Res.* 2016;14(5):431-441.
- 104) Mummidi S, Ahuja SS, Gonzalez E, Anderson SA, Santiago EN, Stephan KT, Craig FE, O'Connell P, Tryon V, Clark RA, Dolan MJ, Ahuja SK. Genealogy of the CCR5 locus and chemokine system gene variants associated with altered rates of HIV-1 disease progression. *Nat Med.* 1998 Jul;4(7):786-93.
- 105) Henrich TJ, Hu Z, Li JZ, Sciaranghella G, Busch MP, Keating SM, Gallien S, Lin NH, Giguel FF, Lavoie L, Ho VT, Armand P, Soiffer RJ, Sagar M, Lacasce AS, Kuritzkes DR. Long-term reduction in peripheral blood HIV type 1 reservoirs following reduced-intensity conditioning allogeneic stem cell transplantation. *J Infect Dis.* 2013 Jun 1;207(11):1694-702.
- 106) Shan L, Siliciano RF. From reactivation of latent HIV-1 to elimination of the latent reservoir: the presence of multiple barriers to viral eradication. *Bioessays.* 2013 Jun;35(6):544-52.
- 107) Archin NM, Liberty AL, Kashuba AD, Choudhary SK, Kuruc JD, Crooks AM, Parker DC, Anderson EM, Kearney MF, Strain MC, Richman DD, Hudgens MG, Bosch RJ, Coffin JM, Eron JJ, Hazuda DJ, Margolis DM. Administration of vorinostat disrupts HIV-1 latency in patients on antiretroviral therapy. *Nature.* 2012 Jul 25;487(7408):482-5. doi: 10.1038/nature11286. Erratum in: *Nature.* 2012 Sep 20;489(7416):460.
- 108) Meinke G, Bohm A, Hauber J, Pisabarro MT, Buchholz F. Cre Recombinase and other Tyrosine Recombinases. *Chem Rev.* 2016 Oct 26;116(20):12785-12820.

- 109) Buchholz F, Stewart AF. Alteration of Cre recombinase site specificity by substrate-linked protein evolution. *Nat Biotechnol.* 2001 Nov;19(11):1047-52.
- 110) Sarkar I, Hauber I, Hauber J, Buchholz F. HIV-1 proviral DNA excision using an evolved recombinase. *Science.* 2007 Jun 29;316(5833):1912-5.
- 111) Mariyanna L, Priyadarshini P, Hofmann-Sieber H, Kreptakies M, Walz N, Grundhoff A, Buchholz F, Hildt E, Hauber J. Excision of HIV-1 proviral DNA by recombinant cell permeable tre-recombinase. *PLoS One.* 2012;7(2): e31576.
- 112) Hauber I, Hofmann-Sieber H, Chemnitz J, Dubrau D, Chusainow J, Stucka R, Hartjen P, Schambach A, Ziegler P, Hackmann K, Schröck E, Schumacher U, Lindner C, Grundhoff A, Baum C, Manz MG, Buchholz F, Hauber J. Highly significant antiviral activity of HIV-1 LTR-specific tre-recombinase in humanized mice. *PLoS Pathog.* 2013;9(9): e1003587.
- 113) Karpinski J, Hauber I, Chemnitz J, Schäfer C, Paszkowski-Rogacz M, Chakraborty D, Beschorner N, Hofmann-Sieber H, Lange UC, Grundhoff A, Hackmann K, Schrock E, Abi-Ghanem J, Pisabarro MT, Surendranath V, Schambach A, Lindner C, van Lunzen J, Hauber J, Buchholz F. Directed evolution of a recombinase that excises the provirus of most HIV-1 primary isolates with high specificity. *Nat Biotechnol.* 2016 Apr;34(4):401-9.
- 114) Karvelis T, Gasiunas G, Siksnys V. Programmable DNA cleavage in vitro by Cas9. *Biochem Soc Trans.* 2013 Dec;41(6):1401-6. doi: 10.1042/BST20130164
- 115) Arnould S, Delenda C, Grizot S, Desseaux C, Pâques F, Silva GH, Smith J. The I-Crel meganuclease and its engineered derivatives: applications from cell modification to gene therapy. *Protein Eng Des*

- Sel. 2011 Jan;24(1-2):27-31. doi: 10.1093/protein/gzq083. Epub 2010 Nov 3. Review. PubMed PMID: 21047873
- 116) Kim YG, Li L, Chandrasegaran S. Insertion and deletion mutants of FokI restriction endonuclease. *J Biol Chem.* 1994 Dec 16;269(50):31978-82.
- 117) Mani M, Kandavelou K, Dy FJ, Durai S, Chandrasegaran S. Design, engineering, and characterization of zinc finger nucleases. *Biochem Biophys Res Commun.* 2005 Sep 23;335(2):447-57. PubMed PMID: 16084494.
- 118) Perez EE, Wang J, Miller JC, Jouvenot Y, Kim KA, Liu O, Wang N, Lee G, Bartsevich VV, Lee YL, Guschin DY, Rupniewski I, Waite AJ, Carpenito C, Carroll RG, Orange JS, Urnov FD, Rebar EJ, Ando D, Gregory PD, Riley JL, Holmes MC, June CH. Establishment of HIV-1 resistance in CD4+ T cells by genome editing using zinc-finger nucleases. *Nat Biotechnol.* 2008 Jul;26(7):808-16.
- 119) Yuan J, Wang J, Crain K, Fearn C, Kim KA, Hua KL, Gregory PD, Holmes MC, Torbett BE. Zinc-finger nuclease editing of human *cxcr4* promotes HIV-1 CD4(+) cell resistance and enrichment. *Mol Ther.* 2012 Apr;20(4):849-59.
- 120) Holt N, Wang J, Kim K, Friedman G, Wang X, Taupin V, Crooks GM, Kohn DB, Gregory PD, Holmes MC, Cannon PM. Human hematopoietic stem/progenitor cells modified by zinc-finger nucleases targeted to CCR5 control HIV-1 in vivo. *Nat Biotechnol.* 2010 Aug;28(8):839-47.
- 121) Maier DA, Brennan AL, Jiang S, Binder-Scholl GK, Lee G, Plesa G, Zheng Z, Cotte J, Carpenito C, Wood T, Spratt SK, Ando D, Gregory P, Holmes MC, Perez EE, Riley JL, Carroll RG, June CH, Levine BL. Efficient clinical scale gene modification via zinc finger nuclease-

- targeted disruption of the HIV co-receptor CCR5. *Hum Gene Ther.* 2013 Mar;24(3):245-58.
- 122) Tebas P, Stein D, Tang WW, Frank I, Wang SQ, Lee G, Spratt SK, Surosky RT, Giedlin MA, Nichol G, Holmes MC, Gregory PD, Ando DG, Kalos M, Collman RG, Binder-Scholl G, Plesa G, Hwang WT, Levine BL, June CH. Gene editing of CCR5 in autologous CD4 T cells of persons infected with HIV. *N Engl J Med.* 2014 Mar 6;370(10):901-10.
- 123) Li L, Krymskaya L, Wang J, Henley J, Rao A, Cao LF, Tran CA, Torres-Coronado M, Gardner A, Gonzalez N, Kim K, Liu PQ, Hofer U, Lopez E, Gregory PD, Liu Q, Holmes MC, Cannon PM, Zaia JA, DiGiusto DL. Genomic editing of the HIV-1 coreceptor CCR5 in adult hematopoietic stem and progenitor cells using zinc finger nucleases. *Mol Ther.* 2013 Jun;21(6):1259-69.
- 124) Yi G, Choi JG, Bharaj P, Abraham S, Dang Y, Kafri T, Alozie O, Manjunath MN, Shankar P. CCR5 Gene Editing of Resting CD4(+) T Cells by Transient ZFN Expression From HIV Envelope Pseudotyped Nonintegrating Lentivirus Confers HIV-1 Resistance in Humanized Mice. *Mol Ther Nucleic Acids.* 2014 Sep 30;3: e198.
- 125) Yao Y, Nashun B, Zhou T, Qin L, Qin L, Zhao S, Xu J, Esteban MA, Chen X. Generation of CD34+ cells from CCR5-disrupted human embryonic and induced pluripotent stem cells. *Hum Gene Ther.* 2012 Feb;23(2):238-42.
- 126) Yuan J, Wang J, Crain K, Fearn C, Kim KA, Hua KL, Gregory PD, Holmes MC, Torbett BE. Zinc-finger nuclease editing of human *cxcr4* promotes HIV-1 CD4(+) T cell resistance and enrichment. *Mol Ther.* 2012 Apr;20(4):849-59.
- 127) Didigu CA, Wilen CB, Wang J, Duong J, Secreto AJ, Danet-Desnoyers GA, Riley JL, Gregory PD, June CH, Holmes MC, Doms

- RW. Simultaneous zinc-finger nuclease editing of the HIV coreceptors *ccr5* and *cxcr4* protects CD4⁺ T cells from HIV-1 infection. *Blood*. 2014 Jan 2;123(1):61-9.
- 128) <http://www.sigmaaldrich.com/life-science/zinc-finger-nuclease-technology/learning-center/what-is-zfn.html>
- 129) Ousterout DG, Gersbach CA. The Development of TALE Nucleases for Biotechnology. *Methods Mol Biol*. 2016; 1338:27-42.
- 130) Benjamin R, Berges BK, Solis-Leal A, Igbiniedion O, Strong CL, Schiller MR. TALEN gene editing takes aim on HIV. *Hum Genet*. 2016 Sep;135(9):1059-70.
- 131) Mussolino C, Alzubi J, Fine EJ, Morbitzer R, Cradick TJ, Lahaye T, Bao G, Cathomen T. TALENs facilitate targeted genome editing in human cells with high specificity and low cytotoxicity. *Nucleic Acids Res*. 2014 Jun;42(10):6762-73.
- 132) Ru R, Yao Y, Yu S, Yin B, Xu W, Zhao S, Qin L, Chen X. Targeted genome engineering in human induced pluripotent stem cells by penetrating TALENs. *Cell Regen (Lond)*. 2013 Jun 18;2(1):5.
- 133) Mock U, Riecken K, Berdien B, Qasim W, Chan E, Cathomen T, Fehse B. Novel lentiviral vectors with mutated reverse transcriptase for mRNA delivery of TALE nucleases. *Sci Rep*. 2014 Sep 18; 4:6409.
- 134) Fadel HJ, Morrison JH, Saenz DT, Fuchs JR, Kvaratskhelia M, Ekker SC, Poeschla EM. TALEN knockout of the PSIP1 gene in human cells: analyses of HIV-1 replication and allosteric integrase inhibitor mechanism. *J Virol*. 2014 Sep 1;88(17):9704-17.
- 135) Ebina H, Kanemura Y, Misawa N, Sakuma T, Kobayashi T, Yamamoto T, Koyanagi Y. A high excision potential of TALENs for integrated DNA of HIV-based lentiviral vector. *PLoS One*. 2015 Mar 17;10(3): e0120047.

- 136) Strong CL, Guerra HP, Mathew KR, Roy N, Simpson LR, Schiller MR. Damaging the Integrated HIV Proviral DNA with TALENs. *PLoS One*. 2015 May 6;10(5): e0125652.
- 137) Joung JK, Sander JD. TALENs: a widely applicable technology for targeted genome editing. *Nat Rev Mol Cell Biol*. 2013 Jan;14(1):49-55.
- 138) Hsu PD, Lander ES, Zhang F. Development and applications of CRISPR-Cas9 for genome engineering. *Cell*. 2014 Jun 5;157(6):1262-78.
- 139) Khalili K, Kaminski R, Gordon J, Cosentino L, Hu W. Genome editing strategies: potential tools for eradicating HIV-1/AIDS. *J Neurovirol*. 2015 Jun;21(3):310-21.
- 140) Ishino Y, Shinagawa H, Makino K, Amemura M, Nakata A. Nucleotide sequence of the *iap* gene, responsible for alkaline phosphatase isozyme conversion in *Escherichia coli*, and identification of the gene product. *J Bacteriol*. 1987 Dec;169(12):5429-33.
- 141) Mojica FJ, Díez-Villaseñor C, Soria E, Juez G. Biological significance of a family of regularly spaced repeats in the genomes of Archaea, Bacteria and mitochondria. *Mol Microbiol*. 2000 Apr;36(1):244-6.
- 142) Jansen R, Embden JD, Gaastra W, Schouls LM. Identification of genes that are associated with DNA repeats in prokaryotes. *Mol Microbiol*. 2002 Mar;43(6):1565-75.
- 143) Barrangou R, Van der Oost J. CRISPR-Cas Systems: RNA-Mediated Adaptive Immunity in Bacteria and Archaea. Heidelberg, Germany: Springer; 2013
- 144) Haft DH, Selengut J, Mongodin EF, Nelson KE. A guild of 45 CRISPR-associated (Cas) protein families and multiple CRISPR/Cas subtypes exist in prokaryotic genomes. *PLoS Comput Biol*. 2005 Nov;1(6): e60.

- 145) Makarova KS, Haft DH, Barrangou R, Brouns SJ, Charpentier E, Horvath P, Moineau S, Mojica FJ, Wolf YI, Yakunin AF, van der Oost J, Koonin EV. Evolution and classification of the CRISPR-Cas systems. *Nat Rev Microbiol.* 2011 Jun;9(6):467-77.
- 146) Deltcheva E, Chylinski K, Sharma CM, Gonzales K, Chao Y, Pirzada ZA, Eckert MR, Vogel J, Charpentier E. CRISPR RNA maturation by trans-encoded small RNA and host factor RNase III. *Nature.* 2011 Mar 31;471(7340):602-7.
- 147) Chylinski K, Le Rhun A, Charpentier E. The tracrRNA and Cas9 families of type II CRISPR-Cas immunity systems. *RNA Biol.* 2013;10: 726–737.
- 148) Makarova KS, Wolf YI, Alkhnbashi OS, Costa F, Shah SA, Saunders SJ, Barrangou R, Brouns SJ, Charpentier E, Haft DH, Horvath P, Moineau S, Mojica FJ, Terns RM, Terns MP, White MF, Yakunin AF, Garrett RA, van der Oost J, Backofen R, Koonin EV. An updated evolutionary classification of CRISPR-Cas systems. *Nat Rev Microbiol.* 2015 Nov;13(11):722-36.
- 149) Zetsche B, Gootenberg JS, Abudayyeh OO, Slaymaker IM, Makarova KS, Essletzbichler P, Volz SE, Joung J, van der Oost J, Regev A, Koonin EV, Zhang F. Cpf1 is a single RNA-guided endonuclease of a class 2 CRISPR-Cas system. *Cell.* 2015 Oct 22;163(3):759-71.
- 150) Garneau JE, Dupuis ME, Villion M, Romero DA, Barrangou R, Boyaval P, Fremaux C, Horvath P, Magadán AH, Moineau S. The CRISPR/Cas bacterial immune system cleaves bacteriophage and plasmid DNA. *Nature.* 2010; 468:67–71.
- 151) Jinek M, Jiang F, Taylor DW, Sternberg SH, Kaya E, Ma E, Anders C, Hauer M, Zhou K, Lin S, et al. Structures of Cas9 endonucleases reveal RNA-mediated conformational activation. *Science.* 2014; 343:1247997.

- 152) Nishimasu H, Ran FA, Hsu PD, Konermann S, Shehata SI, Dohmae N, Ishitani R, Zhang F, Nureki O. Crystal structure of Cas9 in complex with guide RNA and target DNA. *Cell*. 2014; 156:935–949.
- 153) Shah SA, Erdmann S, Mojica FJ, Garrett RA. Protospacer recognition motifs: mixed identities and functional diversity. *RNA Biol*. 2013; 10:891–899.
- 154) Marraffini LA, Sontheimer EJ. Self versus non-self discrimination during CRISPR RNA-directed immunity. *Nature*. 2010; 463:568–571.
- 155) Jinek M, Chylinski K, Fonfara I, Hauer M, Doudna JA, Charpentier E. A programmable dual-RNA-guided DNA endonuclease in adaptive bacterial immunity. *Science*. 2012; 337:816–821
- 156) <https://www.clinicaltrials.gov/ct2/show/results/NCT02793856?term=crispr>)
- 157) Cong L, Ran FA, Cox D, Lin S, Barretto R, Habib N, Hsu PD, Wu X, Jiang W, Marraffini LA, Zhang F. Multiplex genome engineering using CRISPR/Cas systems. *Science*. 2013 Feb 15;339(6121):819-23.
- 158) Fu Y, Foden JA, Khayter C, Maeder ML, Reyon D, Joung JK, Sander JD. High-frequency off-target mutagenesis induced by CRISPR-Cas nucleases in human cells. *Nat Biotechnol*. 2013 Sep;31(9):822-6.
- 159) Hsu PD, Scott DA, Weinstein JA, Ran FA, Konermann S, Agarwala V, Li Y, Fine EJ, Wu X, Shalem O, Cradick TJ, Marraffini LA, Bao G, Zhang F. DNA targeting specificity of RNA-guided Cas9 nucleases. *Nat Biotechnol*. 2013 Sep;31(9):827-32.
- 160) Sander JD, Joung JK. CRISPR-Cas systems for genome editing, regulation and targeting. *Nature biotechnology*. 2014;32(4):347-355.
- 161) Gasiunas G, Barrangou R, Horvath P, Siksnys V. Cas9-crRNA ribonucleoprotein complex mediates specific DNA cleavage for adaptive immunity in bacteria. *Proc Natl Acad Sci U S A*. 2012;109: E2579–86.

- 162) Shen B, Zhang W, Zhang J, Zhou J, Wang J, Chen L, Wang L, Hodgkins A, Iyer V, Huang X, Skarnes WC. Efficient genome modification by CRISPR-Cas9 nickase with minimal off-target effects. *Nat Methods*. 2014; 11:399–402.
- 163) Qi LS, Larson MH, Gilbert LA, Doudna JA, Weissman JS, Arkin AP, Lim WA. Repurposing CRISPR as an RNA-guided platform for sequence-specific control of gene expression. *Cell*. 2013 Feb 28;152(5):1173-83.
- 164) Gilbert LA, Larson MH, Morsut L, Liu Z, Brar GA, Torres SE, Stern-Ginossar N, Brandman O, Whitehead EH, Doudna JA, Lim WA, Weissman JS, Qi LS. CRISPR-mediated modular RNA-guided regulation of transcription in eukaryotes. *Cell*. 2013 Jul 18;154(2):442-51.
- 165) Konermann S, Brigham MD, Trevino A, Hsu PD, Heidenreich M, Cong L, Platt RJ, Scott DA, Church GM, Zhang F. Optical control of mammalian endogenous transcription and epigenetic states. *Nature*. 2013 Aug 22;500(7463):472-476.
- 166) Maeder M L., Linder S. J., Cascio V. M., Fu Y., Ho Q. H., Joung J. K. CRISPR RNA-guided activation of endogenous human genes. *Nat. Meth* 2013b. 10, 977–979.
- 167) Mali P, Yang L, Esvelt KM, Aach J, Guell M, DiCarlo JE, Norville JE, Church GM. RNA-guided human genome engineering via Cas9. *Science*. 2013 Feb 15;339(6121):823-6.
- 168) Fonfara I, Le Rhun A, Chylinski K, Makarova KS, Lécrivain AL, Bzdrenga J, Koonin EV, Charpentier E. Phylogeny of Cas9 determines functional exchangeability of dual-RNA and Cas9 among orthologous type II CRISPR-Cas systems. *Nucleic Acids Res*. 2014 Feb;42(4):2577-90.

- 169) Kaushik A, Jayant RD, Nikkhah-Moshaie R, Bhardwaj V, Roy U, Huang Z, Ruiz A, Yndart A, Atluri V, El-Hage N, Khalili K, Nair M. Magnetically guided central nervous system delivery and toxicity evaluation of magneto-electric nanocarriers. *Sci Rep*. 2016 May 4;6:25309.
- 170) Nair M, Guduru R, Liang P, Hong J, Sagar V, Khizroev S. Externally controlled on-demand release of anti-HIV drug using magneto-electric nanoparticles as carriers. *Nat Commun* 2013; 4: 1707.
- 171) Ebina H, Misawa N, Kanemura Y, Koyanagi Y. Harnessing the CRISPR/Cas9 system to disrupt latent HIV-1 provirus. *Sci Rep* 2013; 3: 2510.
- 172) Hou P, Chen S, Wang S, Yu X, Chen Y, Jiang M, Zhuang K, Ho W, Hou W, Huang J, Guo D. Genome editing of CXCR4 by CRISPR/cas9 confers cells resistant to HIV-1 infection. *Sci Rep*. 2015 Oct 20;5:15577.
- 173) Schumann K, Lin S, Boyer E, Simeonov DR, Subramaniam M, Gate RE, Haliburton GE, Ye CJ, Bluestone JA, Doudna JA, Marson A. Generation of knock-in primary human T cells using Cas9 ribonucleoproteins. *Proc Natl Acad Sci U S A*. 2015 Aug 18;112(33):10437-42.
- 174) Ye L, Wang J, Beyer AI, Teque F, Cradick TJ, Qi Z, Chang JC, Bao G, Muench MO, Yu J, Levy JA, Kan YW. Seamless modification of wild-type induced pluripotent stem cells to the natural CCR5 Δ 32 mutation confers resistance to HIV infection. *Proc Natl Acad Sci U S A*. 2014 Jul 1;111(26):9591-6.
- 175) Wang W, Ye C, Liu J, Zhang D, Kimata JT, Zhou P. CCR5 gene disruption via lentiviral vectors expressing Cas9 and single guided RNA renders cells resistant to HIV-1 infection. *PloS One* 2014; 9: e115987. |

- 176) Li C, Guan X, Du T, Jin W, Wu B, Liu Y, Wang P, Hu B, Griffin GE, Shattock RJ, Hu Q. Inhibition of HIV-1 infection of primary CD4+ T-cells by gene editing of CCR5 using adenovirus-delivered CRISPR/Cas9. *J Gen Virol*. 2015 Aug;96(8):2381-93.
- 177) Zhu W, Lei R, Le Duff Y, Li J, Guo F, Wainberg MA, Liang C. The CRISPR/Cas9 system inactivates latent HIV-1 proviral DNA. *Retrovirology*. 2015 Feb 27; 12:22.
- 178) Zhang Y, Yin C, Zhang T, Li F, Yang W, Kaminski R, Fagan PR, Putatunda R, Young WB, Khalili K, Hu W. CRISPR/gRNA-directed synergistic activation mediator (SAM) induces specific, persistent and robust reactivation of the HIV-1 latent reservoirs. *Sci Rep*. 2015 Nov 5 ;5:16277.
- 179) Saayman SM, Lazar DC, Scott TA, Hart JR, Takahashi M, Burnett JC, Planelles V, Morris KV, Weinberg MS. Potent and Targeted Activation of Latent HIV-1 Using the CRISPR/dCas9 Activator Complex. *Mol Ther*. 2016 Mar;24(3):488-98.
- 180) Hu W, Kaminski R, Yang F, Zhang Y, Cosentino L, Li F, Luo B, Alvarez-Carbonell D, Garcia-Mesa Y, Karn J, Mo X, Khalili K. RNA-directed gene editing specifically eradicates latent and prevents new HIV-1 infection. *Proc Natl Acad Sci U S A*. 2014 Aug 5;111(31):11461-6.
- 181) Wang G, Zhao N, Berkhout B, Das AT. CRISPR-Cas9 can inhibit HIV-1 replication but NHEJ repair facilitates virus escape. *Mol Ther* 2016; 24: 522–526
- 182) Yoder KE, Bundschuh R. Host double strand break repair generates hiv-1 strains resistant to CRISPR/Cas9. *Sci Rep* 2016; 6: 29530
- 183) Ramakrishna S, Kwaku Dad AB, Beloor J, Gopalappa R, Lee SK, Kim H. Gene disruption by cell-penetrating peptide-mediated delivery

- of Cas9 protein and guide RNA. *Genome Res.* 2014 Jun;24(6):1020-7.
- 184) Kaminski R, Chen Y, Fischer T, Tedaldi E, Napoli A, Zhang Y, Karn J, Hu W, Khalili K. Elimination of HIV-1 Genomes from Human T-lymphoid Cells by CRISPR/Cas9 Gene Editing. *Sci Rep.* 2016 Mar 4; 6:22555.
- 185) Kaminski R, Chen Y, Salkind J, Bella R, Young WB, Ferrante P, Karn J, Malcolm T, Hu W, Khalili K. Negative Feedback Regulation of HIV-1 by Gene Editing Strategy. *Sci Rep.* 2016 Aug 16; 6:31527.
- 186) Kaminski R, Bella R, Yin C, Otte J, Ferrante P, Gendelman HE, Li H, Booze R, Gordon J, Hu W, Khalili K. Excision of HIV-1 DNA by gene editing: a proof-of-concept in vivo study. *Gene Ther.* 2016 Aug;23(8-9):696.
- 187) Randhawa S, Cho BS, Ghosh D, Sivina M, Koehrer S, Müschen M, Peled A, Davis RE, Konopleva M, Burger JA. Effects of pharmacological and genetic disruption of CXCR4 chemokine receptor function in B-cell acute lymphoblastic leukaemia. *Br J Haematol.* 2016 Aug;174(3):425-36.
- 188) Yin C, Zhang T, Qu X, Zhang Y, Putatunda R, Xiao X, Li F, Xiao W, Zhao H, Dai S, Qin X, Mo X, Young WB, Khalili K, Hu W. In Vivo Excision of HIV-1 Provirus by saCas9 and Multiplex Single-Guide RNAs in Animal Models. *Mol Ther.* 2017 May 3;25(5):1168-1186.
- 189) Gallia GL, Darbinian N, Tretiakova A, Ansari SA, Rappaport J, Brady J, Wortman MJ, Johnson EM, Khalili K. Association of HIV-1 Tat with the cellular protein, Puralpha, is mediated by RNA. *Proc Natl Acad Sci U S A.* 1999 Sep 28;96(20):11572-7.
- 190) Behringer R. *Manipulating the Mouse Embryo: A Laboratory Manual*, 4th edn. Cold Spring Harbor Laboratory Press: Cold Spring Harbor, NY, USA, 2014.

- 191) Liszewski, M. K., Yu, J. J. & O'Doherty, U. Detecting HIV-1 integration by repetitive-sampling Alu-gag PCR. *Methods* 2009, 47, 254–260.
- 192) Dickie P, Felser J, Eckhaus M, Bryant J, Silver J, Marinos N, Notkins AL. HIV-associated nephropathy in transgenic mice expressing HIV-1 genes. *Virology*. 1991 Nov;185(1):109-19.
- 193) Vahlne A. A historical reflection on the discovery of human retroviruses. *Retrovirology*. 2009 May 1;6: 40.
- 194) Levin A, Loyter A, Bukrinsky M. Strategies to inhibit viral protein nuclear import: HIV-1 as a target. *Biochimica et biophysica acta*. 2011;1813(9):1646-1653.
- 195) Hamy F, Gelus N, Zeller M, Lazdins JL, Bailly C, Klimkait T. Blocking HIV replication by targeting Tat protein. *Chem Biol*. 2000 Sep;7(9):669-76.
- 196) Balachandran A, Wong R, Stoilov P, Pan S, Blencowe B, Cheung P, Harrigan PR, Cochrane A. Identification of small molecule modulators of HIV-1 Tat and Rev protein accumulation. *Retrovirology*. 2017 Jan 26;14(1):7.
- 197) Burton DR, Mascola JR. Antibody responses to envelope glycoproteins in HIV-1 infection. *Nat Immunol*. 2015 Jun;16(6):571-6.
- 198) Dose escalation study of cyclophosphamide in HIV-infected subjects on HAART receiving SB-728-T. Available Online: <http://clinicaltrials.gov/ct2/show/NCT01543152>.
- 199) Schleifman EB, McNeer NA, Jackson A, Yamtich J, Brehm MA, Shultz LD, Greiner DL, Kumar P, Saltzman WM, Glazer PM. Site-specific Genome Editing in PBMCs With PLGA Nanoparticle-delivered PNAs Confers HIV-1 Resistance in Humanized Mice. *Mol Ther Nucleic Acids*. 2013 Nov 19; 2: e135.

- 200) Wong, J.K., Hezareh, M., Guenthard, H.F., Havlir, D.V., Ignacio, C.C., Spina, C.A., Richman, D.D. Recovery of replication-competent HIV despite prolonged suppression of plasma viremia. *Science* 1997 278, 1291–1295
- 201) Sáez-Cirión A, Bacchus C, Hocqueloux L, Avettand-Fenoel V, Girault I, Lecuroux C, Potard V, Versmisse P, Melard A, Prazuck T, Descours B, Guergnon J, Viard JP, Boufassa F, Lambotte O, Goujard C, Meyer L, Costagliola D, Venet A, Pancino G, Autran B, Rouzioux C; ANRS VISCONTI Study Group. Post-treatment HIV-1 controllers with a long-term virological remission after the interruption of early initiated antiretroviral therapy ANRS VISCONTI Study. *PLoS Pathog.* 2013 Mar;9(3): e1003211.
- 202) Persaud D, Gay H, Ziemniak C, Chen YH, Piatak M Jr, Chun TW, Strain M, Richman D, Luzuriaga K. Absence of detectable HIV-1 viremia after treatment cessation in an infant. *N Engl J Med.* 2013 Nov 7;369(19):1828-35.
- 203) Ho YC, Shan L, Hosmane NN, Wang J, Laskey SB, Rosenbloom DI, Lai J, Blankson JN, Siliciano JD, Siliciano RF. Replication-competent noninduced proviruses in the latent reservoir increase barrier to HIV-1 cure. *Cell.* 2013 Oct 24;155(3):540-51.
- 204) Col E, Caron C, Seigneurin-Berny D, Gracia J, Favier A, Khochbin S. The histone acetyltransferase, hGCN5, interacts with and acetylates the HIV transactivator, Tat. *J Biol Chem.* 2001 Jul 27;276(30):28179-84.
- 205) Ott M, Schnölzer M, Garnica J, Fischle W, Emiliani S, Rackwitz HR, Verdin E. Acetylation of the HIV-1 Tat protein by p300 is important for its transcriptional activity. *Curr Biol.* 1999 Dec 16-30;9(24):1489-92.
- 206) Schumann K, Lin S, Boyer E, Simeonov DR, Subramaniam M, Gate RE, Haliburton GE, Ye CJ, Bluestone JA, Doudna JA, Marson A.

Generation of knock-in primary human T cells using Cas9 ribonucleoproteins. Proc Natl Acad Sci U S A. 2015 Aug 18;112(33):10437-42.

APPENDIX A: MOLECULAR CLONING

A1: PCR Products

Three different regions of LTR promoter were amplified (figure 48, LTR -120/+66, -80/+66 and -38/+66 regions) using pNL4-3 DNA virus as the template and the primers listed in table 6 containing the restriction sites for KpnI and XbaI. PCRs were performed under the following conditions:

COMPONENT	VOLUME/REACTION
Fail Safe PCR Enzyme Mix (1.25 Units)	0.5 µl
10 µM primer F	1ul
10 µM primer R	1ul
Buffer D 2X	25 ul
template	300 ng
DNAsI-free water	To 50 ul

Table 7: PCR conditions for the LTR promoter amplification

The cycling conditions of the assay were as follows:

94° C for 3 minutes, 25 cycles (94° C for 30 s, 55° C for 30 s, 72° C for 30s) and 72° C for 7 minutes.

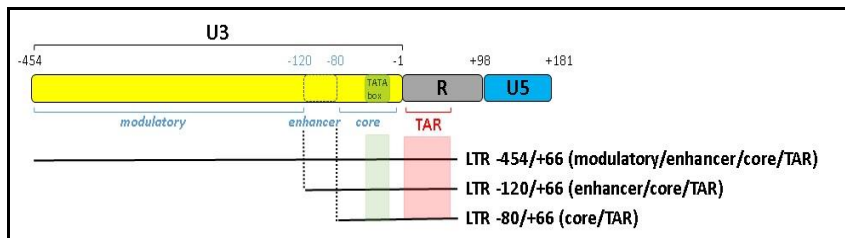


Figure 48: Illustration of the LTR HIV-1 promoter. LTR promoter and portions of LTR promoter for the cloning into the px260 plasmid to test the ability of Tat to activate the

minimal promoter region. (Figure modified from Kaminski et al., 2016, [185], under permission from a Creative Commons CC-BY license]

A2. Gel Purification of PCR products

Gel purification was performed with QIAquick Gel Extraction kit (Qiagen, Germany) using columns that bind DNA in presence of high concentrations of salt, allowing the elimination of all impurities and the elution of pure DNA. Briefly, DNA was separated on agarose gel. The target fragment was cut from the gel and the mass was determined. 5X volume of buffer QG was added and the gel was melted at 56°C for 10 minutes. One volume of isopropanol 100% was added to precipitate the DNA and the sample was loaded to the provided columns and centrifuged at 13,000 rpm for 60 s. The DNA was washed with 750 µl of Buffer PE and centrifuged at 13,000 rpm for 60s. An additional step of centrifugation was performed for 1 min at 13,000 rpm to remove any remaining buffer. DNA was eluted in 25 µl of DNAase free water and centrifugated at 13,000 rpm for 1min.

A3: Ligation of PCR Products and Transformation

To allow one successful cut of the PCR product with the restriction sites created by PCR amplification, the Taq PCR fragments were first directly inserted in TA vector (Life Technologies, CA).

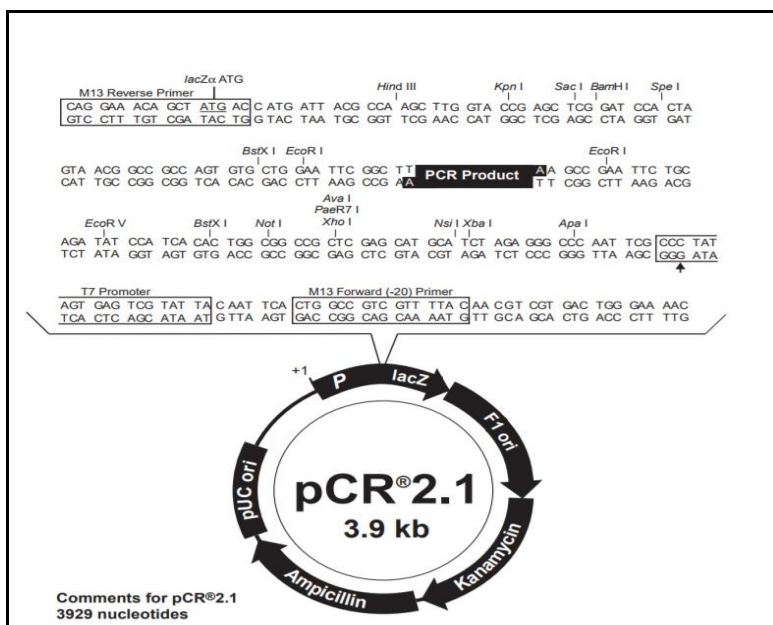


Figure 49: pCR2.1 Vector Map and Sequence [Invitrogen USA, catalog #K2000-01]

The reaction was performed under the following conditions:

COMPONENT	VOLUME/REACTION
ExpressLink™ T4 DNA Ligase (5U)	1ul
5X T4 DNA Ligase Reaction Buffer	2ul
pCR [®] 2.1 vector (25 ng/μL)	2ul
insert	15ng
DNAsi-free water	To 10 ul

Table 8: Ligation Condition for LTR Cloning into the TA Vector: After gel purification LTR product were cloned in 50ng of TA vector at 16°C ON.

The reaction was incubated at 16°C O/N and 5μl of ligation product was transformed using 50 μl of One Shot[®] INV^F Chemically Competent *E. coli* (K2000-01, Life Technologies, CA). Samples were incubated on ice for 30 minutes and then 42°C at 45 seconds (heat shock) and back on ice for 2 minutes. 500 μl of SOC media was added to allow the growth of bacteria

at 37°C. After 1h, 100 µL of suspension was plated on Luria-Bertani (LB) agar plates (LB Medium + 2% agar + ampicillin 100 mg/mL for selective growth) and incubated at 37°C O/N. At the end, single bacterial colony was selected and suspended in LB broth with ampicillin O/N at 37°C for miniprep.

A4: DNA Isolation from Bacteria

The extraction of plasmid DNA was carried out using the Qiagen Plasmid Minikit (Qiagen, Germany). After O/N incubation the bacterial culture was centrifuged at 3000 rpm for 10 minutes and the pellet was resuspended in 300 µl buffer P1 and 300 µl of lysis buffer P2. After a short incubation of 5' on ice 200 µL of buffer P3 was added to stop the lysis process. The clear supernatant, obtained by centrifugation at 14000 rpm for 15 minutes at 4°C, was mixed with isopropanol (1:1) to precipitate the DNA and incubated at -20°C for 1 hour. Samples were then centrifuged at 14000 rpm for 15 minutes and the pellet was resuspended in 80 µl of DNAase free water. The resulting plasmids were sent for sequencing to Genewiz to verify the presence of the insert.

A5: Digestion of pCR™4-TOPO® TA Vector and pX260-U6-DR-BB-DR-Cbh-NLS-hSpCas9-NLS-H1-shorttracr-PGK-puro

After screening the TA vector clones, digestion was performed on the clones containing the insert of interest and on the vector pX260-U6-DR-BB-DR-Cbh-NLS-hSpCas9-NLS-H1-shorttracr-PGK-puro or simply called px260 (Addgene #42229, figure 50) harboring the humanized SpCas9 gene, allowing the creation of a construct where the expression of Cas9 is driven by HIV-1 LTR promoter.

The digestion was performed under the following conditions:

(COMPONENT)	VOLUME/REACTION
KpnI (10U/ul)/XbaI (20U/ul)*	1ul
NcoI*	1ul
Buffer 2.1 10X	5 ul
vector**	2µg
DNaseI-free water	To 50 ul

*New England Biolab

**vector: pCR™4-TOPO® TA vector (Life Technologies, CA) or px260-LTR-Cas9

Table 9: Digestion Conditions for LTR Cloning into px260-U6-DR-BB-DR-Cbh-NLS-hSpCas9-NLS-H1-shorttracr-PGK-puro. TA vector harbouring the minimal LTR promoter and px260-LTR Cas9 were digested with KpnI and XbaI at 37°C for 3h to allow the creation of compatible ends for the ligation step.

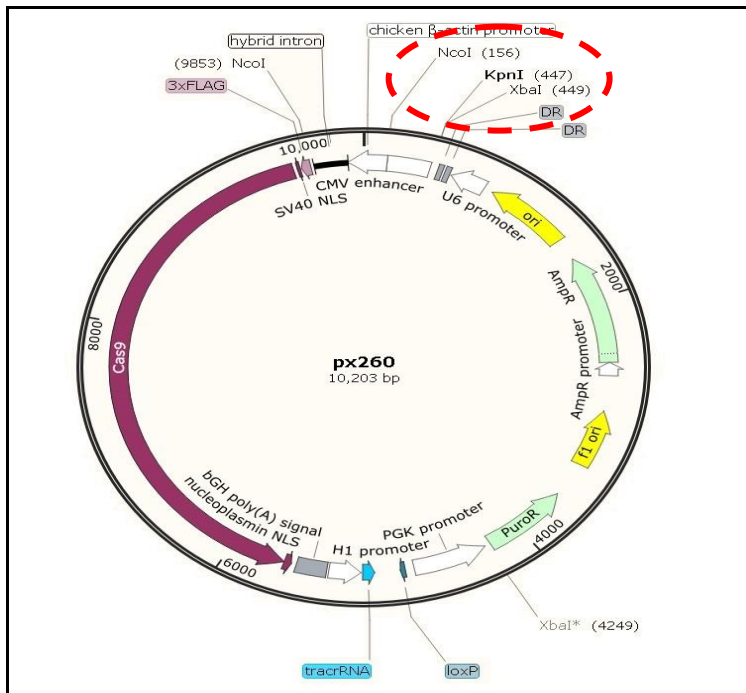


Figure 50: Vector Map of pX260-U6-DR-BB-DR-Cbh-NLS-hSpCas9-NLS-H1-shorttracr-PGK-puro Plasmid [Addgene #42229]. Restriction Enzymes used for the cloning were undelighted in red.

The reaction mixture was incubated at 37°C for 3h and analyzed with a 2% agarose gel. Gel DNA purification was performed using QIAquick Gel Extraction kit (Qiagen, Germany). 50 ng of digested vector and 100 ng of insert were ligated ON at 16°C in a final volume of 20 µl, using T4 DNA ligase (New England, Biolabs, USA).

A6: Creation of LENTI-LTR (-80/+66) Cas9-BLAST Construct

LentiCas9-Blast plasmid (Addgene #52962, figure 51) was digested with NheI and XbaI restriction enzymes following the digestion conditions previously described. PCR amplification (94 °C 3 minutes, 25 cycles (94 °C 30 s, 55 °C 30 s, 72 °C 30s) and 72 °C 7 minutes) was performed using primers described in table 6 and pNL4-3 as template. The reaction was separated with a 2% agarose gel and purified and cloned to the TA vector. Positive clones were digested with XbaI and NheI (restriction sites introduced in LTR promoter by PCR amplification) and ligated with the digested LentiCas9-Blast plasmid.

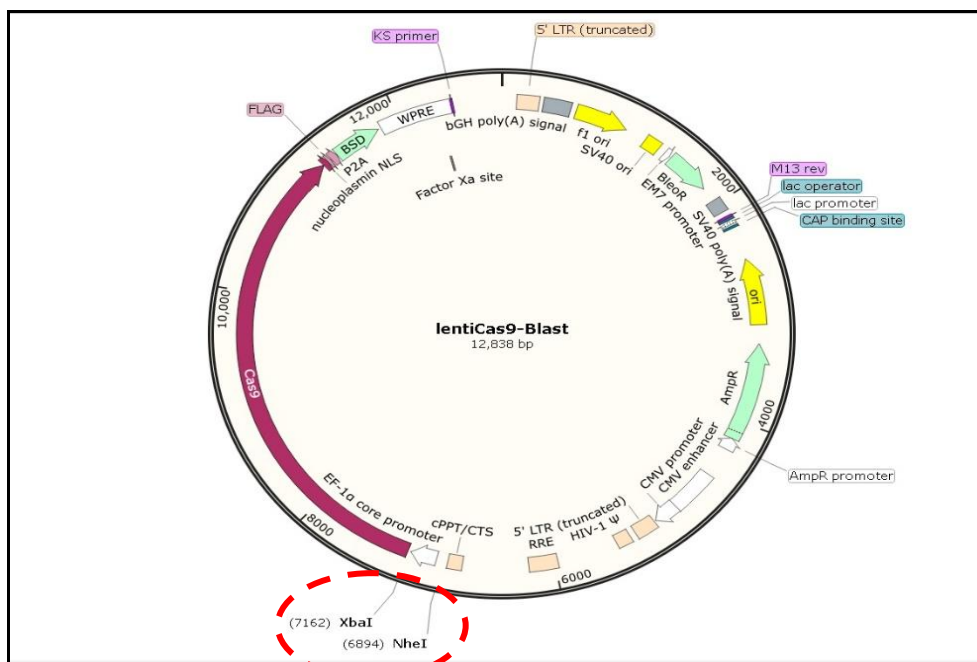


Figure 51: LentiCas9-Blast Plasmid Vector Map [Addgene # 52962]. Restriction Enzymes used are circled in red

A7: Creation of px601-CMV/saCas9-LTR1-GagD

2 μg of px601-AAV-CMV:NLS-saCas9-NLS-3xHA-bGHpA;U6::Bsa1-SgRNA (Addgene #61591, figure 52) vector was digested with 1 μl of BsaI in 50 μl of reaction mixture for 3h at 37°C. The digestion mix was purified using QIAquick Gel Extraction kit (Qiagen, Germany) and treated with CIP under the following conditions:

COMPONENT	VOLUME/REACTION
CIP (10 U/ul) *	1 ul
10X CutSmart® Buffer	5 ul
Digested vector	2ul
DNAase-free water	To 50 ul

*New England, Biolabs

Table 10: De-phosphorylation conditions of px601-AAV-CMV:NLS-saCas9-NLS-3xHA-bGHpA;U6:Bsa1-SgRNA after Bsa1 digestion. Digested vector was treated with CIP enzyme to allow the dephosphorylation of its extremities at 37°C for 30 minutes.

The reaction was incubated at 37°C for 30 minutes and purified using QIAquick PCR Purification Kit (Qiagen, Germany) following the manufacturer's instructions.

Oligonucleotides specific for LTR1 and GagD regions were used to generate gRNA sequences. Oligonucleotides were annealed according to the following method:

- 5µl of oligonucleotides 10 µM (final volume of 10 µl) added in a 1.5 ml microfuge tube were incubated at 95°C for 5 minutes
- the mix was cooled to room temperature after which it was phosphorylated and annealed using T4 Polynucleotide Kinase (PNK) under the following condition:
- Reaction was incubated at 37°C for 30'.
- 100 nM of reaction mixture was ligated at 14°C ON with 50 ng of p601 SaCas9 LTR1 BsaI linearized

COMPONENT	VOLUME/REACTION
T4 PNK (10U/µl)	0,5 µl
T4 buffer 10X	2 µl
Annealed mixture	10 µl
Deionized water	7.5 µl

Table 11: Phosphorylation of Annealed Oligonucleotides Mixture

COMPONENT	VOLUME/REACTION
Insert*	100 ng
T4 DNA ligase**	1µl
T4 DNA Ligase Reaction Buffer 10X	1µl
Vector Bsal digested***	50 ng
DNAase-free water	To 10 µl

*phosphotilated oligonucleotides mixture

** New England Biolabs

***px601 SaCas9 LTR1 Bsal linearized

Table 12: Ligation Condition for Phosphorylated Oligonucleotides with the px601 Vector.

5 µl of ligation product was transformed in competent cells and clones were screened to check the presence of gRNA. The same protocol was used to generate two different px601 constructs containing the sequence of the gRNA LTR1 or GagD. Later 2 µg of px601 SaCas9 LTR1 vector was digested with 0.5 µl of EcoRI (20U/µl) and 1 µl of KpnI (10U/µl). A PCR was performed using px601SaCas9GagD construct as template to amplify GagD gRNA using the primers T795 and T796 (donated by Dr. Hu). The PCR product was treated with infusion kit (Takara Bio, USA) to fuse GagD gRNA sequence and the digested px601 SaCas9 LTR1 vector EcoRI/KpnI. Reaction conditions are described below:

COMPONENT	VOLUME/REACTION
PCR fragment (insert)	50ng
Linearized vector	100 ng
5X In-Fusion HD Enzyme Premix	2 µl
Deionized Water	To 10 µl

Table 13: Infusion treatment conditions to create px601 LTR1 GagD construct.

Insert and vector were treated with the enzyme premix for 15 minutes at 50°C and 5µl of reaction mix was transformed in the competent cells.

The mix was incubated for 15 minutes at 50°C, and after that 5µl of reaction mixture was transformed using 50 µl of Stellar competent cells, sold in In-Fusion HD Plus kits, following the standard protocol of transformation. Digestion with BamHI or EcoRI plus NotI was performed for the screening of positive clones.

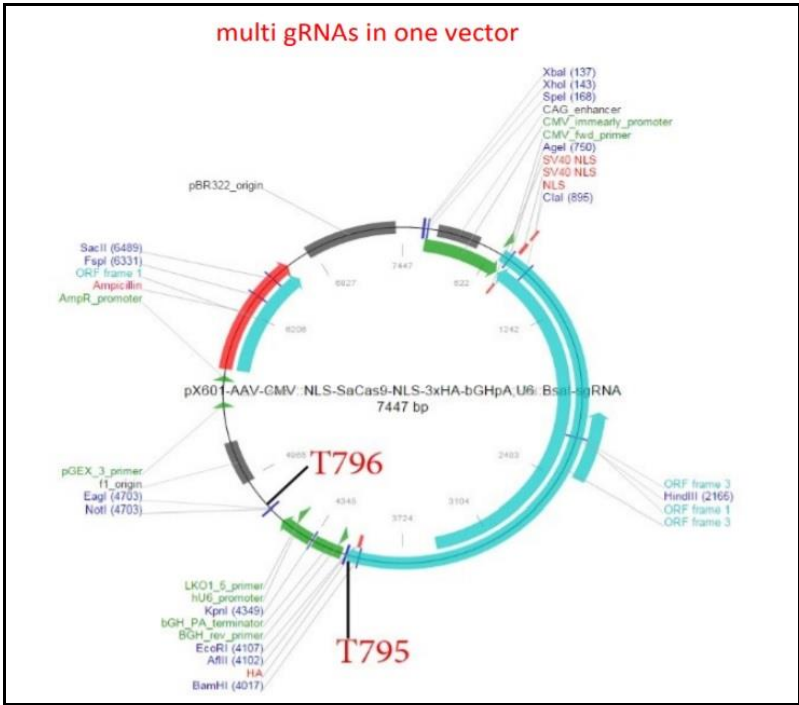


Figure 52: Position of the T795 and T796 primers in px601. These primers were used to amplify the gRNA sequence for the cloning of multi-gRNAs in one px601 Vector [Addgene # 61591].

APPENDIX B: Lentiviral packaging

HEK 293 cells were transfected using CaPO₄ precipitation with 15 µg of pLENTI LTR- 80/+ 66-Cas9-Blast, 10 µg of psPAX2 containing Gag, Pol, Rev and Tat and 6 µg pCMV-VSV-G expressing envelope protein in 450 µl of water, supplemented with 50 µl of 2.5M CaCl₂. The DNA mixed with calcium generates a precipitate that facilitates the entry of DNA into the cell by endocytosis. The mixture was added dropwise into 0.5 ml warm HNP buffer. The mix was added on the cells, plated on 100 mm dishes in presence of 10 ml of growth medium and 50 µM of cloroquine. Fresh medium was supplemented after 24h and supernatant was harvested 48 and 72h later. The same protocol was used to package pKLV-U6-LTR A/B-PGKpuro2ABFP, using the amounts of DNA founded in the table below.

Per 100 mm dish see below:

	pCW-Cas9 (1,7µg/µl)	psPAX2 (2.2 µg/µl)	pCMV-VSV-G (1.8µg/µl)	Lenti-LTR-Cas9-blast (2µg/µl)
1	15 µg	10 µg	6 µg	-
2	-	10 µg	6 µg	15 µg
	pKLV-gRNA empty (1.28 µg/µl)	pMDLg/Prre (2 µg/µl)	pRSV-Rev (2 µg/µl)	pCMV-VSV-G (1.8 µg/µl)
1	10µg	8 µg	5 µg/	3 µg

Table 14: Lentiviral vector packaging conditions. HEK 293 cells were transfected with 15 µg of pLENTI LTR- 80/+ 66-Cas9-Blast, 10 µg of psPAX2 and 6 µg pCMV-VSV-G. The same protocol was used to package pKLV-U6-LTR A/B-PGKpuro2ABFP, using pMDLg/Prre, pRSV-Rev and PCMV-VSG-G.

APPENDIX C: Western Blot

Western blotting was performed as follows. The cells were washed in PBS, harvested and centrifuged at 1200 rpm for 5 minutes. The cell pellet was suspended in 350 μ l of TNN buffer supplemented with 1X protease inhibitor cocktail for mammalian cells (Cayman Chemical, USA). Cellular lysates were kept in agitation at 4°C for 30 min and then centrifuged at 14,000 rpm at 4°C for 15 minutes. After the preparation of stacking gel (30% Acrylamide/0,8% bisacrilamide, 4X Tris Cl/SDS pH 6.8, 10% APS, TEMED, distilled water) and running gel 9% (30% Acrylamide/0,8% bis-acrilamide, 4X Tris Cl/SDS pH 8.8, 10% APS, TEMED, distilled water), 100 μ g of proteins were mixed with 6 μ l of loading dye solution 1x and TNN buffer (40 μ l final volume), denatured at 95°C for 5 min and loaded into the gel. 8 μ l of protein marker (Colorplus prestained protein marker, Broad range (7-175kDa), New England Biolabs, USA) was loaded in the first well. After 30 minutes of run at 100 Volt for 2h in 1X Running Buffer (Tris-Glycine-SDS, TGS) (Biorad, USA) the proteins were transferred from the gel to a membrane in 1x Transfer Buffer (Tris-Glycine, TG) (Biorad, USA) with 200 mL of methanol O/N at 4°C at 60 milliamps. The following day the membrane was blocked in 5% non-fat dry milk in PBST (50ml), (0.1% Tween 20 in 1X PBS) at RT for 1 hour. The primary antibody was added for 3 hours at room temperature, mouse anti-flag M2 monoclonal antibody (1:1000, Sigma, USA) and mouse anti- α -tubulin monoclonal antibody (1:2000, Sigma, USA), or rabbit anti GFP protein (1:1000, Sigma, USA) and rabbit anti-HIV-1-Tat (1:1000, Abcam, USA). The membrane was washed 3 times for 5 min with TBST and the secondary antibody solution was added at RT for 1 hour, Goat Anti-Mouse IgG FITC conjugated and horse anti rabbit rhodamine conjugated, diluted 1:5000 in in 5% No fat dry milk in PBST. The membrane was washed 3 times for 5 min with PBST

and scanned using an Odyssey Infrared Imaging System (LI-COR Biosciences, USA).

APPENDIX D: DNA and RNA analysis

D1: Genomic DNA Extraction from Cells and Tissues

Nucleospin Tissue Kit (Macherey Nagel, Germany) was used for the DNA purification. The procedure was carried out as follows: 25 mg of tissues were homogenized in 250 μ l of buffer T using a combination of different beads following the manufacturer's protocols and the Bullet Blender homogenizer (Next Advance, USA) and. The lysate was incubated O/N in presence of proteinase K, lysed with 210 μ l of B3 lysis buffer at 75°C for 15', precipitated with 210 μ l of ethanol and loaded into the column that binds specifically the DNA. After centrifugation at 11,000g for 1 minutes, the DNA was subject to two steps of wash and at the end, the DNA was eluted in 100 μ l of DNAase free water. DNA from 10^7 cells and from blood was purified using the manufacturer's directions.

D2: RNA Isolation from Cells and Blood

RNeasy Mini Kit (Qiagen, Germany) was used for the RNA extraction under the following instructions: 1×10^7 cells were harvested and lysed in 350 μ l of buffer RTL. The lysate was loaded into a QIAshredder spin column, centrifuged for 2 min at maximum speed and the eluted product was mixed with 350 μ l of 70% ethanol and incubated for 1' at RT. Then the mixture was loaded into a RNeasy spin column and centrifuged for 15 seconds at $\geq 8000 \times g$. 350 μ l of buffer RW1 was added on the column and the samples were centrifuged for 15 seconds at $\geq 8000 \times g$. 80 μ l of DNase solution (10 μ l of DNase I stock solution in 70 μ l of buffer RDD) was added into the membrane and incubated for 15 min at RT. 350 μ l of buffer RW1

was added on the column and after centrifugation at $\geq 8000 \times g$ for 15 seconds, two wash steps were performed with 500 μl of Buffer RPE. Samples were centrifuged for 15 s at $\geq 8000 \times g$ and an additional step of centrifugation for 1 minute at full speed was performed to eliminate any residual buffer. RNA was eluted in 40 μl of RNase-free after centrifugation for 1 min at $\geq 8000 \times g$.

D3: Retrotranscription

RNA was retrotranscribed using M-MLV reverse transcription enzyme (Invitrogen, USA). Briefly 1 μg of total RNA was mixed with 1 μl of oligo dT (500 $\mu\text{g}/\text{ml}$), 1 μl of 10 mM dNTP mix (10 mM of each nucleotide) and distilled water in a final volume of 12 μl . The mix was incubated at 65°C for 5 minutes and then on ice. 4 μl of 5X first strand buffer, 2 μl of 0.1M DTT and 1 μl of RNase OUT recombinant ribonuclease inhibitor (40U/ μl) were added to the mixture and incubated at 37° C for 2 minutes. 1 μl of M-MLV RT (200U) was added to each mix and the samples were incubated at 37° C for 50 minutes. The reaction was inactivated at 70° C for 15 minutes. cDNA was quantified using spectrophotometric technology (Biorad, USA) and analyzed by TaqMan qPCR.

D4: RNA Extraction from Rat Tissues

TRIzol (Thermo fisher scientific, USA) is a chemical solution used for the extraction of RNA, DNA and proteins. Briefly 25 mg of tissue was homogenized using specific bead combinations and the bullet blender homogenizer (Next Advance, USA) in 500 μl of Trizol. The lysate was centrifuged at max speed for 1 minute and 250 μl of reaction was mixed with 750 μl of Trizol and incubated at RT for 5 minutes. 200 μl of chloroform was added to the mixture and incubated at RT for three minutes. The mix was centrifuged at 12,000xg for 15 seconds at 4°C to

allow the separation into different phases, the lower red phenol-chloroform phase, an interphase and a colorless upper aqueous phase containing the RNA. The top phase was collected and mixed with 500 μ l of 100% isopropanol at RT for 10 minutes. Samples were centrifuged at 12,000xg for 10' at 4°C. The pellet was washed with 1ml of 75% ethanol and centrifuged at 7500 g for 5 minutes at 4°C. RNA was resuspended in 40 μ l of RNase free water and stored at -70 C.

D5: PCR on TZM-b1 Cells

300 ng of DNA purified from TZM-b1 cells transduced with lenti SpCas9 LTR -80/ +66 and gRNAs A and B in presence of different concentrations of Tat was subjected to LTR PCR amplification (94 °C 5 min, 30 cycles (94°C 15 s, 55°C 30 s, 72°C 30 sec) and 72°C 5min) using Fail Safe kit, buffer D (Epicentre, USA) and 0.2 μ M of the primers listed in table 6. The same PCR was performed on TZM-b1 lenti LTR-80/+66 Cas9 stable line transduced with different amounts of gRNAs and infected with HIV-1_{JRFL} and HIV-1_{SF162}.

D6: qPCR on Jurkat 2D10 cells

RNA purified from Jurkat 2D10 cells was assessed by qPCR using Platinum Taq DNA polymerase (Invitrogen, USA). Each sample was analyzed in triplicate, such as the standards.

The reaction was prepared as follows:

COMPONENT	VOLUME/REACTION
Platinum™ Taq DNA polymerase*	0,1 µl
Buffer 10X	2 µl
dNTPs mix (25 uM)	0,16 µl
50 mM MgCl ₂	1.2 µl
forward Primer (100 µM)	0,1µl
reverse Primer (100 µM)	0,1 µl
probe 100 µM)	0,1 µl
DNA sample	50 ng
Deionized Water	To 20 µl

*Thermo Fisher Scientific (#10966034)

Table 15: qPCR Conditions to detect viral DNA in Jurkat 2D10 cells. Reactions were performed in 50 µl using two LTR FAM conjugated probe to detect the ratio between truncated versus full length LTR as index of efficiency of viral excision.

D7: PCR on Jurkat 2D10 cells

PCR was performed on a conventional PCR machine (T100 Thermal Cycler, Biorad, CA, USA) in 25 µl of buffer D, 1µl of Fail Safe enzyme and 300 ng of DNA sample. PCR specific for LTR region was performed in Jurkat 2D10 -80/+66 Cas9 cell line transduced with different amounts of gRNAs in presence or absence of Tat. PCR product was resolved on 2% agarose gel detecting one 427 base pairs wild type LTR fragment and one 227 base pairs truncated LTR fragment. Specific PCRs for 5'UTR, env and B-actin were performed on DNA purified from Jurkat cells transduced with Cas9 and gRNAs A/B and HIV-1 infected using primers listed in table 6. The sizes of the amplicons were 139, 150 and 270 base pairs respectively. LTR PCR revealed one 395 base pairs wild type fragment and one 205 base pairs truncated LTR. PCR conditions were as follows: 94 °C 5 min, 30 cycles (94 °C 15 s, 55 °C 30 s, 72 °C 30 sec and 72C 5 min.

APPENDIX E: TG26 Mice and Rat Model

Tg26 mice were crossed into the C57BL/6L background to generate animals able to survive to 12 months of age and where clinical manifestation, associated to a low level of expression of viral transcripts, is largely reduced. Tg26 mice and rats were used for studies *in vivo* to test the ability of the construct AAV9 saCas9 LTR1/GagD. Both animal models encompass a sequence of HIV-1_{NL4-3} with a deletion of a 3.1 kb from the C-terminal of the Gag gene to the N-terminal of the Pol gene (Figure 53). This delivery system is associated with the use of saCas9, derived from *Staphylococcus aureus*, 1 kb shorter than spCas9 allowing the use of one vector for the delivery of Cas9 and gRNAs together.

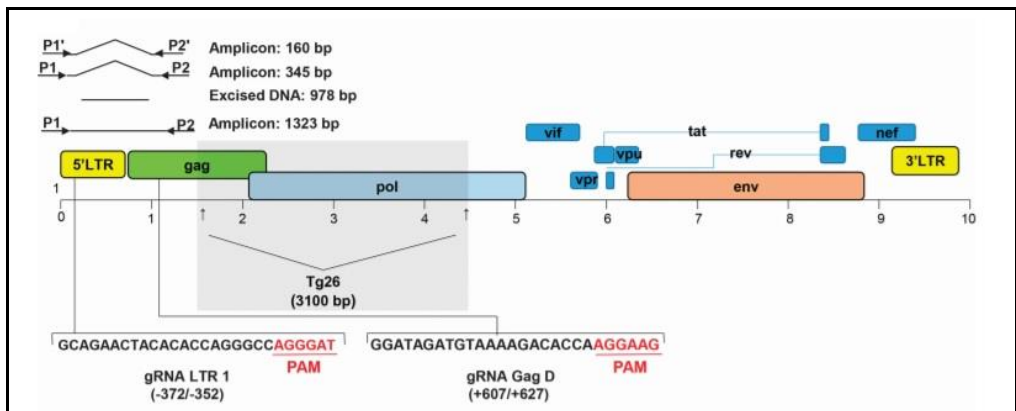


Figure 53: Schematic representation of the Tg26 mouse containing HIV-1 DNA. The mice harbour HIV-1 genome with a missing portion between gag and pol region. The region covered by the primers used for to detect viral excision are illustrated on the top of the figure. The position of the LTR1 and GagD gRNAs is shown by arrows. (Figure reproduced with permission from Kaminski R. *et al.*, 2016 and Nature Publishing group) [186].

APPENDIX F: Humanized Mice Model and AAV9/CRISPR/Cas9 Treatment

Nod/Cg-Prkdc^{scid} Il2rg^{tm1wj}/SzJ (NSG) mice were used for study the ability of AAV9SaCas9LTR1GagD to induce gene editing in humanized animal model. The experiments on humanized mice were performed by collaborators from the University of Nebraska Medical Center. Briefly 10⁴ human peripheral blood lymphocytes (PBLs) were injected by intrahepatic injection for each newborn mouse, previously irradiated with C9cobalt60. 18 weeks old mice were infected with HIV-1_{NL4-3} (10⁵ tissue culture infective dose 50/ml); of the following mice, 5 received no antiretroviral treatment and one injection of AAV9 construct, and 13 were treated with a long acting slow effective release ART therapy (LASER ART) using 40-45 mg of a cocktail of antiretroviral drugs such as rilpivirine, myristolyated dolutegravir, lamivudine and abacavir. After 6 weeks of ART therapy the animals under retroviral drugs were successively divided in non Cas9 treatment (4 mice) and Cas9 treated (9 mice). Five control mock animals were used as negative control. Tissues were harvested after 5 weeks from CRISPR treatment in absence of antiretroviral treatment.

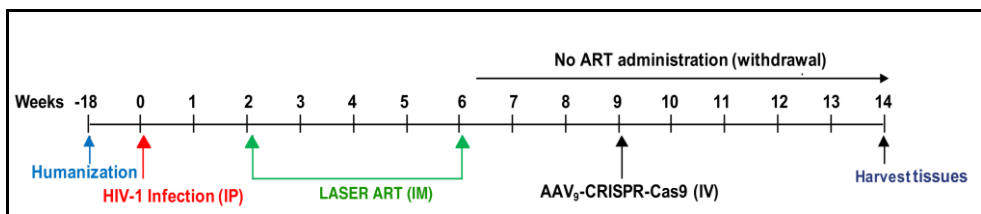


Figure 54: Schematic representation of mouse humanization, viral infection, ART initiation and CRISPR/Cas9 treatment. Infection was performed at week 0, a combination of antiretroviral drugs was somministrated for 4 weeks, three weeks later one single injection of AAV₉-CRISPR-Cas9 was injected and tissues were harvested at week 14.

SCIENTIFIC PRODUCTS

1. Delbue S, Elia F, Signorini L, **Bella R**, Villani S, Marchioni E, Ferrante P, Phan TG, Delwart E. Human polyomavirus 6 DNA in the cerebrospinal fluid of an HIV-positive patient with leukoencephalopathy. *J Clin Virol.* 2015 Jul; 68:24-7. IMPACT FACTOR: 3.466
2. Serena Delbue, **Ramona Bella** and Mariano Ferraresso. Reactivation of the Human Herpes Virus 6 in Kidney Transplant Recipients: An Unsolved Question. Editorial: *J Transplant Technol Res* 2015, 5: e134
3. Signorini L, Croci M, Boldorini R, Varella RB, Elia F, Carluccio S, Villani S, **Bella R**, Ferrante P, Delbue S. Interaction Between Human Polyomavirus BK and Hypoxia Inducible Factor-1 alpha. *J Cell Physiol.* 2016 Jun;231(6):1343-9. IMPACT FACTOR: 3.839
4. Cason C, Campisciano G, Zanotta N, Valencic E, Delbue S, **Bella R**, Comar M. SV40 Infection of Mesenchymal Stromal Cells From Wharton's Jelly Drives the production of Inflammatory and Tumoral Mediators. *J Cell Physiol.* 2017. Nov;232(11):3060-3066. IMPACT FACTOR: 3.839
5. **Bella R**, Dolci M, Ferraresso M, Ticozzi R, Ghio L, Rizzo J, Signorini L, Villani S, Elia F, Ferrante P, Delbue S. Human Herpes Virus-6 DNAemia in children and young adult patients after kidney transplantation. *Future Virology* (Accepted 2015, September 30). IMPACT FACTOR: 1.011

SCIENTIFIC PRODUCTS RELATED TO THIS WORK

Society for NeuroImmune Pharmacology (SNIP) 22nd Scientific Conference, Krakow, Poland April 2016

Eradicating HIV-1 from Brain Compartment Using Tat Inducible Crispr/Cas9 Gene Editing Strategy

Kaminski, R, Chen, Y, Salkind, J, **Bella, R**, Hu, W, Md, Khalili K.

Poland

Abstract

City-Wide NeuroAIDS Discussion Group Held in conjunction with the 2016 International Symposium on Molecular Medicine and Infectious Disease, September 14, 2016, 245 N. 15th Street, Philadelphia.

Negative Feedback Regulation of HIV-1 by Gene Editing Strategy

Bella R.*, Kaminski R., Chen Y., Salkind J., Young WB, Ferrante P.*, Karn J., Malcolm T., Hu W., Khalili K.

Philadelphia

1. Kaminski R, Chen Y, Salkind J, **Bella R**, Young WB, Ferrante P, Karn J, Malcolm T, Hu W, Khalili K. Negative Feedback Regulation of HIV-1 by Gene Editing Strategy. Scientific Reports. Accepted July 20. IMPACT FACTOR 4.259
2. Kaminski R, **Bella R**, Yin C, Otte J, Ferrante P, Gendelman HE, Li H, Booze R, Gordon J, Hu W, Khalili K. Excision of HIV-1 DNA by gene editing: a proof-of-concept in vivo study. Gene Ther. 2016 May 19. IMPACT FACTOR 3.11
3. Prasanta. K. Dash[#], Rafal Kaminski[#], **Ramona Bella[#]**, Hang Su, Taha M. Ahooyi, Chen Chen, Saumi Mathews, Pietro Mancuso, Rashan Sariyer, Pasquale Ferrante, Brady Sillman, Zhiyi Lin, Mary Banoub, Monalisha Elangao, R. Lee Mosley, Larisa Poluektova,

JoEllyn McMillan, Aditya N. Bade, Santhi Gorantla, Won-Bin Young, Benson Edagwa, Jeffrey M. Jacobson, Kamel Khalili, Howard E. Gendelman. Combinations of CRISPR-Cas9 and Long-acting Antiretroviral Therapy Eliminates HIV-1 Infection in Humanized Mice". In preparation

#Equal contributions made

ACKNOWLEDGMENTS

I would like to thank Dr. Pasquale Ferrante and dott.ssa Serena Delbue for their scientific support and help during these years. I would like to thank Dr. Kamel Khalili for the opportunity to work in his laboratory in America and allow me to learn a lot and live this amazing experience. I would like to thank all my colleagues, for their technical and scientific support. I would like to thank my Italian and American friends for all moment spent together. I would like to thank my family for all moral support and continuous interest for my research and allow me to follow my dreams. I would like to thank Michael Craigie for help me a lot in these two years spent in America, help me to learn English language, and for being a constant presence in lab and in life.